2014

CALIBRATION OF NON-NUCLEAR DEVICES FOR CONSTRUCTION QUALITY CONTROL OF COMPACTED SOILS

Joshua E. R. Wells
University of Kentucky, joshua.wells@uky.edu

STUDENT AGREEMENT:

I represent that my thesis or dissertation and abstract are my original work. Proper attribution has been given to all outside sources. I understand that I am solely responsible for obtaining any needed copyright permissions. I have obtained needed written permission statement(s) from the owner(s) of each third-party copyrighted matter to be included in my work, allowing electronic distribution (if such use is not permitted by the fair use doctrine) which will be submitted to UKnowledge as Additional File.

I hereby grant to The University of Kentucky and its agents the irrevocable, non-exclusive, and royalty-free license to archive and make accessible my work in whole or in part in all forms of media, now or hereafter known. I agree that the document mentioned above may be made available immediately for worldwide access unless an embargo applies.

I retain all other ownership rights to the copyright of my work. I also retain the right to use in future works (such as articles or books) all or part of my work. I understand that I am free to register the copyright to my work.

REVIEW, APPROVAL AND ACCEPTANCE

The document mentioned above has been reviewed and accepted by the student's advisor, on behalf of the advisory committee, and by the Director of Graduate Studies (DGS), on behalf of the program; we verify that this is the final, approved version of the student's thesis including all changes required by the advisory committee. The undersigned agree to abide by the statements above.

Joshua E. R. Wells, Student

Dr. L. Sebastian Bryson, Major Professor

Dr. Y.T. Wang, Director of Graduate Studies

CALIBRATION OF NON-NUCLEAR DEVICES FOR CONSTRUCTION QUALITY CONTROL OF COMPACTED SOILS

THESIS

A thesis submitted in partial fulfillment of the
requirements for the degree of Master of Science
in Civil Engineering in the College of Engineering
at the University of Kentucky

By

Joshua Eli Robert Wells

Lexington, Kentucky

Director: Dr. L. Sebastian Bryson, Associate Professor of Civil Engineering

Lexington, Kentucky

2014

ABSTRACT OF THESIS

CALIBRATION OF NON-NUCLEAR DEVICES FOR CONSTRUCTION QUALITY CONTROL OF COMPACTED SOILS

Inadequate compaction of a soil subgrade can lead to detrimental outcomes that are not only costly but dangerous to the general public. To avoid this, quality control (QC) devices such as the nuclear density gauge (NDG) are currently being used to monitor the compaction and moisture content of soil subgrades. However, regulatory concerns associated with the NDG have encouraged federal and state agencies, as well as the heavy civil construction industry to consider non-nuclear devices for QC testing of compacted soils. One such non-nuclear device is the Soil Density Gauge (SDG), which utilizes electromagnetic wave propagation to obtain soil properties such as wet unit weight and moisture content. This research shows that through using soil-specific trend lines, the SDG has the capability of obtaining an equivalent NDG wet unit weight. Alongside the SDG, two dielectric moisture probes were also evaluated and through a calibration process on compacted soils, a general moisture content trend line was developed. This general moisture content trend line related outputted volumetric moisture contents from the moisture probes to gravimetric moisture contents. Field data were then plotted along with the general moisture content trend line to show that these devices have the potential of predicting gravimetric moisture contents.

By combining the results of the SDG and moisture probe analyses, graphs were then developed that relate SDG wet unit weights to NDG dry unit weights using soil and moisture-specific trend lines.

KEYWORDS: Nuclear Density Gauge, Soil Density Gauge, Dielectric Constant, Hydra Probe, Theta Probe.

Joshua Eli Robert Wells

May 29, 2014

CALIBRATION OF NON-NUCLEAR DEVICES FOR CONSTRUCTION QUALITY CONTROL OF COMPACTED SOILS

By

Joshua Eli Robert Wells

Dr. L. Sebastian Bryson
Director of Thesis

Dr. Y.T. Wang
Director of Graduate Studies

May 29, 2014

ACKNOWLEDGEMENTS

I would first like to acknowledge my advisor Dr. L. Sebastian Bryson. Not only was Dr. Bryson an advisor but he was a mentor and a role-model as well. He guided me through every level of research, expanded my knowledge in geotechnical engineering and genuinely cared about my well-being. Dr. Bryson managed to take time out of his busy day to allow for any questions or concerns that I may have had and did his best to solve them. Furthermore, I will always be grateful that I had the privilege of being in the presence of such a great individual.

I would like to thank Clark Graves and the Kentucky Transportation Cabinet for allowing me to perform testing with their devices. I would also like to thank my professors from whom I have had the privilege of learning at the University of Kentucky. Dr. L. Sebastian Bryson, Dr. Michael Kalinski, Dr. Edward Woolery, and Dr. Jerry Rose have offered the knowledge and technical background for me to become a successful Geotechnical Engineer.

My completion of my Master's degree would have not been possible without the help of my colleagues at the University of Kentucky. I would like to thank Ryan Ortiz, Aaron Daley, Xu Zhang, Corrie Walton-Macaulay, Malinda Jean-Louis and Kobina Sekyi for not only helping me with school related work but being friends as well.

Finally, I would like to acknowledge my family. No matter the situation, my mother Diana, my father James and my two sisters Jessica and Jami, were supportive every step of the way. They were always there to talk and listen to any struggles that I experienced. My parents raised me to the best of their ability and I feel they did an excellent job and I thank them for that.

TABLE OF CONTENTS

LIST OF TABLES

LIST OF FIGURES

CHAPTER 1

1 Introduction

1.1 Background

Many federal and state agencies, as well as the heavy construction industry, perform construction quality control (QC) of compacted subgrades using a Nuclear Density Gauge (NDG). However, the NDG has many regulatory concerns that make the use and storage of the device cost-prohibitive in some cases. For example, the costs associated with the NDG include training and certification for each technician, semi-annual leak tests, yearly verifications, and bi-annual calibrations; along with licensing, storage, special handling, and shipping of a hazardous material (Brown, 2007).

To replace the NDG, non-nuclear density gauges (NNDG) have been examined as a viable option. One option is the Soil Density Gauge 200 (SDG), a NNDG manufactured by TransTech, Inc. headquartered out of Schenectady, New York. The SDG utilizes electromagnetic wave propagation theory to obtain frequency-dependent electrical measurements in a soil mass which are related to soil properties such as moisture content and unit weight. The SDG is of particular interest to the construction industry because the device is non-intrusive to the soil and has no regulatory concerns.

Whereas the SDG infers both unit weights and gravimetric moisture contents through onboard calculations, there are also dielectric-based devices that measure the volumetric moisture content of the soil. These devices have an array of probes, arranged at certain distances from each other, to infer moisture contents of a known soil volume. An evaluation was performed on such two devices; the Hydra Probe II, manufactured by Stevens Water Monitoring Systems Inc. headquartered out of Portland Oregon, and the

ML2x Theta Probe manufactured by Delta-T Devices headquartered out of Cambridge, UK. These devices were evaluated with the SDG because previous research (Berney et al., 2011; Sotelo, 2012; and Sabesta et al., 2012) with the SDG has shown the SDG does not produce reliable moisture contents in some situations.

1.2 Research Tasks Description

This research focused on relating wet unit weights and moisture contents outputted by the SDG to NDG wet unit weights and oven moisture contents, respectively. Algorithms used by the SDG to calculate unit weights and moisture contents are proprietary and not made available to this research. However, by reclassifying 32 case study soils to an "Adjusted" Unified Soil Classification System (USCS), soil-specific trend lines were developed relating SDG to NDG equivalent wet unit weights. This research also discusses factors that appear to influence the outputted SDG moisture contents in relation to oven moisture contents as well.

In addition, this research evaluated two dielectric moisture probes and developed a general moisture content trend line to obtain field gravimetric moisture contents from device outputted volumetric moisture contents. This was performed in the laboratory, prior to field testing, on compacted soils using a standard proctor mold. Nine soils, which included two sands, two silts and five clays, were used to develop this general moisture content trend lines. For the space of simplicity, the onboard default soil models (i.e. linear regression models) for the moisture probes were used to develop the correlations. Field data were later gathered and related to the general moisture content trend line and evaluated for reliability.

The equations from the developed soil-specific trend lines and the general moisture content trend lines were then used to develop graphs relating SDG wet unit weights to NDG dry unit weights. The developed graphs are soil-specific and obtain equivalent NDG dry units through the use of moisture-specific trend lines and outputted SDG wet unit weights. A statistical analysis was then performed to evaluate the reliability of the developed soil-specific trend lines for the SDG and a percent error analysis was performed on the field data retrieved from the moisture probes as it related to the general moisture content trend line.

1.3 Objectives of Research

The objectives of this research are as follows:

1) To further understand how the SDG operates and to how this device obtains its outputted values of moisture content and wet unit weight.
    - Field test the SDG at active construction sites near Lexington, Kentucky and evaluate its reliability in obtaining outputted parameters of wet unit weight and moisture content. Then discuss the SDG's ability to obtain the outputted values relative to a sand cone and oven moisture contents.
    - Perform an error analysis for the SDG regarding inputted material properties. Asses the effects of inputting incorrect material properties on the SDG performance.
    - Compile and plot outputted SDG wet unit weight and moisture content data from case studies. Group the plotted data to a developed adjusted USCS to observe if any trends develop per adjusted soil type

- Apply soil-specific trend lines based on the adjusted USCS to reliably obtain an equivalent NDG wet unit weight from an outputted SDG wet unit weight.

2) To further analyze and develop a general moisture content trend line for two dielectric moisture probes that obtains gravimetric moisture contents from device outputted volumetric moisture contents.

- Perform laboratory calibrations with the Theta Probe and Hydra Probe on soils that were compacted in a proctor mold at standard energy.
- From the laboratory calibration, develop general moisture content trend lines based on default soil models that can be used to obtain gravimetric moisture contents from device volumetric moisture contents for compacted soils
- Perform a field performance evaluation with the two dielectric probes to asses the ability of the probes to obtain moisture contents relative to the developed general moisture content trend lines
- Use the general moisture calibration trend line equations and soil-specific wet unit weight trend line equations to develop a method to relate SDG wet to NDG dry unit weight through moisture-specific trend lines.

1.4 Contents of Thesis

Chapter 2 presents the technical background of the SDG, Theta Probe and Hydra Probe. A discussion of the theory behind these devices is presented as well, along with related research and a section regarding the need for further research.

Chapter 3 shows laboratory testing and a calibration procedure for the moisture probes, developed on compacted soils at standard energy. Through this calibration procedure a general moisture content trend line was developed.

Chapter 4 presents the methods and procedures for using the devices during field testing. Inputted material properties were varied and an error analysis based on those variations was performed to assess the influence of the inputted material properties. The SDG and moisture probes were also evaluated on performance in the field.

Chapter 5 shows case studies involving the SDG. An evaluation was performed regarding the outputted wet unit weights and moisture contents. An adjusted USCS was presented and soils from the case studies were reclassified accordingly. Soil-specific trend lines from the reclassified soils were then made to obtain equivalent NDG wet unit weights from SDG wet unit weights. The equations from the developed soil-specific trend lines and the general moisture content trend lines were then used to develop graphs relating SDG wet unit weights to NDG dry unit weights using moisture-specific trend lines. Confidence intervals and percent error graphs were developed to show the reliability of the developed trend lines.

Chapter 6 shows how well the outputted volumetric moisture contents from the Theta Probe were able to predict gravimetric moisture contents through the use of the general moisture content trend lines. Comparisons between different calibration methods with the SDG were performed as well.

Chapter 7 presents the conclusions from this research. By using the SDG and the Theta Probe or Hydra Probe together, gravimetric moisture contents and equivalent dry unit weights can be obtained, making the devices a possible reliable form of QC for monitoring compacted subgrades.

Appendix A presents graphs to obtain equivalent NDG dry unit weights using the Theta Probe and SDG in tandem.

Appendix B presents graphs to obtain equivalent NDG dry unit weights using the Hydra Probe and SDG in tandem.

Appendix C presents graphs to obtain equivalent NDG wet unit weights from outputted SDG wet unit weights along with confidence interval graphs.

Appendix D shows the moisture probe laboratory calibration line data.

Appendix E presents the data sheets for the soil material properties tested in the laboratory.

CHAPTER 2

2 Technical Background

2.1 Complex Permittivity in Soil

The devices evaluated in the research all have a common theme of operation in that measurements of complex permittivity are used to infer outputted values of either moisture content or unit weights. Complex permittivity is given as

$$\varepsilon^* = \varepsilon' - j\varepsilon'' \quad \textbf{(1)}$$

where complex permittivity , ε^*, contains both the real dielectric permittivity, ε', and imaginary dielectric permittivity, ε'' and $j=\sqrt{-1}$. How each device obtains these outputted values are unique to the device through dependencies on frequencies and onboard calculations. The frequencies can either be a single frequency or a range of frequencies and the calculations, based on the readings of the soil permittivity, changes between each device.

Mitchell and Soga (2005) define complex permittivity as a measure of the ease with which molecules can be polarized and orientated in an electric field. Complex permittivity contains both real and imaginary parts where the real component describes the energy storage and imaginary component describes the energy losses experienced in the presence of an applied electric field. Both components are used to describe the behavior of molecules in a conducting media.

When an alternating current is introduced to a conducting material (e.g. saturated and partially saturated soil) a process of polarization occurs. Through polarization, the dipoles of the soil and pore water molecules that are being influenced align in the direction of the applied current flow. In the case of soil, the dipoles behavior is dependent on the

moisture content and the soil type. Water molecules tend to polarize to a greater extent than the soil molecules in the presence of an electric field. Thus, water content tends to be directly related to measures of electric current flow in a conducting material (Stevens, 2008). Figure 2.1 shows the concept of molecule polarization.

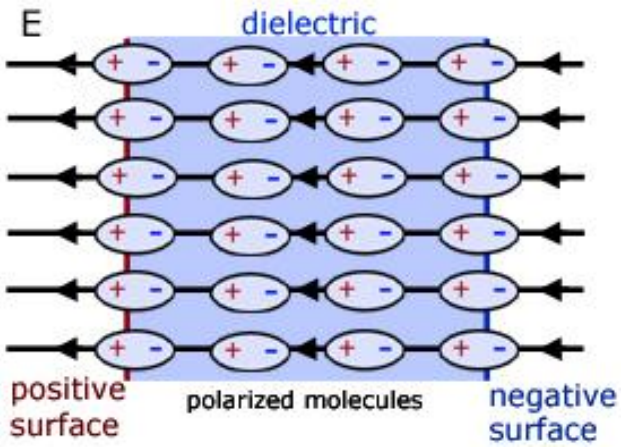

Figure 2.1: Concept of Molecule Polarization

The frequency at which the electromagnetic field is applied also influences the process polarization. When the frequencies are low, the polarity of the applied field changes slow enough to where the molecules dipoles are able to keep up with the change and align in the direction of the current flow. At higher frequencies, the molecules dipoles are not able keep up with the changes in polarity. This process of not being able to keep up is referred to as relaxation, meaning that some of the energy applied is dissipated. This causes a phase lag between the applied field and the materials response, which is where the real and imaginary parts of complex permittivity present themselves.

Often when dealing with materials such as soils, the complex permittivity is normalized with the free space of permittivity, ε_0, to obtain what is known as relative permittivity, ε_r^*, given as

$$\varepsilon_r^* = \frac{\varepsilon^*}{\varepsilon_0} = \frac{\varepsilon'}{\varepsilon_0} - j\frac{\varepsilon''}{\varepsilon_0} = \varepsilon_r' - j\varepsilon_r'' \quad \textbf{(2)}$$

where, ε_0 is the free space of permittivity equals 8.8542x10^{-12} C^2/J·m. In Equation 2 the relative real component $\varepsilon'/\varepsilon_0$ is typically referred to as the dielectric constant because at certain operating frequencies the real component is much greater than the imaginary component. Normally at around 21 degrees Celsius the dielectric constant of water ranges from 79 to 82, dry soil ranges 2 to 5 and for air it is 1 (Hu et al., 2010). So when observing the dielectric constants of a soil it is assumed that the effects of air and the soil are negligible. Thus, the dielectric constant of a soil is most influenced by the water contained in the soil.

These readings of dielectric permittivity are also frequency dependent in that at different frequencies the responses of the real and imaginary components respond differently. The response of the real component and imaginary component at differing frequencies can be seen in Figure 2.2

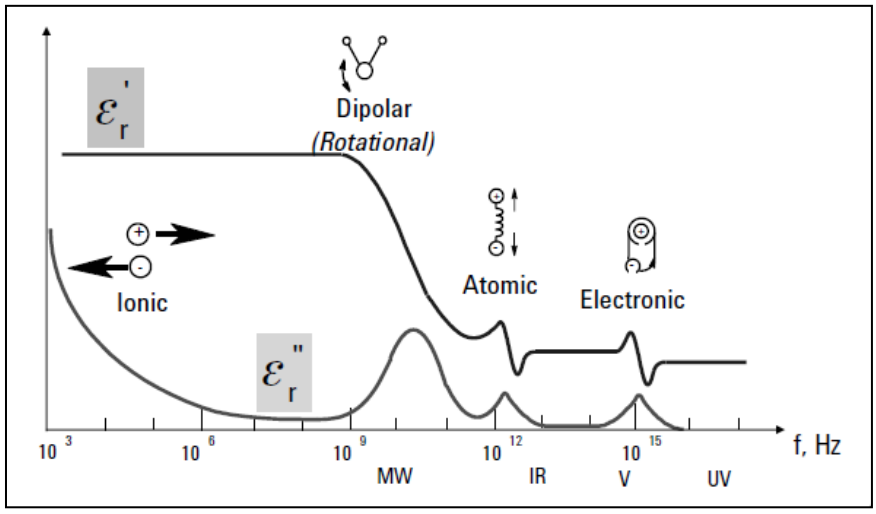

Figure 2.2: Frequency dependence of permittivity in water (Agilent Technologies, 2006)

The real component of permittivity is fairly constant in a frequency range from approximately 1 kHz to 1 GHz, while the imaginary component tends to vary significantly between 1kHz to 1MHz. Many dielectric devices operate in the range from 1MHz to 1GHz. However, there is not one single best frequency and many researchers have experimented with a wide variety of frequencies (Topp et al., 1980; Campbell, 1990; Lee, 2005).

2.2 Device Overview and Concepts of Operation

2.2.1 SDG Overview

The NDG is considered a reliable device to monitor compaction and moisture content of a subgrade soil but because of regulatory concerns, and specialized training and disposal requirements, the NDG is costly to operate. Along with these concerns, for the NDG to be within regulation; storage, transportation and handling have to be documented correctly or heavy fines could be implemented. Thus, researchers have developed non-nuclear devices that can potentially replace the NDG. The SDG is a commercially-available non-nuclear device currently being marketed as a NDG replacement. The SDG is shown in Figure 2.3.

Figure 2.3: Soil Density Gauge 200 developed by TransTech Systems Inc.

The SDG uses electromagnetic wave propagation to generate measurements of in situ unit weights and moisture contents of compacted soils (Pluta et al., 2009). This device is also non-intrusive, which allows for rapid measurements to be taken while in the field. The main housing unit sits on a circular ring that rests on top of the ground surface. This is different compared to the NDG, which requires a spike to be driven into the ground.

While the SDG has characteristics of being efficient, there are also some deficiencies associated with the device. The SDG has on-board proprietary algorithms that determine the values of wet unit weight and volumetric moisture content. Because the algorithms are proprietary, researchers cannot adjust the equations for varying conditions such as differing soil types. Therefore, there is no means to calibrate or adjust the outputted values internally. However, the SDG does allow the operator to input material properties which implies that the inputted material data is used during on-board calculations. How

the material properties data affects the outputted values of unit weights and moisture contents is not known.

2.2.2 SDG Concepts of Operation

The SDG is a self-contained device. A user-operated interface is attached to a signal-producing body that uses electrical impedance spectroscopy (EIS) to infer the soil's volumetric moisture content and wet unit weight of the soil. Specific information about the algorithms implemented to calculate unit weights and moisture content from the obtained EIS reading is proprietary. However, a few published works give a general idea of the working theory.

EIS is the measurement of electrical permittivity based on the interaction of an external field and electric dipole moment of the material (Pluta, et al., 2009). The current-voltage relationship of an external AC electric field takes the simplified form of the Equation 3

$$Z = \frac{V}{I} \tag{3}$$

where were Z is the impedance, V is the frequency-dependent voltage and I is the frequency-dependent current. The complex impedance can be measured in the terms of resistance (R) and reactance (X), These measured parameters include the natural impedance of the probe, the cable, electrode effect, and the soil itself. Thus, if the impedance due to the probe, cable and electrode configuration is known and remains constant, the impedance of the soil can be readily determined. Electrical impedance can be calculated from the Equation 4

$$Z = R + jX = \sqrt{R^2 + X^2}\, e^{j\Phi} \tag{4}$$

where Φ is the phase angle and j is a constant (Parilkova, et al., 2009). The relationship between frequency and electrical permittivity of soil is limited by the Maxwell-Wagner relaxation effect, which relates a qualitative representation of dielectric properties of wet soils as a function of frequency (Drnevich, et al., 2001), as seen in Figure 2.4.

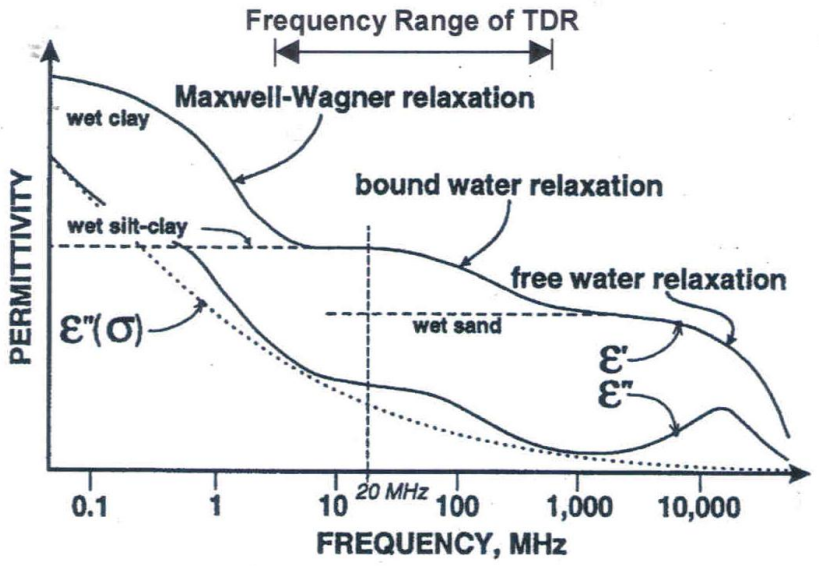

Figure 2.4: Qualitative representation of dielectric properties of wet soils as a function of frequency (Drnevich, et al., 2001).

The SDG operates at a range from 300 kHz to 40 MHz and within that range, the Maxwell-Wagner effect is used with an empirically derived soil dielectric mixing equation to develop a soil model. Wet unit weight and moisture content are identified from a pattern in the fitted frequency spectra equations. Soil gradation was found to affect the frequency response of the SDG, thus the specific surface area of the tested material was calculated and the empirical inversion model was adjusted (Pluta, et al., 2009).

The SDG measures the wet density and volumetric moisture content of the soil during each test. The wet density is the total mass of material per unit volume and the volumetric

moisture content is the volume of water per unit volume. From these measurements the device calculates the dry density and gravimetric moisture content, both of which are outputted for the operator to view. The dry density is calculated by the difference between wet density and volumetric moisture content as seen in Equation 6

$$\gamma_{dry} = (\gamma_{wet})_{measured} - ((\theta)_{measured})\gamma_w \quad \textbf{(5)}$$

where the γ_{dry} is the calculated dry density, $(\gamma_{wet})_{measured}$ is the measured wet density, $(\theta)_{measured}$ is the measured volumetric moisture content and γ_w is the unit weight of water. Once the dry density is calculated a gravimetric moisture content is calculated shown in Equation 6

$$\omega = \left(\frac{(\theta_{measured})\gamma_w}{(\gamma_{dry})_{calculated}} \right) * 100 \quad \textbf{(6)}$$

where ω is the calculated gravimetric moisture content as a percentage of dry density, γ_w is the unit weight of water and $(\gamma_{dry})_{calculated}$ is the dry density calculated in Equation 6. With the outputted measurements of dry density and gravimetric moisture content, the values can then be related to maximum dry densities and optimum moisture contents for QC.

2.2.3 Moisture Probe Overview

The probes evaluated in this research infer the volumetric water content of the soil through the measurement of the dielectric properties of a unit volume of soil. Figure 2.5 shows the two devices evaluated for this research.

(A) (B)

Figure 2.5: (A) Delta-T Theta Probe ML2x; (B) Stevens Hydra Probe II

Figure 2.5(A) shows the Theta Probe and Figure 2.5(B) shows Hydra Probe. Each probe has onboard (ie. pre-programmed) default soil models, which infer volumetric moisture contents that the operator can choose from depending on the soil type is being tested. The soil models are simply regression models that relate dielectric and voltage measurements to volumetric moisture content measurements. The Theta Probe has two default onboard soil models consisting of mineral and organic, while the Hydra Probe has four on board soil models consisting of clay, silt, loam and sand. The user also has the capability of developing a soil-specific model that then can be inputted into each device. A calibration procedure to develop a soil-specific model increases the devices ability to accurately obtain moisture contents as seen in research from (Kalieita et al., 2005; Saito et al., 2013; and Carteret et al., 2013).

2.2.4 Hydra Probe Concepts of Operation

The Hydra Probe, as seen in Figure 2.6, is classified as a ratiometric coaxial impedance based sensor that measures the complex permittivity of a soil. The device consists of a 25

mm diameter stainless steel base plate that is attached to a head with four 3 mm diameter tines that extend 58 mm away from the head. Three tines surround a central tine to form an equilateral triangle with 22 mm sides (Seyfried et al., 2005)

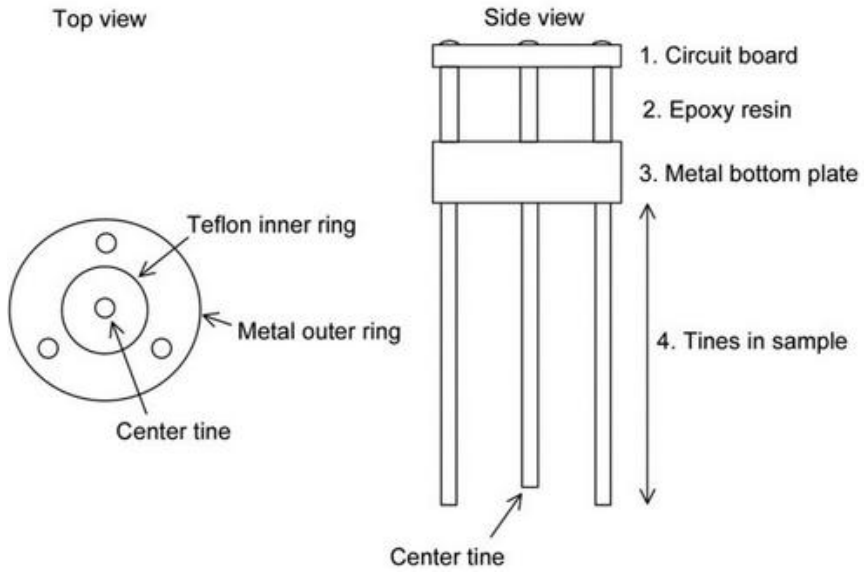

Figure 2.6: Schematic of the bottom portion of the Hydra Probe (Kelleners et al., 2009)

The probe creates an electromagnetic signal at a frequency of 50 MHz that is generated in the head and transmitted via planar waveguides to the tines, which constitute a coaxial transmission line that has a characteristic impedance of, Z_0 (Seyfried and Murdock, 2004). To obtain the real and imaginary component of permittivity the Hydra Probe has to calculate the impedance of the probe, Z_P, through Equation 7

$$Z_P = \frac{Z_0}{\sqrt{\varepsilon_r^*}} \cot\left(\frac{\omega \sqrt{\varepsilon_r^*} L}{c} j \right) \quad \textbf{(7)}$$

where ε_r^* is the relative permittivity, j = $\sqrt{-1}$, ω is the angular frequency of the sensor, L is the electrical length of the probe, and c is the speed of light. However, to solve for Z_P, a measurement of the incident and reflected voltage has to be made. When a voltage is applied through the coaxial cable, a signal is reflected and related to the impedance of the coaxial cable, Z_C. This relationship is calculated through Equation 8

$$\frac{Z_P}{Z_C} = \frac{1+\Gamma}{1-\Gamma} \quad \textbf{(8)}$$

where Z_C is the impedance on the coaxial cable, and Γ is the ratio on the behavior of the reflected voltage and incident voltage. By determining Γ, Z_p can be calculated by using Equation 8 and then inputted into Equation 7 to solve for the relative permittivity. By measuring the relative permittivity, on-board soil specific equations can then be used to calculate a volumetric moisture content.

2.2.4.1 Hydra Probe Default Calibrations equations

Default calibration equations, i.e. soil-specific models, are used to calculate volumetric water contents. Depending on the default soil type selected of Clay, Silt, Sand or Loam, the Hydra Probe calculates volumetric moisture contents using one of the three equations as follows

$$\theta = A + B(\varepsilon'_{r,TC}) + C(\varepsilon'_{r,TC})^2 + D(\varepsilon'_{r,TC})^3 \quad \textbf{(9)}$$

$$\theta = A + B(\varepsilon'_r) + C(\varepsilon'_r)^2 + D(\varepsilon'_r)^3 \quad \textbf{(10)}$$

$$\theta = A\sqrt{\varepsilon'_r} + B \quad \textbf{(11)}$$

where θ is the calculated volumetric water content, ε'_r is the real dielectric permittivity, $\varepsilon'_{r,TC}$ is the temperature corrected real dielectric permittivity and the coefficients of A,B,C

and D are a function of the soil texture that is selected (Bellingham, 2007). These coefficient values were developed on different soil types and can be seen in Table 2.1.

Table 2.1: Default soil type coefficient values (Bellingham, 2007)

Soil Texture	Equation	Coefficients			
		A	B	C	D
Sand	9	-8.63	3.216	-9.54E-02	1.57E-03
Silt	9	-13.04	3.819	-9.12E-02	7.30E-04
Clay	10	-20.93	6.553	-0.246	3.24E-03
Loam	11	0.109	-0.179		

2.2.5 Theta Probe Concepts of Operation

The Theta Probe is impedance based probe that has the capability of outputting volumetric moisture contents and voltage readings. The Theta Probe consists of an input/output cable, probe body and a sensing head. The cable allows for power supply and transmits output readings to the operator. The probe body is a water proof casing that houses an oscillator, transmission line and measuring circuitry. The sensing head has an array of four tines, where three of the tines surround a central signal rod in a triangular fashion as seen in Figure 2.7

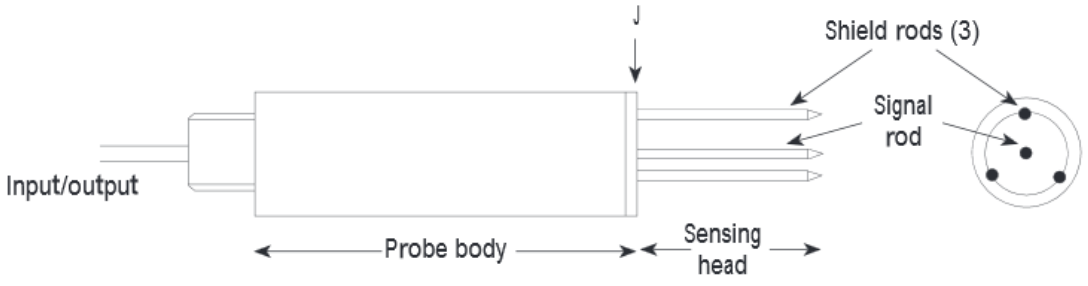

Figure 2.7: Schematic of the Theta Probe showing the probe body and sensing head (Miller and Gaskin, 1999)

The Theta Probe is able to calculate infer the volumetric moisture content by utilizing measurements from a simplified free standing wave to determine the impedance of a sensing rod array. By measuring amplitude difference between the voltages, the impedance of the probe can be measured then related to the dielectric constant of the soil. To obtain this amplitude difference a reflection coefficient, ρ, is calculated as follows

$$\rho = \frac{(Z_M - Z_L)}{(Z_M + Z_L)} \quad \textbf{(12)}$$

where Z_L is the impedance of the transmission line and Z_M is the impedance of the probe inserted into the soil. This is then used to calculate the difference in amplitude by the following relationship

$$V_J - V_0 = 2a\rho \quad \textbf{(13)}$$

where V_0 is the transmission lines peak voltage and V_J is the reflected peak voltage and (a) is the amplitude of the oscillator output. The impedance of the array of tines affects the reflection of the 100 MHz signal that is produced by the Theta Probe. So when the reflected signals combine with applied signals a voltage standing wave is formed. From this, an output analogue voltage is shown which is proportional to the difference in amplitude of the standing wave at two points (Miller and Gaskin, 2009).

2.2.5.1 Theta Probe Default Calibration Equations

With this outputted voltage, volumetric moisture contents and square root of the dielectric constants can be calculated. The Theta Probe uses two on-board soil models of Mineral and Organic to calculate volumetric moisture contents. Equation 14 shows the general form of the equation used to calculate the volumetric moisture contents.

$$\theta = A(V)^3 + B(V)^2 + C(V) + D \quad \textbf{(14)}$$

where θ is the calculated volumetric moisture content of the soil and V is the voltage that is recovered from the interaction of the applied and reflected waves. Table 2.2 shows the values of the coefficients for each of the on-board models.

Table 2.2: Coefficient values for the on-board soil models

Soil Model	Coefficients			
	A	B	C	D
Mineral	0.560	-0.762	0.762	-0.063
Organic	0.610	-0.831	0.831	-0.030

Likewise, the square root of the dielectric constant, $\sqrt{\varepsilon_r'}$, can be calculated from the outputted voltage by either using a 3rd degree polynomial seen in Equation 15 or by a linear equation shown by Equation 16.

$$\sqrt{\varepsilon_r'} = 1.07 + 6.4V - 6.4V^2 + 4.7V^3 \quad \textbf{(15)}$$

$$\sqrt{\varepsilon_r'} = 1.1 + 4.44V \quad \textbf{(16)}$$

When choosing which equation to use to obtain a dielectric constant, there is little difference in accuracy between the two when volumetric moisture contents are below 50%. However if moisture contents are above 50%, the 3rd degree polynomial is suggested to be used (Delta-T Devices, 1999).

2.2.6 NDG Overview and Concepts of Operation

The nuclear density gauge (NDG) is currently the most widely used field method to determine soil unit weight and moisture content because of its simplicity of use, speed of measurement, and perceived accuracy (Rathje et al., 2006). The procedure for operation

consists of a large spike being hammered into the ground and removed to provide a hole. A rod from the NDG is lowered into this hole with a cesium or radium source in the tip. High energy photons are emitted by the radioactive material and interact with the electrons in the soil mass. The Geiger-Mueller receiver in the base of the NDG counts the number of incoming high energy photons. A higher density soil contains a higher number of electrons in the soil mass, which results in a lower number of high energy photons counted at the receiver (Ayers et al., 2008). The moisture content derived by the NDG is actually a count of Hydrogen particles. High energy neutrons are emitted from the nuclear source and loose energy as they come into contact with Hydrogen. The NDG receiver detects the very slowest (thermalized) neutrons and infers the moisture content based off the percentage detected (Evett, 2000).

2.3 Previous Studies

2.3.1 SDG Previous Studies

Since the development of the SDG 200, researchers (Berney et al., 2011; Sotelo, 2012; and Sabesta et al., 2012) have been trying to quantify how this device obtains outputted values of unit weights and moisture contents. Different procedures have been presented to achieve more reliable results when compared to accepted standards. Those methods are discussed in this section along with conclusions based on the data collected.

Pluta et al., (2009) presented some of the initial performance data for the SDG. The data presented by these researchers gave general insight in how the SDG performs for various soil types. For the Pluta et al., (2009) study, five granular non-plastic soils were tested in a laboratory at various states of compaction and moisture contents, which were relative to maximum dry unit weights and optimum moisture contents. SDG performance data were

compared to wet unit weight obtained from the NDG. Figure 2.8 shows the results of the Pluta et al. (2009) study.

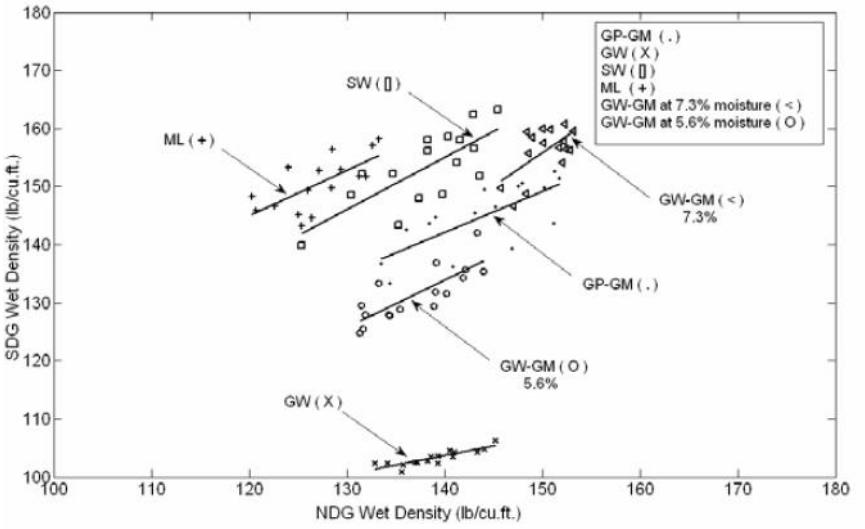

Figure 2.8: NDG Wet Density versus SDG Wet Density without Specific Surface Area Adjustment (Pluta et al., 2009)

The figure shows the SDG predicted higher wet unit weights than the NDG for soils with greater amounts of fines (% passing the #200 sieve) such as the ML and SW soils. However, the SDG predicted low wet unit weights than the NDG for the Gravels. To better correlate the SDG with the NDG, Pluta et al. (2009) applied bulk specific surface area adjustments that were developed using the specific surface area of idealized particles. However, the method of applying the specific surface area adjustments is proprietary information but Figure 2.9 shows the results after the adjustments were made.

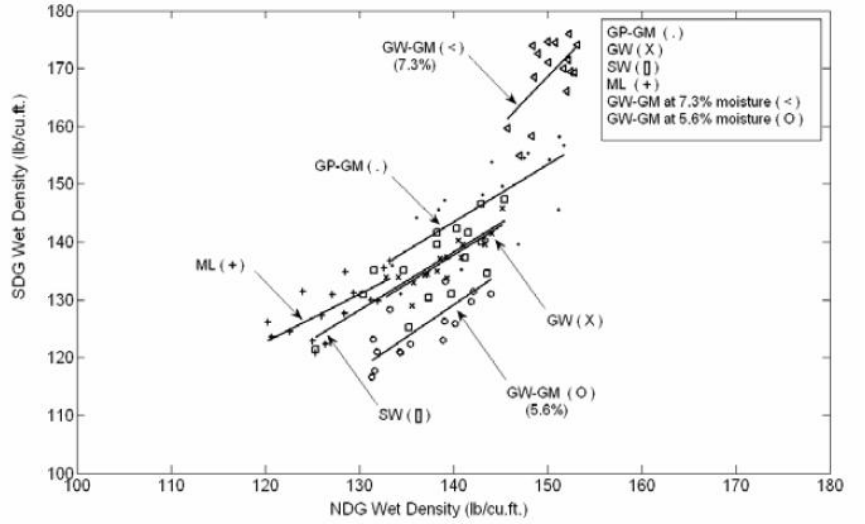

Figure 2.9: NDG Wet Density versus SDG Wet Density with Specific Surface Area Adjustment (Pluta et al., 2009)

Two studies were conducted by the U.S Army Engineer Research and Development Center (ERDC). Berney et al. (2011) compared moisture content data obtained from various field moisture content methods that included the NDG, SDG, Electrical Density Gauge (EDG), and a field open flame gas burner. The other study conducted by Mejias-Santiago et al. (2013) also focused on the SDG 200 and compared outputted dry unit weights to NDG dry unit weights.

Berney et al. (2011) compared the outputted SDG gravimetric moisture contents to oven gravimetric moisture contents and it was concluded that when calibrated, the SDG performed very well. The testing took place in a field setting and calibrations were made by applying linear offsets to the outputted moisture contents obtained from the SDG. To obtain these linear offsets, a moisture content from the SDG was subtracted from an oven moisture content during the first baseline test and the difference was applied to subsequent SDG outputted moisture contents. Figure 2.10 shows the field data compared

to the oven moisture contents. Data for both the raw and corrected are plotted and as can be seen, there were improvements.

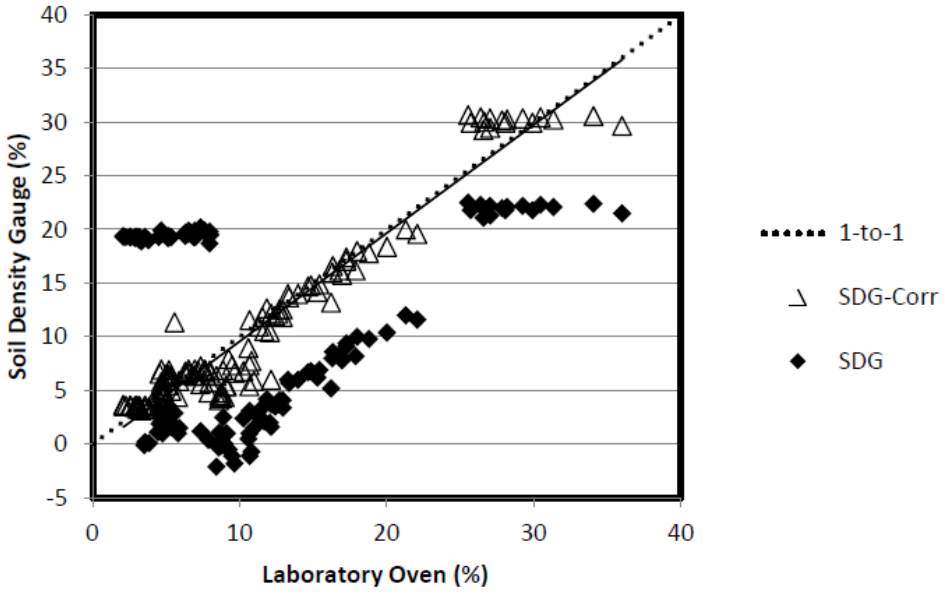

Figure 2.10: Laboratory oven versus SDG moisture content (Berney et al., 2011)

R^2 values were also presented for the adjusted data and achieved a value of 0.93. However, even though the SDG was able to give acceptable values after applying linear offsets, it was suggested that the SDG not be viewed as a reliable device for QC purposes if a calibration procedure cannot be implemented.

Mejias-Santiago et al. (2013) tested 16 different soils with the SDG. The device was evaluated on reliability of obtaining dry unit weights compared to a NDG. The test soils were in a compacted state at moisture contents below, near, and above optimum moisture content. An initial graph was developed to show how the uncorrected SDG data dry unit weights data compared to the NDG data. However, when calculating R^2 for the uncorrected data a correlation of only 0.17 was achieved. To improve this correlation, an equation was applied to the data taking the material properties of each soil into

consideration. Equation 17 shows the developed equation that was applied to each outputted reading from the SDG to obtain a NDG dry unit weight.

$$\gamma_{dry}(NDG) = a1 + a2 * SGD + a3 * SGM + a4 * C + a5 * PI + a6 * PL + a7 * COR \quad \textbf{(17)}$$

where SGD is the SDG outputted dry density, the SGM is the SDG moisture content, C is the parameter derived from the SDG's frequency spectrum, PI is the soil plasticity index and the PL is the soil plastic limit. A (COR) variable was applied at the end of the equation that further improved the correlation. The COR variable was calculated by the numeric difference between one NDG dry density and its companion SDG reading. The coefficients of C, a1, a2, a3, a4, a5, a6, and a7 as seen in Table 2.3, were developed using a multiple-linear regression to determine the significance of the SDG internal parameters and soil properties based on laboratory testing to improve accuracy (Mejias-Santiago et al., 2013).

Table 2.3: Statistical variables and coefficient values for regression analysis (Mejias-Santiago et al., 2013)

Variable	r value	Coefficient	All Soils	All Soils	Fine	Coarse
Constant		a1	130.188	92.300	90.596	167.936
SDG Wet Density	0.261	a2	-0.320	0.124	0.132	-0.377
SDG Moisture Content	0.233	a3	1.068	-0.426	-0.101	1.434
C Value	0.289	a4	0.811	0.970	0.738	1.634
Plasticity Index (PI)	0.683	a5	-0.793	-0.118	-0.186	-0.647
Plastic Limit (PL)	0.810	a6	-0.647	-0.404	-0.486	-3.511
Dry Density Correction	0.792	a7*		0.698	0.645	2.638
		Overall r =	0.911	0.944	0.953	0.704
		r^2 =	0.83	0.89	0.91	0.50

Depending on the soil type, different coefficients values were inputted into Equation 17 which allowed for higher correlations between the SDG and NDG. Figure 2.11 shows the

final data for the NDG dry density versus statistically corrected and calibrated SDG dry density.

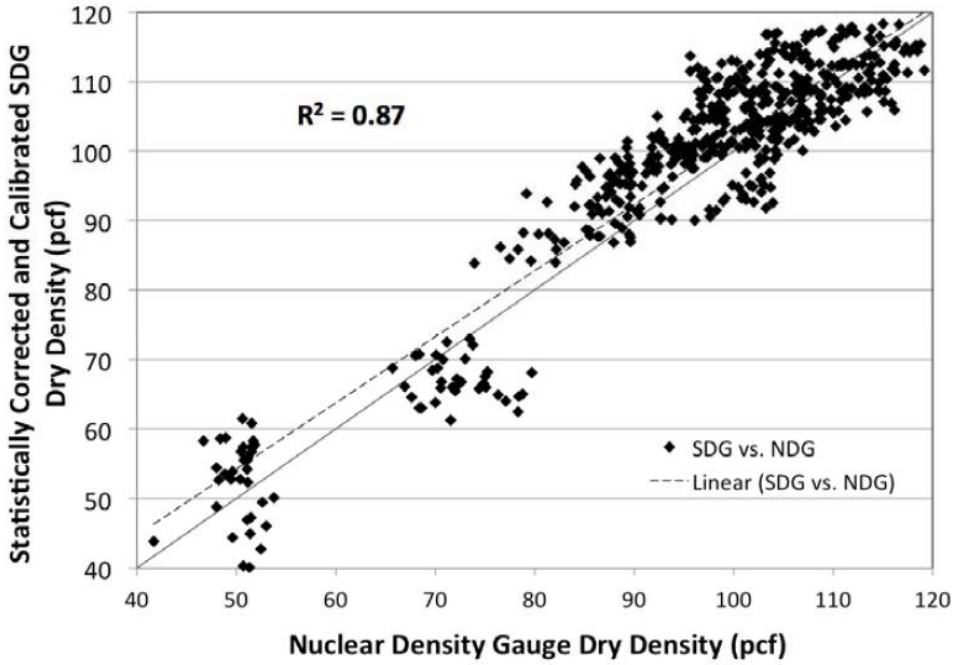

Figure 2.11: NDG dry density versus corrected SDG dry density (Mejias-Santiago et al., 2013)

By applying the equation to each of the raw outputted data for the SDG, a R^2 value of 0.87 was achieved which was a significant improvement from the uncorrected data for the SDG. Although there were improvements in data, it was still recommended that the SDG not be viewed as an acceptable QC device if no calibration is performed.

Sotelo (2012) evaluated several non-nuclear devices for the determination of moisture content and dry unit weights of compacted soils. The experiments were laboratory-based and the soil was compacted into a cylindrical mold, 0.5 m in diameter and 0.6 m in depth. The soil was placed in 50 mm lifts and compacted at the end of each lift to heights of 0.3 m for the first test then 0.6 m for the second test. Moisture content samples were taken every 50 mm to obtain oven moisture contents that were later compared with outputted

SDG moisture contents. These values were recorded from the SDG and were compared to a known dry unit weights and oven moisture contents. Figure 2.12 shows an example of the data that were produced.

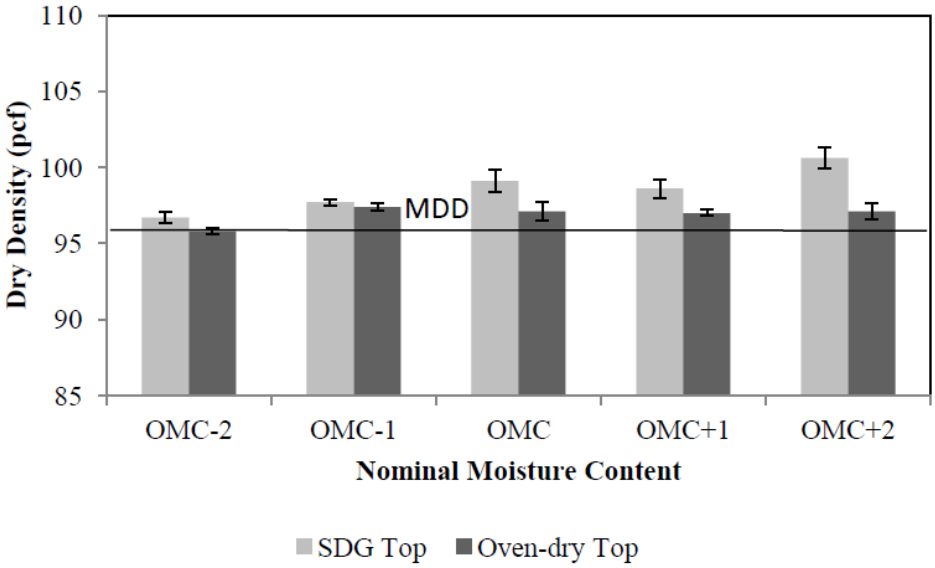

Figure 2.12: Bar Graph showing Dry Density Comparisons at Varying Moisture Contents (Sotelo, 2012)

The tests were performed at varying moisture contents for each soil type that were presented in the study. The data presented in Figure 2.12 are for a highly plastic clay and the SDG outputted data shows correlations to the known unit weight signified by the horizontal black line. However, this was not the case for every soil type tested and it seemed that as the moisture content increased the less correlation the SDG had with the actual unit weights. Sotelo (2012) concluded that the SDG was affected by the changes in the material properties from each soil and predicted moisture contents and dry densities accurately for only certain soil types. However, further research is needed.

Sebesta et al. (2012) worked with the Texas Department of Transportation and the Federal Highway Administration to evaluate multiple non-nuclear devices for reliably

obtaining unit weights and moisture contents of a flexible base. The flexible base consisted of a large amount of gravel but still had a level of plasticity. The AASHTO classification given to the soil was Type A Grade 4. The tests with the SDG were performed in a 0.2 m^3 meter box and the flexible base was compacted in two lifts. Material was then collected for moisture contents and the SDG and NDG outputted values were compared. Following the box test, the SDG was evaluated in the field on the same flexible base that was as the subgrade for a roadway project. During the field testing the SDG was compared to oven moisture contents and as the actual moisture content increased the outputted SDG readings did not increase. When obtaining dry unit weights the SDG tended to under-predict and when compared to the other devices tested, none displayed a higher level of performance.

Rose (2013) researched several non-nuclear devices, including the SDG, and compared outputted values to a NDG or sand cone for wet and dry unit weights and oven moisture contents. A 1-point correction factor or 3-point correction factor were applied to outputted SDG values in order to achieve more repeatable results. To perform the 1-point correction during testing, the first reading from the SDG was compared to a known measurement and the difference between the two was calculated. Whatever the difference was it was then applied to subsequent outputted SDG readings thereafter. The same was done for the 3-point correction factor except this was performed at the first three testing spots and the differences from the known measurements at those testing locations were averaged together. The averaged result was then applied to subsequent test thereafter as well. Figure 2.13 shows the improvements that were experienced when the 1-point and 3-point corrections were applied to the subsequent outputted SDG values.

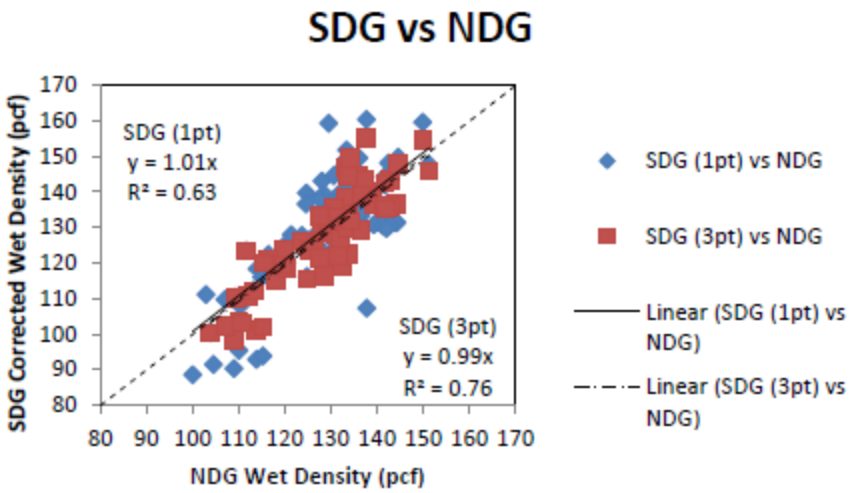

Figure 2.13: 1-point and 3-point correction results (Rose, 2013)

The correlation between the SDG and NDG wet unit weights achieved R^2 values of 0.63 for the 1-point correction and 0.76 for the 3-point correction. These improvements were also experienced with the outputted dry unit weights and gravimetric moisture contents as well and can be seen in (Rose, 2013). However with these improvement, it was determined that the SDG performs well when corrections are applied to the outputted SDG readings, but when the corrections are not used then the SDG is not reliable.

2.3.2 Moisture Probe Previous Studies

Several studies have been performed with the Theta Probe and Hydra Probe that investigate different applications such as; moisture content observance, outputted value evaluations of dielectric properties, and calibrations per soil type. Vaz (2013) presented a review of published papers that were available for Hydra Probe and Theta Probe. Table 1 from Vaz (2013), there were 39 published papers for the Theta Probe and for the Hydra Probe there were 21 published at that time. With so many published papers, these devices are well documented and because of their versatility of use, researchers have used them in many applications.

Hu et al. (2010) performed a study with three dielectric probes consisting of the Theta Probe, CS616, and the SM200. The research focused on developing calibration trend lines on an expansive clay soil. Up to this point, much research had been performed on granular soils but little with expansive fine grained soil. This paper compared calibration trend lines from other studies to calibration trend lines developed in this paper as seen in Figure 2.14.

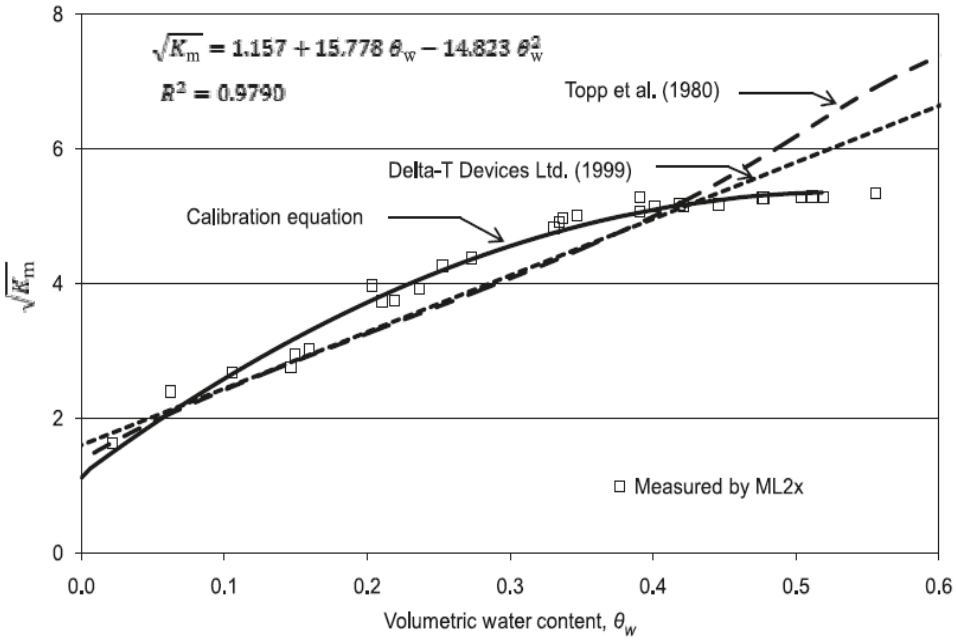

Figure 2.14: Volumetric Moisture versus Square Root Bulk Dielectric Constant (Hu et al., 2010)

Calibrations trend lines were developed for each of the devices and the differences between the developed curves and the curves from other studies were observed. For this particular clay, the observed dielectric values were higher than that of the predicted values. It was recommended that further research to be done to quantify if the higher plasticity of the soil has an effect on the dielectric readings.

Schmutz and Namikas, (2011) developed a relationship comparing the Theta Probes outputted voltages to gravimetric moisture contents for two beach sands. While doing this, probe insertion depths were varied and the outputted voltages based on varying probe depths were recorded. The reasoning behind this evaluation was to see how outputted voltages changed as the insertion depth went from full insertion of the probe at 60 mm, to just the tip of the probes at 5 mm. To vary the depths of the insertion of the probes, pre-cut foam blocks were made and the rods of the probes were placed through the blocks during field testing. Figure 2.15 shows the results of voltage versus gravimetric moisture for the Theta Probe at varying insertion depths.

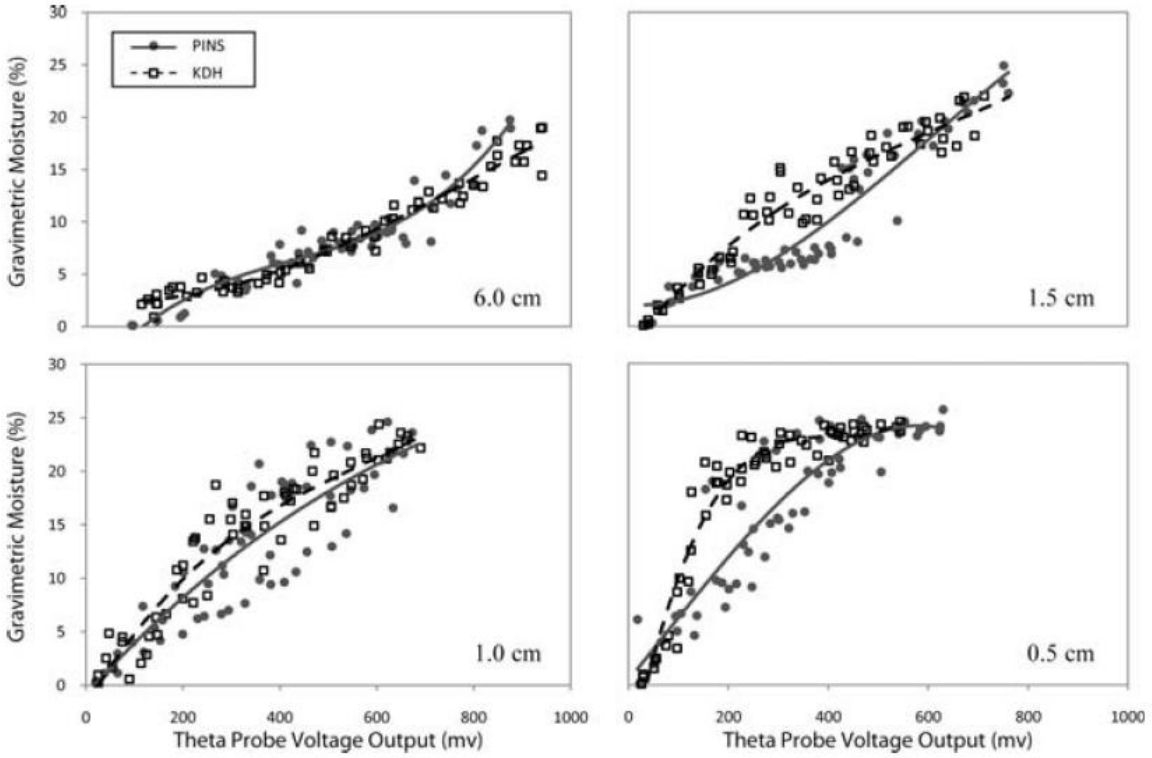

Figure 2.15: Graphs showing Theta Probe Voltage versus Gravimetric Moisture Content at varying Insertion Depths (Schmutz and Namikas, 2011)

While the insertion decreased the probes output range decreased as well. As a result the Theta Probe became less sensitive to moisture increases as the insertion depth decreased.

Carteret et al. (2013) used the Hydra Probe to relate how different installation and calibration methods of the probe affected the readings outputted by the device. This study was tested on gravelly course-grained material and several installation methods were assessed and compared to installation methods used on fine-grained materials. It was observed that the typical installation methods used on the gravelly material led to inconsistent outputted data. To improve results, an alternative method of installation was developed and recommended because of its ability to improve the reliability and accuracy of the outputted data. Also, the calibration curve presented for granular soils produced inconsistent volumetric water contents when compared to oven moisture contents. Figure 2.16 shows the experimental soil, the manufacturers and other researcher relationships of the real component of dielectric permittivity as compared to volumetric water content.

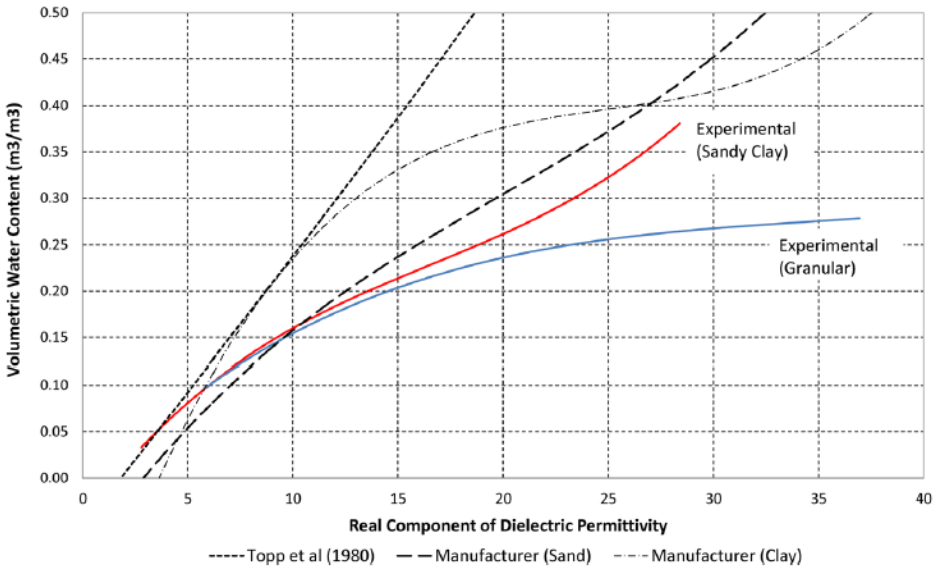

Figure 2.16: Comparison of Material-Specific and Standard Volumetric Moisture-content Relationships (Carteret et al., 2013)

The experimental data presented showed significant differences than that of previous research. Observing this, general recommendations were given to improve data along

with showing that a material specific calibration led to higher accuracy when determining volumetric water content.

2.3.3 Conclusion of Previous Studies

As has been presented, there have been several studies analyzing the reliability and repeatability of the SDG. Adjustment and correction factors were required to make the SDG data better align with the NDG data. Recommendations were given by each study and further research was suggested in order for the SDG to be a viable QC device to replace the NDG.

The Theta Probe and the Hydra Probe have various published studies that evaluated the factors that influence the performance of the devices. Various studies have also evaluated moisture content reliability, measurements of dielectric constants, calibrations and installation methods of the devices. These moisture probes are capable of producing reliable volumetric moisture contents from test to test whether using on-board soil models or developing soil-specific models. To use these moisture probes as acceptable QC assurance devices for roadway compaction, further field testing is going to have to be performed but laboratory research shows that it is possible.

2.3.4 Need for Further Research

Despite the fact that the algorithms to obtain outputted values of wet and dry unit weight and moisture contents are not known for the SDG, what can be inferred is that the calculations are partially based on the material properties inputted into the device. Researchers have recognized this and have presented various calibration equations to minimize the difference that are seen with the SDG when compared to an accepted standard. However, what these calibration equations do not address is to how individual

inputted material properties affect the outputted values. Often times during roadway construction, multiple soil types can be mixed together and then compacted. During this situation, it would be up to the operator to choose which material properties to input into the device. This problem is not seen with the NDG because the material properties of the soil are not required to obtain measures of unit weight and moisture content. Therefore, it is imperative that the influence of the inputted material properties be quantified for the SDG. It is also important to investigate if grouping soils according to USCS or AASHTO soil classification systems will help develop soil-specific adjustment procedures.

The moisture probes have been used in a multitude of ways, but little research has been performed on compacted subgrade soils. One reason is because of the difficulty associated inserting the tines into a compacted soil and the other is due to the variability of soils during construction could lead to inconsistent results. To resolve this, a general calibration methodology needs to be performed on compacted soils.

CHAPTER 3

3 Laboratory Testing and Calibration

3.1 Goals for Laboratory Testing

Before evaluations in the field with the SDG, Hydra Probe and Theta Probe, laboratory testing and calibrations had to be performed. For the SDG, grain sizes and material properties of the soil have to be determined in the laboratory before testing in the field can be performed. For the moisture probes, development of soil-specific calibrations was needed to improve the accuracy of moisture content predictions.

To achieve these calibrations and obtain soil properties, the laboratory goals were to:

- Perform material property tests according to the appropriate ASTM standard so that the material properties could be inputted into the SDG
- Group soils according to the USCS classifications to observe if trends developed during calibrations
- Calibrate the probes for soils compacted in a proctor mold at standard energy. Also, relate the outputted volumetric moisture contents to gravimetric oven moisture contents
- From this calibration process, develop a general moisture content trend line that encompasses soil types similar to the ones in this study.

3.2 Test Soils

Nine soils were evaluated in the laboratory and the material properties were recorded. As seen in Table 3.1 a wide variety of properties were obtained or computed per soil type. The soils were separated into corresponding USCS classifications showing the variety of soils types that consisted of: four low plasticity clays, two low plasticity silts, one highly

plastic clay and two poorly graded sands. The names for each of the soils seen in the soil identity column were given based on the location of the construction sites around Lexington, Kentucky.

Table 3.1: Material properties of the test soils

Soil Identity	USCS Class	PI (%)	LL (%)	D_{10} (mm)	D_{30} (mm)	D_{60} (mm)	% Fines	Clay Fraction (%)	SSA (mm^{-2})	G_s	MDUW (kN/m^3)	OMC (%)
Messer Construction	CL	20	46	-	-	0.009	74.0	40.69	3149381	2.77	15.851	21.3
Band Stoll Field	CL	13	37	-	-	0.007	91.6	39.98	2931048	2.68	16.166	18.8
Wild Cat Den	CL	18	36	-	-	0.020	61.8	39.2	1343419	2.82	15.160	27.3
Jane Lane	CL	19	41	-	-	0.011	80.5	34.48	2013106	2.69	15.828	21.8
Kiddville Rd.	ML	11	36	-	-	0.007	86.6	47.12	5310889	2.74	16.260	20.5
Ramp D Silt	ML	19	48	-	-	0.006	79.5	39.67	3471181	2.81	16.456	20.0
BNE	CH	28	57	-	-	0.002	89.2	57.04	5187865	2.76	15.592	23.8
Ohio Valley River Sand	SP	-	-	0.300	0.490	0.780	6.9	-	191	2.73	18.341	14.0
Kentucky River Sand	SP	-	-	0.120	0.170	0.210	5.6	-	1307	2.69	15.828	17.0

PI= Plasticity Index; LL= Liquid Limit; D_{10}=Grain diameter for which 10% of the sample is finer
D_{30}=Grain diameter for which 30% of the sample is finer; D_{60}=Grain diameter for which 60% of the sample is finer
% Fines= Percentage of material smaller than #200 sieve; Clay Fraction= Material smaller than 0.002 mm;
SSA= Specific surface area; MDUW= Maximum Dry Unit Weight; OMC= Optimum Moisture Content as a percentage

All of the soils, except the two poorly graded sands, were gathered from construction sites and brought back to the lab for testing before field evaluations were performed. This allowed for calibrations and material property testing to be performed on the soil. All of the material properties were obtained in accordance with the appropriate ASTM standard. It is noted that the specific surface area was calculated from the Kozeny-Carman method as seen in Equation 18

$$SSA = \frac{P}{100} * \left(\frac{6}{\sqrt{d_1 * d_2}} \right) * f \qquad \textbf{(18)}$$

where SSA is the specific surface area, P is the proportion of total mass for a selected particle size range, d_1 and d_2 equal the particle size ranges and f is an angularity factor

value that depends on the soil type being tested. Appendix E shows the test results and process for obtaining the material properties for all of the soils.

3.3 Laboratory Testing, Preparation and Procedures

3.3.1 Materials and Soil Preparation

As was mentioned earlier, the test soils were compacted in a standard proctor mold per (ASTM D698) at standard energy. The mold that was used for testing is shown in Figure 3.1.

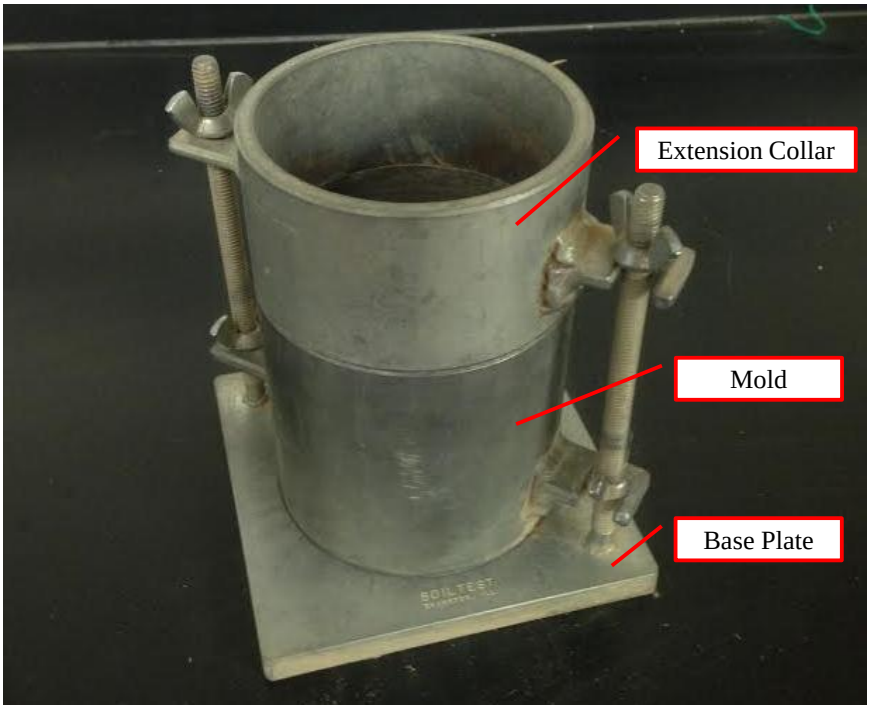

Figure 3.1: Standard Proctor Mold used for calibrating Soils

Both the Theta Probe and Hydra Probe were inserted into the compacted soil to obtain volumetric moisture contents. However before testing, preparation of the soil was the same for each test soil to allow for consistent results from test to test.

The following steps were used for preparing the soil.

- Once the soil was retrieved from either the field site or from the stock pile in the laboratory, it was separated into smaller portions and placed in an oven at 60 degrees Celsius until the sample was completely dry
- After cooling, the soil was separated into particle sizes that could pass the #4 sieve.
- 10 kg of soil was weighed from the material that passed the #4 sieve and separated into four samples weighing 2.5 kg each.
- Water was then added to each of the samples to roughly achieve moisture contents below, near and above OMC.
- The soil samples were allowed to cure for 24 hours after the water was added. The curing process allowed the moisture content to be evenly distributed throughout the soil sample. Curing of the soil was important because uneven moisture content significantly affects the performance of the probes.

3.3.2 Laboratory Calibration Procedures

Following the soil preparation process, calibration in the standard proctor mold took place. Figure 3.2 shows the moisture probes inserted into the compacted soil for the calibration procedures.

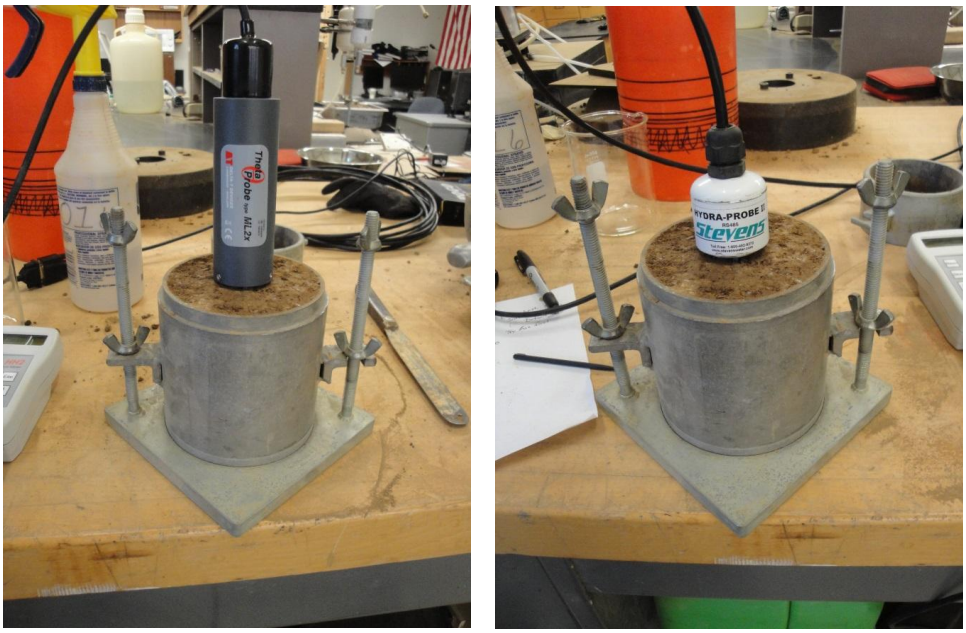

(A) (B)

Figure 3.2: Inserted moisture probes after soil compaction; (A) Theta Probe; (B) Hydra Probe

The procedures that took place for every soil calibration test were as follows:

- After curing, the soil was removed from the container and placed into a pan to be thoroughly mixed.
- The soil was compacted in three lifts, in accordance with ASTM D698
- Following compaction, the extension collar was removed and the soil was then trimmed with a straightedge to be level the soil to the top of the mold.
- The moisture probes were then inserted vertically into the soil. The tines of the probes were fully inserted to where the head of the probe came into contact with the soil.
- Once inserted, tests to obtain the moisture contents for both devices commenced. The on-board Theta Probe Mineral soil model and the on-board Hydra Probe Clay

Model (Note, the Silt Model was used for silty soils and the Sand Model was used for sandy soils) were chosen to retrieve the moisture contents of the soil.

- The probes were then extracted from the compacted soil and the soil was extruded from the mold weighed and placed in the oven for at least 24 hours to obtain oven moisture contents.

For some of the points on the dry side of OMC, difficulty was experienced while inserting the moisture probes into the compacted soil. Although the manufacturers recommend that these devices not be used in compacted soils, there has been research regarding different methods for inserting these probes into compacted soil as seen in (Carteret et al., 2013). For the current study, regular insertion of the tines and a method of using a device to make guide holes for the tines called a jig, were evaluated and little difference was seen in outputted moisture content values. Therefore, the process of using the jig to insert the probes into hard compacted soils became the preferred approach.

3.4 A General Soil Moisture Content Trend Line

3.5 Development of the Trend Line

The outputted volumetric content values for each compacted point were then compared to the oven gravimetric moisture contents. Graphs were developed showing the relationships of the outputted volumetric contents from the moisture probes versus the gravimetric oven moisture contents for each sample. These data are shown in Figure 3.3. Each of the soils were plotted per soil type to show if any trends developed for the test soils.

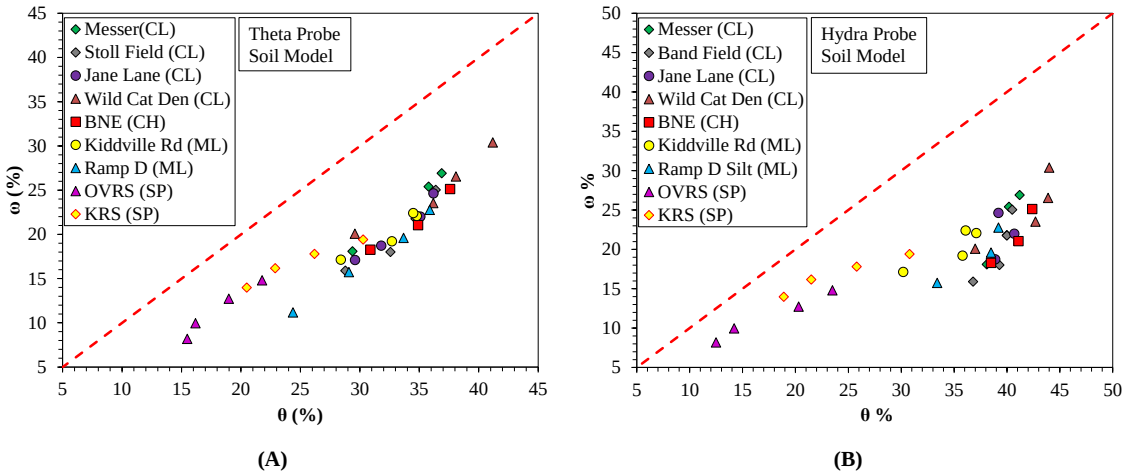

Figure 3.3: Device Volumetric moisture content vs Gravimetric Oven Moisture Content per soil type; (A) Theta Probe; (B) Hydra Probe.

Figure 3.3 shows that although soil types tended to group together the performance of the probes was somewhat independent on soil type. It can be seen in there are some differences in the outputted values per device. This is because each device uses different onboard models to calculate the volumetric moisture content. Each probe operates at different frequencies which affect the measurements of the dielectric properties that are used to infer the moisture contents of the probes (Campbell, 1990). Frequency dependence of the real and imaginary parts of permittivity complicates sensor calibration, and for this reason permittivity calibration remain instrument specific (Kelleners et al., 2005).

Figure 3.3 shows that while the relationships are offset from the dashed line-of-unity, a trend line can be applied to allow for a calibration to be developed. Since the soils followed a similar trend, linear and 2nd order polynomial trend lines were applied to the plotted data as seen in Figure 3.4. The Theta and Hydra Probe data also showed a fairly linear trend constant between all the soil types plotted.

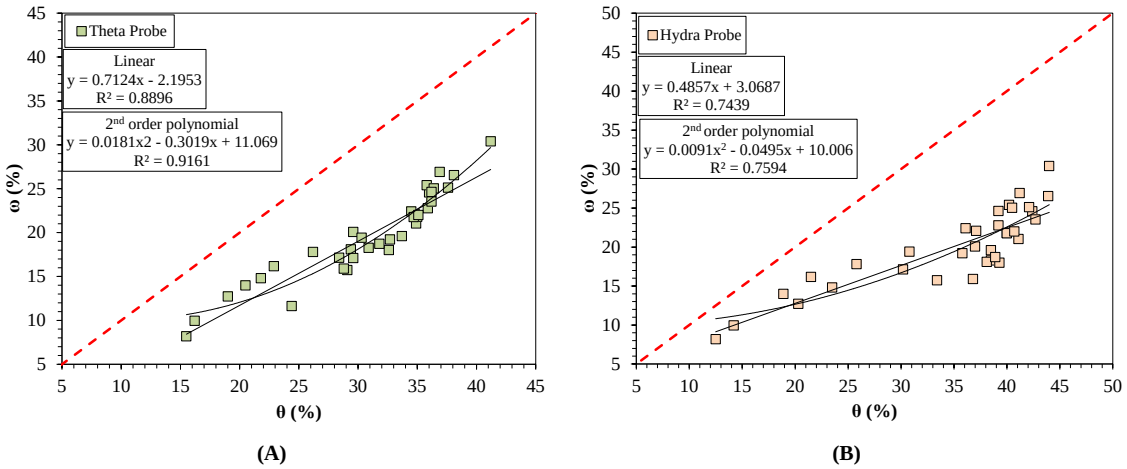

Figure 3.4: General Moisture Content Trend Lines relating Volumetric to Gravimetric Oven moisture Content; (A) Theta Probe; (B) Hydra Probe.

For both the devices, the 2nd order polynomial general moisture trend line resulted in a higher correlation between outputted volumetric moisture content and the gravimetric moisture contents. The Theta Probe data shown in Figure 3.4(A) was able to obtain a linear trend line R^2 value of 0.88 and 0.91 for 2nd order polynomial trend line. The Hydra Probe data did not obtain as high of R^2 values, but was still able to obtain a 0.74 of the linear and 0.76 for the 2nd order polynomial trend line. From these trend lines, equivalent gravimetric moisture content can be obtained from outputted volumetric moisture content from the devices

3.6 Methods for Obtaining Equivalent Gravimetric Moisture Contents

From the developed trend lines, an equivalent gravimetric moisture content can be obtained from the outputted volumetric moisture content using either graphical procedures or analytical procedures.

Figure 3.5 shows an example to how an operator would graphically obtain the equivalent gravimetric moisture content from the outputted volumetric moisture content when using

the Theta Probe. This example shows the use of the linear trend line, but the 2nd order polynomial trend line could be used as well.

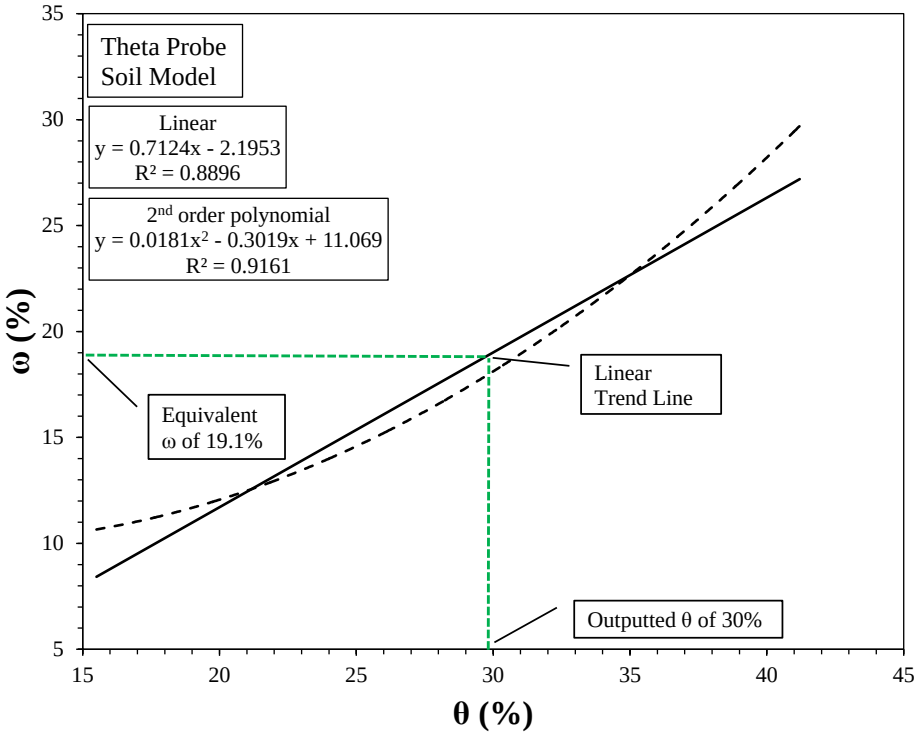

Figure 3.5: Obtain equivalent gravimetric moisture contents graphically

The following steps present how an equivalent gravimetric moisture content can be obtained from and outputted volumetric moisture content graphically

- An outputted volumetric moisture content from the Theta Probe happened to be 30%, as seen on the x-axis.
- After obtaining the value the operator would go vertically towards the linear trend line, signified by the vertical dashed line, until an interception of the linear trend line occurred.
- Once at the linear line, the operator would then go horizontally towards the y axis, following the horizontal dashed line, until reaching the y axis. The operator would

then read the scale and obtain an equivalent gravimetric moisture content, in this case 18.9%.

This method is simple and if the operator had this graph in hand out in the field, equivalent gravimetric moisture content could be obtained quickly. However, if higher accuracy is needed, the equations from the general trends lines should be used. These equations can be seen on the graph in Figure 3.5 for the Theta Probe and are given in general form as

$$\omega_{EQ} = A_1(\theta_p) - B_1 \quad \textbf{(19)}$$

$$\omega_{EQ} = A_2(\theta_P)^2 - B_2(\theta_P) + C_2 \quad \textbf{(20)}$$

Table 3.2: Linear and 2nd order polynomial trend line coefficient values

Probe	Linear		2nd order polynomial		
	A_1	B_1	A_2	B_2	C_2
Theta Probe	0.7124	-2.1953	0.0181	-0.3019	11.069
Hydra Probe	0.4857	3.0687	0.0091	-0.0495	10.006

Equation 12 represents the linear trend line equation and Equation 13 represents the 2nd order polynomial trend line equation. ω_{EQ} is the calculated equivalent gravimetric moisture contents and θ_P is the outputted volumetric moisture content retrieved from the Theta Probe. Table 3.2 shows the coefficient for the linear and 2nd order polynomial trend lines for both probes. As it can be seen Equation 19 is much simpler to use than Equation 20. However, the 2nd order polynomial equation yields a higher R^2 value. So for determining which equation to use, that would be up to the operator.

3.7 Conclusions of Laboratory Testing and Calibration

Comparing volumetric moisture content to gravimetric moisture content is normally not performed because two different quantities are described. Gravimetric moisture content describes the amount of water in a sample in terms of a mass per mass of solids and volumetric moisture contents describes the amount of water in a sample in terms of volume per total unit volume. Studies such as Hu et al. (2010) show volumetric-to-volumetric comparisons or relate dielectric properties to volumetric water content (Campbell, 1990; Lee, 2005; Carteret et al., 2013).

If the Theta Probe and Hydra probe were used in the field to obtain gravimetric moisture contents without the use of the developed general trend line, another device would have to be used along with the moisture probes. The other device would have to obtain measurements of either dry or wet unit weight and with the outputted volumetric moisture content from the moisture probes gravimetric moisture content could be calculated. What the comparison of this current study shows is that these devices can be used in the field to directly obtain gravimetric moisture content through the use of the trend line.

CHAPTER 4

4 Field Evaluation of Devices

4.1 Goals for Field Evaluation

Since the SDG and moisture probes are to be used in the field during construction, a field evaluation was performed for the SDG and moisture probes to observe the reliability of the devices under field conditions. Field testing was performed at active construction sites around Lexington, Kentucky and multiple tests were conducted at each site. The processes of testing the devices are discussed and the outputted values are evaluated based on performance. The outputted data from the moisture probes were related to the trend line previously discussed and the outputted data from the SDG was related to unit weights obtained from sand cone device and oven moisture contents.

Multiple studies (Berney et al., 2011; Rose, 2013; Mejias-Santiago et al., 2013) have observed that the material properties inputted into the SDG could potentially influence the outputted values. To further examine this concern, multiple tests were performed with the SDG that adjusted inputted material properties. Afterwards, an error analysis was performed to assess how the differing inputted material properties affected outputted values.

4.2 Site Preparation and Testing Process

The devices were tested at active construction sites that differed in compaction, moisture content and soil type as seen in Table 4.1. Of the six sites tested, four of the soil types were clay while the other two consisted of silt. The table also represents the material properties that were inputted into the SDG before the testing process begun.

Table 4.1: Soil material properties that are inputted into the SDG

Soil Identity	Soil Index Properties					Grain Size Properties				
	USCS Class	MDUW (kN/m^3)	OMC (%)	PL (%)	LL (%)	C_c	C_u	% Gravel	% Sand	% Fines
Messer Construction	CL	15.83	21.3	26	46	0	0	3.4	22.4	74.0
Jane Lane	CL	15.82	21.8	22	41	0	0	1.4	18.1	80.5
Band Stoll Field	CL	16.11	18.8	24	37	0	0	0.1	8.3	91.6
Wild Cat Den	CL	15.16	27.3	18	36	0	0	26.2	11.4	61.8
Kiddville Rd.	ML	16.26	20.5	25	36	0	0	0.4	13.0	86.6
Ramp D Silt	ML	16.45	20.0	29	48	0	0	0.6	19.9	79.5

MDUW= Maximum dry unit weight; OMC= Optimum moisture content; LL= Liquid limit; PL=Plastic limit
C_c=Coefficient of curvature; C_u= Coefficient of uniformity; % Gravel= Percentage of soil larger than #4 sieve
% Sand= Percentage of soil between #4 and #200 sieve; % Fines= Percentage of soil smaller than #200 sieve

To ensure the tests at each construction site were consistent to one another, a soil testing area was prepared at each site prior to testing with the devices. For each site, the areas were leveled so that the base of the SDG and the heads of the moisture probes, once inserted, would be flush with the soil. To achieve this, a shovel was used to smooth and remove any major obtrusions present on top of the surface and a 0.6 m by 0.6 m by 0.05 m thick plywood board was placed on the smoothed area. The soil was then compacted with a 25 kg weight by lifting the weight to a height of 30 cm and dropping the weight 50 times.

The SDG was typically tested first at each site. The device was placed in the center of the prepared area at the beginning of testing and operated according to the manufactures instructions. Figure 4.1 shows an example of the prepared area where the testing with the SDG took place. Figure 4.1(A) shows the weight, shovel, and plywood board used to prepare the area for testing. It can be observed in the figure that flattened area to the right of plywood board is more compacted compared to the rest of the soil. Not only did the manual compaction achieve higher compaction to the testing area, but it flattened the

testing to allow the devices to rest evenly on the soil as seen with the SDG in Figure 4.1(B).

(A) (B)

Figure 4.1: Test area prepared: (A) Tools used for preparation; (B) SDG during testing.

Figure 4.2 shows examples of the testing that was conducted with both the Theta Probe and Hydra Probe. Figure 4.2(A) shows the Hydra probe during testing on a compacted area at the test site Band Stoll Field test site. Figure 4.2(B) shows both the Theta and Hydra probe at the Kiddville Road roadway construction site. At the Kiddville Road site, the soil was already compact by the contractors so there was no need to compact the soil manually. However, the areas tested were smoothed to remove any obtrusions that may have caused interference with the testing.

(A) (B)

Figure 4.2: Moisture probe testing; (A) Hydra probe; (B) Both Theta and Hydra Probe during testing on a compacted roadway

The Hydra probe was used at every construction site because it was available during the start of the field testing. The Theta Probe was ordered later in the research and was only used at Kiddville Road, Ramp D Silt, and Messer sites. The Hydra Probe had the option using different soil models depending on the soil type being tested. For the Kiddville Road and Ramp D Silt sites the soils were classified as a silt so the Silt Soil Model was used. Likewise, for the Messer, Jane Lane, Band Stoll Field, and Wild Cat Den sites the Clay Soil Model was used because the soils were classified as a clay. While testing with the Theta Probe, the default Mineral Soil Model was used because soils types, according to the manufacturer silt, clay and sand are considered to be mineral. Since the Kiddville Road, Ramp D Silt, and Messer sites were either a silt or clay, the Mineral Soil Model was used. To compare the actual unit weights of the sites soils to the outputted values from the SDG, a sand cone test was performed in accordance with ASTM 1556. Samples of the site soils were also collected to be later used to calculate oven moisture contents.

4.2.1 Performance of the SDG

Figure 4.3 shows the performance values of the outputted SDG compared to sand cone wet unit weights.

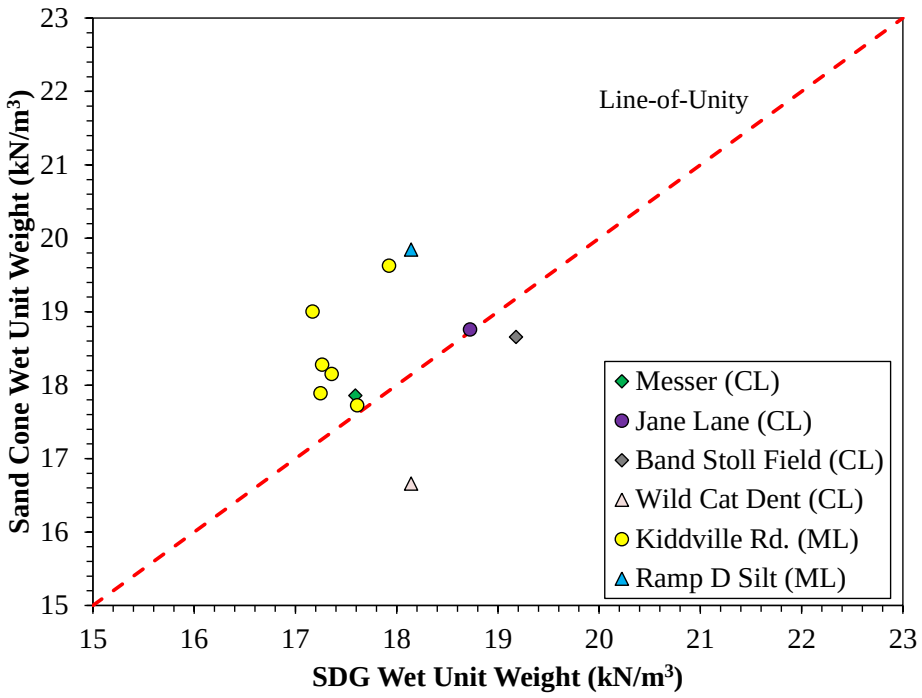

Figure 4.3: Performance of the SDG versus the sand cone

The plotted data is differentiated from each other based on soil type and the site where the testing took place. What Figure 4.3 shows is that the silty soils at Kiddville Road and Ramp D Silt, the SDG under predicted the wet unit weights but data grouped together based on soil type. For the clayey soil sites, data also grouped together according to soil type and the SGD tended to better match to the sand cone wet unit weights more reliably with the exception of Wild Cat Den. A reason for this could have been that Wild Cat Den contained 26.2% gravel which is more than any of the other sites. A further discussion of soils grouping together and idea of material properties affected the outputted data will be shown in the next subsequent sections

A performance evaluation was also performed with the outputted SDG moisture contents and compared to oven moisture contents as seen in Figure 4.4.

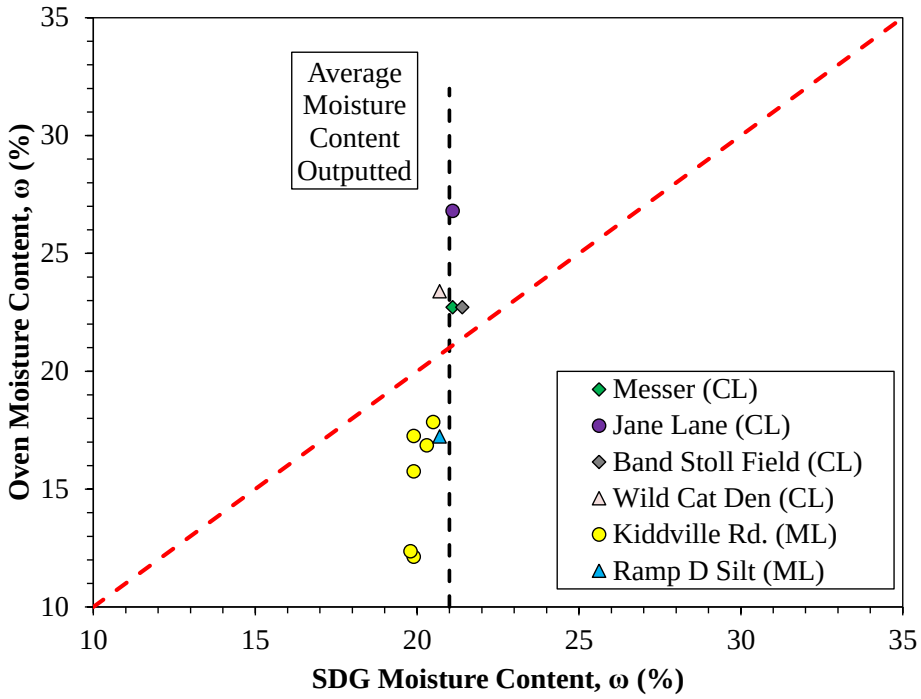

Figure 4.4: SDG moisture content versus oven moisture content

Observing the outputted moisture data from the SDG, a pattern developed showing that no matter the actual oven moisture content the SDG outputted moisture contents around 21%, represented by the vertical dashed line. The actual oven moisture contents ranged from as low as 12% to as high as 31%, but regardless the SDG outputted roughly the same moisture content. The reason for this behavior is not known. However, there are similarities in the material properties inputted into the SDG for these soils. Other studies (Berney et al., 2011; Sotelo et al., 2014) also experienced the SDG outputting moisture contents around 21% and in both studies the soil types were classified as clays.

The internal algorithms that convert the electrical signals to measures of moisture content are based on the inputted material properties (Pluta et al., 2009). Thus, if a particular

algorithm was adversely affected by a particular input parameter, it is quite possible that similar behavior of the device would occur in similar soils.

4.3 Inputted Material Property Values

Not knowing the proprietary algorithms that calculate output values for the SDG is problematic for investigating the factors that affect performance. However, it can be inferred that the outputted SDG values are functions of the soil material properties that are inputted into the device. The degree to which the inputted material properties affect the SDG calculations was investigated by adjusting the inputted material properties and observing changes to the outputted values of wet unit weight and moisture content, relative to the actual reading during the baseline test.

4.3.1 Error Inputted Value Analysis

For the baseline test, the actual material property values were inputted into the SDG and the outputted values of wet unit weight and moisture content were recorded. After the baseline test, adjusted error material property values were then inputted into the device at 10% and 25% error above and below the actual material property value. This percentage of error was arbitrary and it was applied to observe if significant amounts of material property error would affect the outputted SDG readings. Table 4.2 shows the actual values that were inputted into SDG at the site Band Stoll Field along with the error adjusted values.

Table 4.2: Error adjustments made at Band Stoll Field

Material Property	Actual Soil Index Property	Error Adjusted From Actual Value			
		(+)10%	(+)25%	(-)10%	(-)25%
MDUW	16.1	17.7	20.1	14.5	12.1
OMC	18.8	20.6	23.4	16.9	14.1
PL	24.0	26.4	**30.0**	21.6	18.0
LL	37.0	40.7	46.3	33.3	**27.8**
C_c	No Value	No Value	No Value	No Value	No Value
C_u	No Value	No Value	No Value	No Value	No Value
% > 3"	0.0	0.0	0.0	0.0	0.0
% > 3/4"	0.0	0.0	0.0	0.0	0.0
% Gravel	0.1	0.1	0.1	0.1	0.1
% Sand	8.3	9.1	10.3	7.4	6.2
% Fines	91.6	***Above 100%***	***Above 100%***	82.4	68.7

MDUW= Maximum dry unit weight; OMC= Optimum moisture content; C_c= Coefficient of curvature
C_u= Coefficient of uniformity; LL= Liquid limit; PL= Plastic limit; %>3"= % of soil larger than 3"
%>3/4"=% of soil between 3/4" and 3"; % Gravel= % of soil between 3/4" and #4 sieve
% Sand= % of soil between #4 and #200 sieve; % Fines= % of soil smaller than #200 sieve

The influences of the inputted data were evaluated by changing one inputted property at a time, while keeping the other properties constant. A slight deviation to the error analysis approach was required for tests adjusting the grain size distributions, which had to add up to 100% between all the grain sizes. If this did not happen, an error would be displayed on the screen forcing the operator to fix the grain size proportions to add up to 100%. For example, when adjusting the percent fines to -10% of its actual value, 9.2 % was taken from the percent fines and then added to the percent sand. In other cases adjustment were applied and the grain size value became larger than 100%, signified bold italicized letters in Table 4.2. During that case, the test was skipped and another test was performed adjusting another material property.

After obtaining the outputted values of wet unit weight and moisture content, two error tests showed a significant change in output values compared to the baseline test. This

happened for values of 30 for PL and 27.8 for LL, which are underlined and bolded in Table 4.2.

The error inputted PL is significant because when subtracted from the actual LL, a PI of 7 is obtained. Likewise, the error inputted LL is also significant because when the actual PL is subtracted from this LL a PI of 4.8 is retrieved. According to the flow chart for classifying soils, referenced in Section 9 of ASTM D2487, PI values of 4.8 and 7, change the classification of the soil to a silt instead of the original classification of a clay.

Along with the flow chart, the plasticity chart within ASTM D2487 was referenced. The plasticity chart distinguishes between silts and clays using the A-line. Soils that plot above the A-line are considered clay of varying plasticity and soils that plot below the A-line are considered silt of varying plasticity. Figure 4.5 presents the plasticity chart showing the actual plasticity of the soils along with the error plasticity associated with each test.

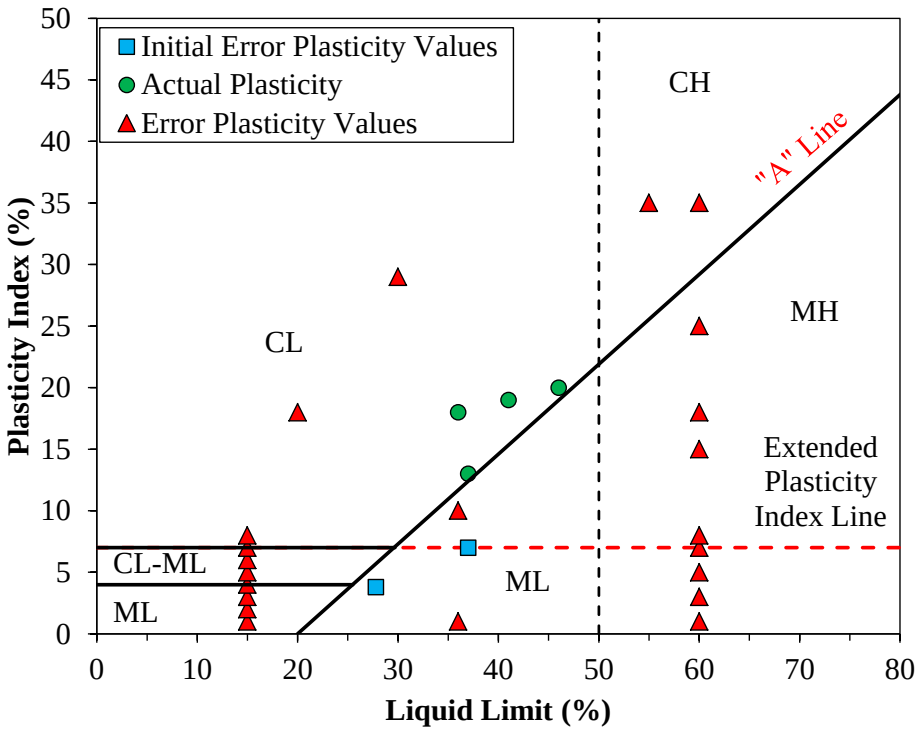

Figure 4.5: Plasticity Chart showing plasticity of soils tested and error plasticity associated with each test.

In Figure 4.5 the circle symbols represent the actual plasticity of the soils tested during the error analysis. According to the plasticity chart the soils were considered lean clays. Along with the actual plasticity, the two square symbols represent where the initial error adjustment values of 30 for PL and 27.8 for LL plotted. Compared to the actual plasticity at Band Stoll Field which classified the soil as a clay, this error adjustment classified the soil as a silt causing the outputted SDG values to be different than that of the baseline test.

To further investigate the significance of the error inputted LL and PL experienced at Band Stoll Field, a follow up evaluation took place at the same site. During this evaluation only the LL and PL were varied, which in turn varied the PI. The PL and LL were adjusted as high of 65% higher than the actual material property and are represented

by the triangle symbols. The vertical dashed line represents the boundary that separates low plasticity soils from high plastic soils, depending on LL. The horizontal dashed line represents the PI value of seven. As explained in the next section, any PI greater than seven had the same output values.

4.3.2 Outputted SDG Values from Error Analysis

Figure 4.6 shows the outputted wet unit weight from the SDG from each of the PI error inputted material property adjustments.

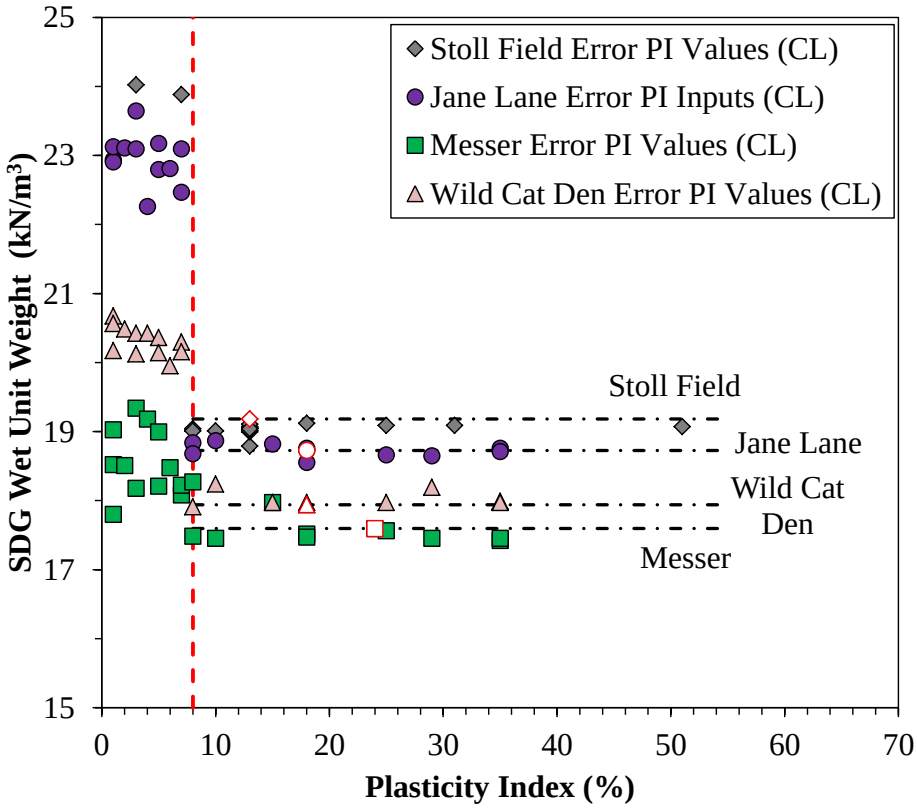

Figure 4.6: Plasticity index versus outputted SDG wet unit weight

When plotting the PI versus the SDG wet unit weight, any combination of the LL and PL to produce a PI of eight and above yielded a constant SDG wet unit weight value unique to that site. However, when the PI was seven and below, the outputted values varied from

where the actual value plotted, signified by the open symbol. The SDG was also able to differentiate between levels of compaction experienced at each site. The vertical dashed line signifies a PI of eight where the significant change in outputted values took place during the error testing. As mentioned before, this PI of eight and above differentiates the soil type as being a clay and not a silt. The implication is the SDG could be using an algorithm to calculate wet unit weight that is partially based on the USCS.

Likewise, the influence of the plasticity index of the outputted moisture content was evaluated as well. Figure 4.7 relates the PI of the error inputted values to SDG outputted moisture contents.

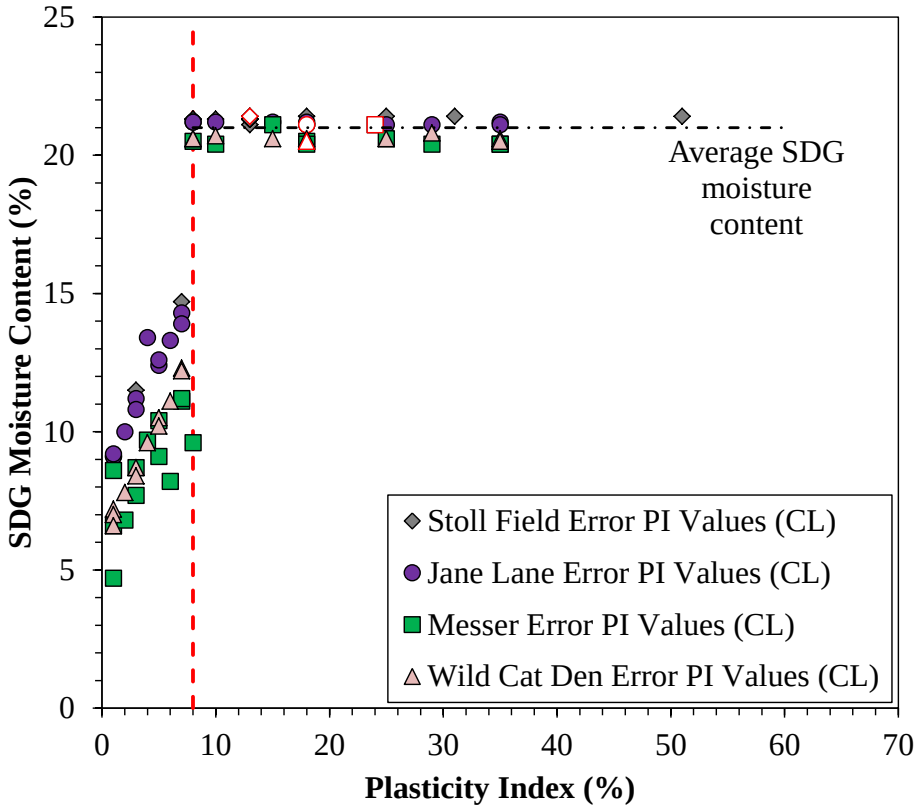

Figure 4.7: Plasticity index versus outputted SGD moisture content

Like the outputted wet unit weights, the vertical dashed line signifies a PI of eight. It is again seen that significant change in outputted values occurs as the soil classification transitions from silt to clay.

The horizontal dashed-dot lines, seen in both Figure 4.6 and Figure 4.7, represent the variance the error outputted values experienced from the actual index values (represented by open symbols). As seen in Figure 4.6, the SDG was able to output different wet unit weights during baseline testing at each site, represented by the open symbols. During the error adjustment tests, when the PI was eight and above, there was little variance from the baseline test. However, when the PI was seven and below the outputted values greatly differentiated from the baseline test value. This was also seen with the outputted values of moisture content. Any error adjusted value with a PI of seven and below, greatly differentiated from the outputted baseline test value. But unlike the outputted wet unit weights, the SDG outputted moisture contents around 21%, regardless of the actual moisture contents as experienced during the field performance evaluation.

4.4 Conclusions of Field Evaluations

The performance evaluation showed that the SDG produced wet unit weights comparable to the sand cone equipment at each site. For the silty soil sites of Kiddville Road and Ramp D Silt, the SDG under predicted the wet unit weights but was able to group the outputted values together. The same was experienced with the clayey soil sites of Jane Lane, Messer, and Band Stoll Field but the SDG achieved better correlations when compared to the sand cone. This is significant because it shows that the SDG could be outputting values based on different classifications of soil type. If so, a calibration could be applied to soil types individually to obtain higher wet unit weight correlations.

When observing the outputted SDG gravimetric moisture content values, a value of 21% was experienced during every test. Unlike the outputted wet unit weights, the SDG was not able to distinguish between soil type and actual gravimetric moisture content. This outputted value of 21% has been experienced with other studies (Berney et al., 2011; Sotelo et al., 2014) for soil types that were similar to the soil types presented in this study.

From the field performance with evaluation of the SDG it can be concluded that that functionality of the device can be greatly improved if calibrations are made based on soil type as seen with outputted wet unit weights during the field performance. However, the SDG moisture contents, based on this field evaluation, were not satisfactory. Constant outputted moisture contents around 21% were seen and this was experienced at every test site regardless of the actual gravimetric moisture content. A reason for this happening could be in relation to the PI of the soils tested which were all eight and above. As shown through the error adjustment testing, when there was a PI of eight and above, a constant moisture content of 21% was experienced.

Constraints were noticed with the error inputted material data seen while adjusting the LL and PL of the soils. Significant deviation from the actual outputted data were noticed when a PI of seven or less. The PI of seven is significant because separates soil types of silts and clays while using the plasticity chart in ASTM D2487. Thus, it appears that the SDG algorithm for calculating wet unit weight and moisture content are based on the USCS.

CHAPTER 5

5 Case Study of SDG Data

5.1 Gathering Data from Case Studies

To investigate if certain classifications have an impact on the outputted SDG values, five case studies were evaluated regarding the outputted SDG unit weights and moisture contents as compared to NDG unit weights and oven moisture contents. At the conclusion of the field performance evaluation, it was observed that the outputted values tended to group together according to similar liquid limits and plasticity indexes. To capitalize on this, the soils were reclassified based on an adjusted USCS. The reasoning was that similar soils would behave in a consistent manner and thus would facilitate soil-specific calibration (ie. the development of trend lines). With a soil-specific calibration the operator of the SDG will be able to take the raw outputted SDG wet unit weights and relate them to a NDG wet unit weights. A procedure of using the moisture probes in conjunction with the that SDG is also introduced that relates the outputted SDG wet unit weights to obtain equivalent NDG dry unit weights through the use of volumetric moisture content specific trend lines.

5.2 Adjusted USCS

The adjusted USCS is partially based on the British Soil Classification System (BSCS) plasticity chat. Implementing the adjusted classification system caused some of the soils from the case studies to be reclassified. However, this reclassification only applied to soils that had some level of plasticity, and silty soils that had no plasticity. For the soils that were considered non-plastic and course grained, the original classification per report was used and the soil was not reclassified under the adjusted USCS. Figure 5.1 shows how the soils were classified based on the plasticity.

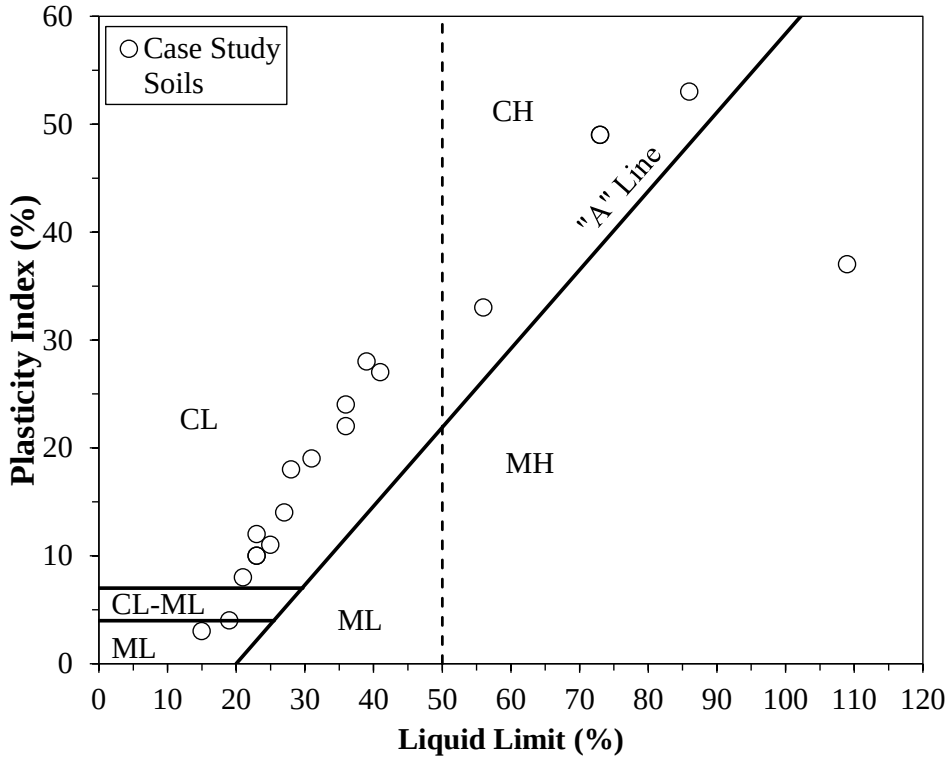

Figure 5.1: Original USCS plasticity chart showing plasticity of case study soils

Figure 5.1 shows the original USCS plasticity chart referenced in ASTM D2487. The degree of plasticity of a soil is designated with an (L) meaning low plasticity or an (H) meaning high plasticity and separated by a LL of 50%. This chart encompasses both silts and clays, and the two are separated by the A-line. Soils that plot above this A-line are classified as clay and soils that plot below are classified as silt.

Figure 5.2 shows the adjusted USCS plasticity chart, which is partially based on the BSCS. The same data were plotted as in Figure 5.1 but groupings of soil types are more specific.

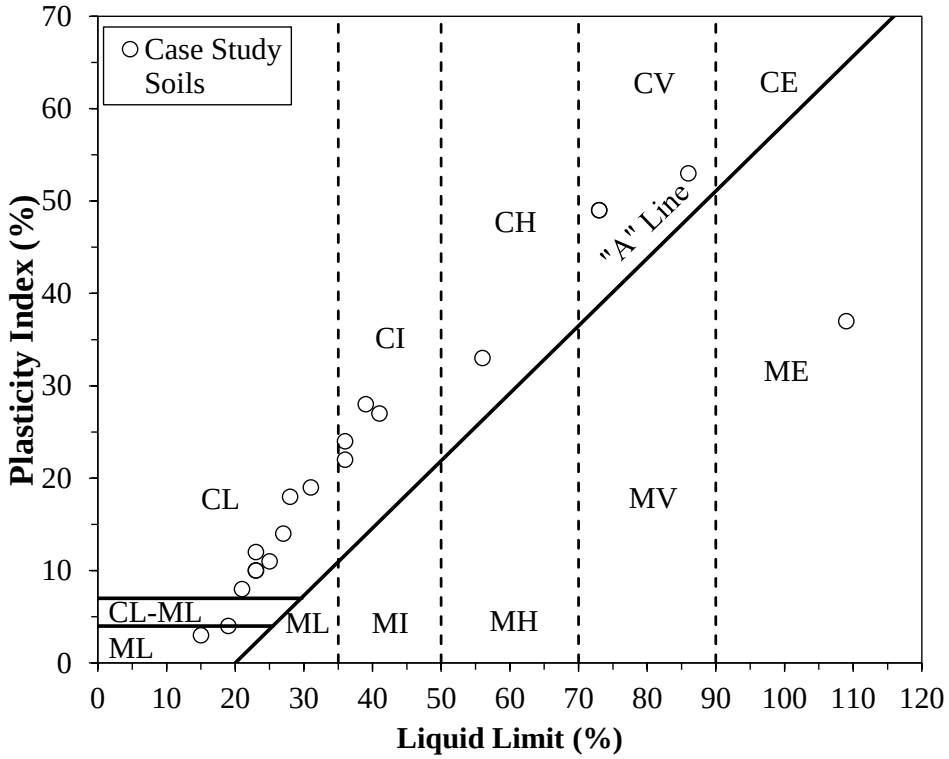

Figure 5.2: Adjusted USCS plasticity chart showing plasticity of case study soils

The plasticity chart designates degree of plasticity as L for low for LL < 35; I for intermediate for 35 ≤ LL ≥ 50; H for high for 50 ≤ LL ≥ 70; V for very high for 70 ≤ LL ≥ 90; and E for extremely high for LL > 90. As with the original USCS plasticity chart, the A-line separates the soil types as clay or silt. For example, a soil with a LL of 40 and PI of 30 would be considered a CL using the original USCS plasticity chart. But when using the adjusted USCS plasticity chart, the soil would now be considered a CI.

5.3 Soil Properties from Case Studies

Roughly, 33 different soils were collected ranging from non-plastic gravels, silts and sand to varying levels of plastic clays and silts. Table 5.1 presents the different soil types, the report the soil data came from (signified by a number of 1 through 5) and the soil ID per report. Next to the soil ID per report, the soils reclassification is given using the adjusted

USCS ID. These soils were tested with the SDG and the material properties inputted into the device are presented. Also, in some cases the same soil is listed twice as seen with soils used in Report 1 and Report 2, this is because the same soil was used in different projects performed by the ERDC.

Table 5.1: Material properties of soils from case studies

Report	Soil ID Per Report	Adjusted (USCS) Soil ID	MDUW (kN/m^3)	OMC (%)	LL (%)	PL (%)	PI (%)	% Fines (%)	% Sand (%)	% Gravel (%)
1	ML	**ML**	17.20	15.8	NP	NP	NP	87.8	11.0	1.2
1	SM	**SM**	19.13	10.0	NP	NP	NP	50.3	47.0	2.7
1	CL-1	**CL**	18.77	12.0	27	13	14	56.9	42.1	1.0
1	CL-3	**CL**	19.89	9.4	21	13	8	55.4	40.5	3.8
1	SC-3	**SCL**	19.28	10.3	28	10	18	49.6	49.7	0.7
1	SC-1	**SCL**	19.21	10.9	31	12	19	40.0	55.0	5.0
1	SC-2	**SCL**	19.29	11.3	25	14	11	32.1	66.0	1.9
1	SP-SC	**SCL**	20.23	8.0	23	13	10	8.0	50.7	41.3
1	CH-3	**CI**	17.06	14.8	36	14	22	64.9	32.4	2.7
1	CL-2	**CI**	18.15	14.2	39	11	28	64.1	34.0	1.9
1	CH-1	**CI**	17.42	16.5	41	14	27	61.8	37.0	1.2
1	SC-4	**SCI**	19.21	11.1	36	12	24	35.1	61.3	3.6
1	CH-2	**CH**	14.50	25.9	56	23	33	82.0	17.6	0.4
1	CH-ERDC	**CV**	13.46	24.6	73	24	49	95.1	4.9	0.0
1	MH	**ME**	8.75	62.0	109	72	37	97.5	2.5	0.0
1	SP	**SP**	17.23	1.9	NP	NP	NP	3.1	92.0	4.9
2	SP-SC	**SCL**	20.23	8.0	23	13	10	8.0	50.7	41.3
2	ML-1	**ML**	17.20	15.8	NP	NP	NP	87.8	11.0	1.2
2	ML-2	**ML**	19.13	10.0	NP	NP	NP	50.3	47.0	2.7
2	SM	**SM**	20.38	7.8	NP	NP	NP	24.9	45.9	29.2
2	SP	**SP**	17.23	1.9	NP	NP	NP	3.1	92.0	4.9
2	GP-GM	**GP-GM**	17.20	15.8	15	12	3	5.3	40.9	52.8
2	CH	**CV**	13.46	24.6	73	24	49	95.1	4.9	0.0
3	A-4/M	**ML**	18.08	9.4	NP	NP	NP	58.5	41.5	0.0
3	A-2-4/SM	**SM**	16.21	15.2	NP	NP	NP	27.0	73.0	0.0
3	A-6/CL	**SCL**	17.62	11.4	23	11	12	45.0	55.0	0.0
3	A-7-6/CH	**CV**	13.89	25.4	86	33	53	97.2	2.8	0.0
4	ML	**ML**	19.64	10.3	NP	NP	NP	64.4	32.7	2.9
4	GP-GM	**GP-GM**	21.57	8.5	NP	NP	NP	10.4	41.4	48.2
4	GW-GM(1)	**GW-GM**	7.63	22.2	NP	NP	NP	10.3	36.1	53.6
4	GW-GM(2)	**GW-SM**	7.63	22.2	NP	NP	NP	9.4	49.8	40.8
4	SW	**SW**	21.24	8.1	NP	NP	NP	7.8	82.1	10.0
4	GW	**GW**	21.47	9.5	NP	NP	NP	5.1	29.9	64.0
5	GCL-ML	**GCL-ML**	21.02	8.0	19	15	4	13.0	23.0	64.0

Report 1- Mejias-Santiago et al. (2013); Report 2- Berney et al. (2012)
Report 3- Sotelo et al. (2014); Report 4 - Pluta et al. (2009) Report 5- Sebesta et al. (2012)

The material properties given in Table 5.1 were taken directly from the referenced report. Some of the material properties that are required to be inputted into SDG are not listed in this table and are as follows; coefficient of uniformity, coefficient of curvature, the amount of material in between ¾" and 3" and the amount of material greater than 3". Zeroes were assumed for the amount of material in between ¾" and 3" and the amount of material greater than 3". The justification for this assumption is the amount for each grain size listed in Table 5.1 (% fines, % sand and % gravel) when combined add to 100%, which is the maximum amount. The coefficient of uniformity and coefficient of curvature are not listed because these parameters appeared to have very little influence on the performance of the SDG in coarse grain soils.

As seen in Table 5.1, the soils are listed according to the adjusted USCS plasticity chart and given a new plasticity designation of L,I,H,V or E. Also some of the soils were originally classified as (ML), meaning a low plasticity silt, but as reported the soil had no plasticity. In this case, the classification was kept the same even though the soils were non-plastic. The original classifications were also kept the same for soils that were not plastic and course grained.

5.4 Outputted SDG Values based of the Adjusted USCS

The case study soils has were reclassified to the adjusted USCS and the outputted moisture contents and wet unit weights from the SDG were compared to oven moisture contents and NDG wet unit weights, respectively. Graphs were developed and the plotted data were grouped based on the adjusted USCS given to each soil type. Once grouped, the soils were analyzed per adjusted USCS grouping to develop soil-specific calibrations for both the outputted moisture content and wet unit weights.

5.4.1 Outputted Moisture Content

The outputted gravimetric moisture contents from the case studies were related to oven gravimetric moisture contents. 755 data points were collected and plotted as shown in Figure 5.2. Each of the data points are color coated based on the soil type and described as either having zero plasticity or some level of plasticity based on the liquid limit. The red dashed line represents the 1:1 relationship between the outputted SDG moisture content and oven moisture content and the vertical dashed black lines signify trends that were seen with the outputted moisture contents from the case studies.

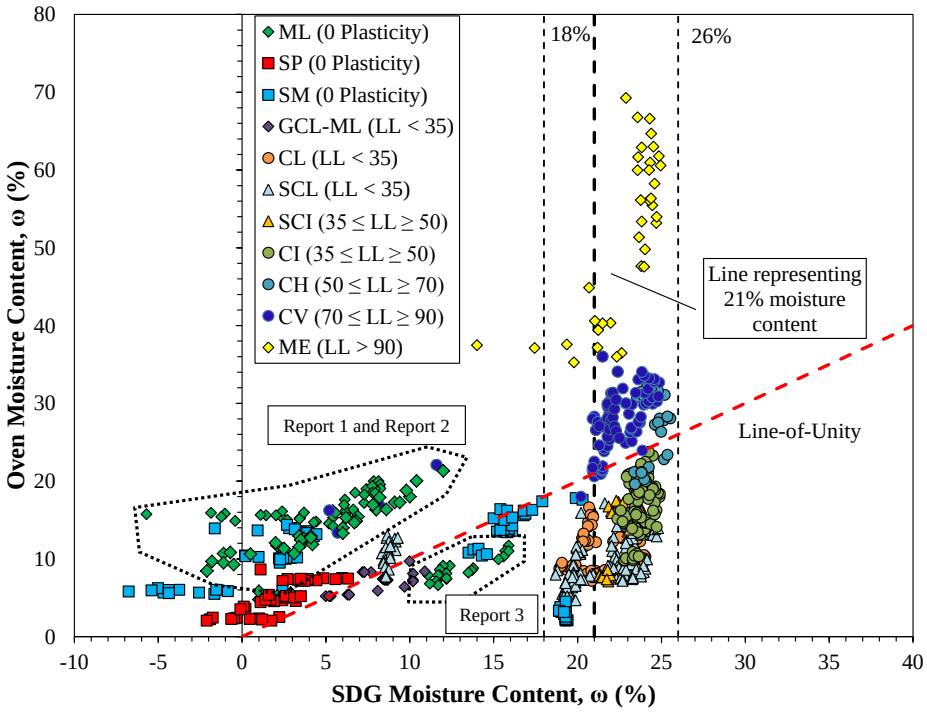

Figure 5.3: Graph of outputted SDG gravimetric moisture content versus oven moisture content

The soils were plotted per adjusted USCS soil type. As seen in Figure 5.3, performance appeared to group according to soil types ML, SP and SM. Two groupings of soil type (ML) appeared where in one case the SDG under-predicted the moisture contents,

signified by the enclosed dotted line labeled Report 1 and Report 2, and in another case over-predicted, also signified by the enclosed dotted line but labeled Report 3. Although Reports 1 and 2 were different studies, the soil still grouped together based on the adjusted USCS. Report 3 did not follow the same trend but in all three studies, the individual groupings were parallel to the line-of-unity. This was also seen with the soil types SP and SM where some groupings were parallel with the line-of-unity and in some cases accurately obtained moisture contents. For an individual grouping of soils to be parallel to the line-of-unity is significant because an adjustment, offset or some type of calibration could be applied to the outputted data from the SDG, to obtain reliable moisture contents. The SDG also outputted negative gravimetric moisture contents for the soil types of M, SP and SM. The reason for this is not known but it appears to only occur when testing with granular or non-plastic soil types.

Along with the non-plastic soil types, the soils having some level of plasticity, were plotted as well. One trend did develop in that majority of the outputted moisture contents from the plastic soils plotted in between 18% and 26% moisture, while the actual moisture contents ranged from around 5% to 75%. This average line of 21% follows the trend from the case studies and shows that the SDG could possibly be differentiating outputted moisture contents based on soil types. The plastic soils encompass a wide range of plasticity's but regardless; the SDG still had difficulty obtaining correct moisture contents. The plastic soil types of GCL-ML and a SCL grouping did not follow the trend experienced with the other plastic soils. The SCL grouping was able to reliably obtain moisture contents, per that grouping, and the GC-ML soil type followed a non-plastic soil type trend where the plotted data were parallel to the line-of-unity.

As stated, the non-plastic soil types could be possibly calibrated to obtain equivalent oven moisture contents but for the plastic soils it may be hard to achieve accuracy once calibrated. For all of the outputted values, plotted within the moisture boundaries, only varied 8% regardless of the actual moisture content. However, the moisture contents of the soil types in Figure 5.3 are typical for coarse and fine grained soils around OMC. It could be that the coarse grained soils have a max moisture content of 18% and the fine grain soils, when compacted, have OMC in between 18% and 26%. To make a conclusive assessment of if grouping soils according to the adjusted USCS improves the performance of the device in regards to outputted gravimetric moisture contents, more data and research is needed.

5.4.2 Outputted Wet Unit Weight

The SDG wet unit weights were plotted against the NDG wet unit weights and soil-specific trend lines were developed based on the grouping of the soil types. These soil-specific trend lines allowed for an equivalent NDG wet unit weight to be obtained from outputted SDG wet unit weights. It should also be noted that out of the five case studies presented evaluated, only three reports had data relating to wet unit weights. The three reports included Pluta et al. (2009); Sebesta et al. (2012); Mejias-Santiago et al. (2013)

5.5 Development of Soil-specific Trend Lines

Figure 5.4 shows the SDG wet unit weight as compared to the NDG wet unit weight for non-plastic soils.

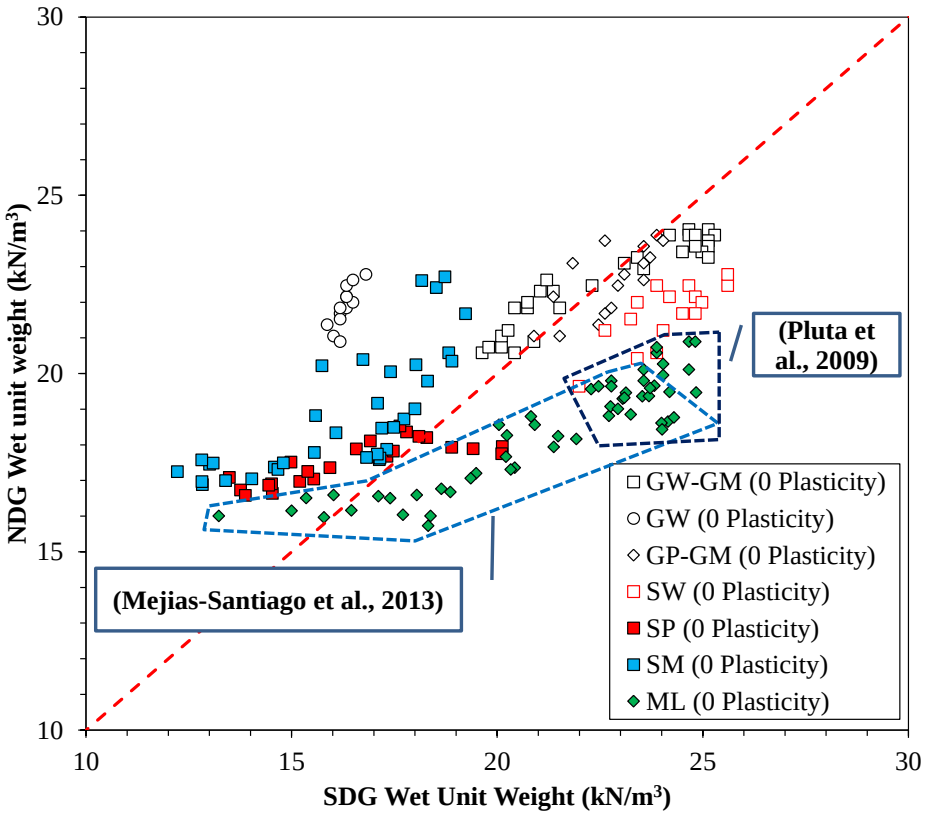

Figure 5.4: SDG wet unit wet versus NDG wet unit weight for non-plastic soils

As it can be seen, certain trends develop depending on the adjusted USCS. In Figure 5.4, each of the soils plotted developed trends that were distinguishable from each other. However, it could be said that the soil trends developed were only unique to the site at which the testing took place. To show that is not the case, the soil type (ML) is referenced because the data for this soil type came from both Pluta et al. (2009) and Mejias-Santiago et al. (2013) case studies. Where the data plotted is shown by the enclosed dashed lines. When plotted, the data followed the same soil specific trend and was not specific to a certain site. For the other soil types seen in Figure 5.4 a possible reasoning for differentiating trends could be the material that makes up each soil types such as the amount of gravel, and sand that would be inputted into the SDG.

Trends were also experienced in Figure 5.5 when the soil was separated based on the plasticity's. Depending on of the level of plasticity from low to extreme, each soil group trended together based on that qualification. The lower plasticity soils tended to plot more towards the line of unity and for the higher plasticity soils the SDG tended to over predict the actual wet unit weights.

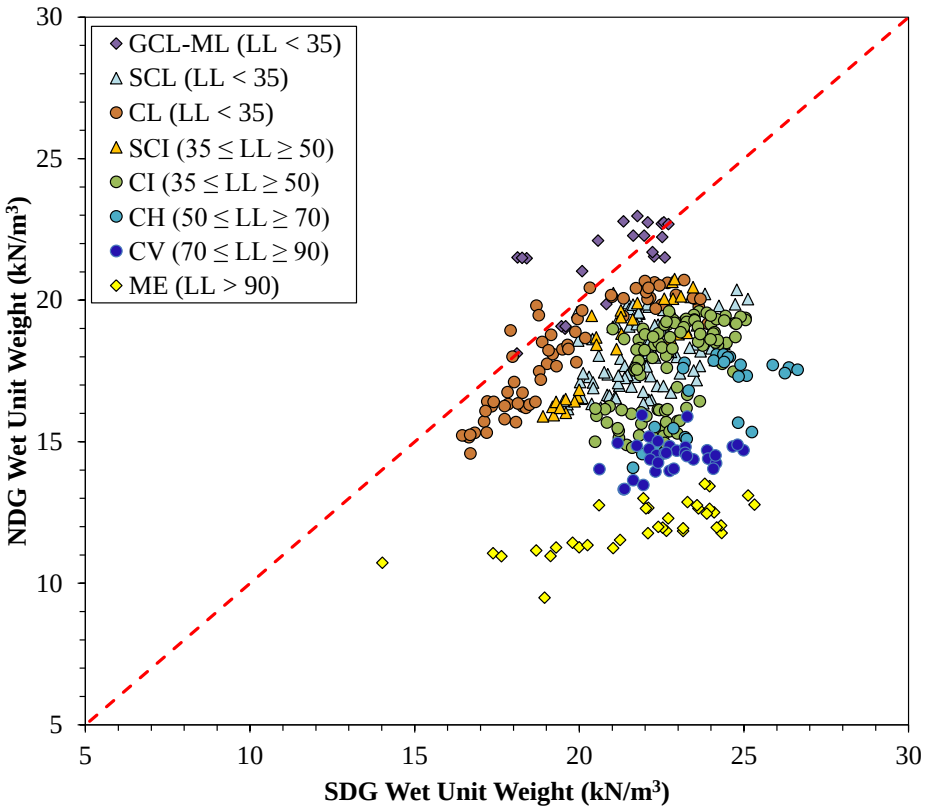

Figure 5.5: SDG wet unit wet versus NDG wet unit weight for plastic soils

From these trends, lines were fitted through the data based on the classification given to that soil type. As seen in Figure 5.6, lines were fitted through the non-plastic soils individually.

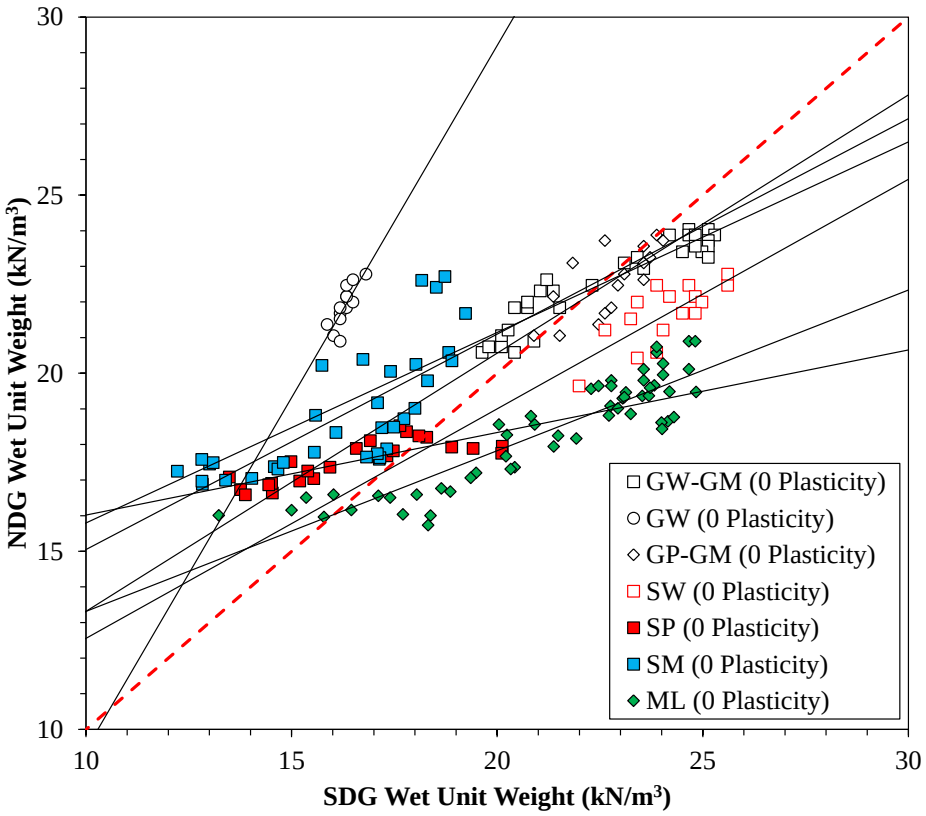

Figure 5.6: SDG wet unit weight versus NDG wet unit weight trend lines for each non-plastic soil type

However, the trend lines create confusion because many of them are overlapping. To simplify the non-plastic soil specific trend lines, soil types were combined based on similarities of the soils material properties and trend line slopes. The first combination of soil types was applied to the soils SM, GP-GM and GW-GM. The slopes of the soils were similar and each had some percentage of silt. Other soil types that were combined were the SP and SW soils and differentiate by one soil is poorly graded and the other is well graded.

After developing the combination trend lines, a new graph was constructed as seen in Figure 5.7. By combining the soil types, with the exception of the GW soil, the trend line no longer overlapped and as it can be seen there are clear distinctions between each line.

One possibility for this distinction could be that the material properties inputted into the SDG affected the SDG calculations in interpreting wet unit weights. As seen with the (GW), the data plotted by itself and the trend line was not similar to the others. This soil type also had the highest percentage of gravel compared to the other soils. It could be possible that this large amount of gravel, when in putted into the SDG, had an effect on the calculations for the wet unit weight.

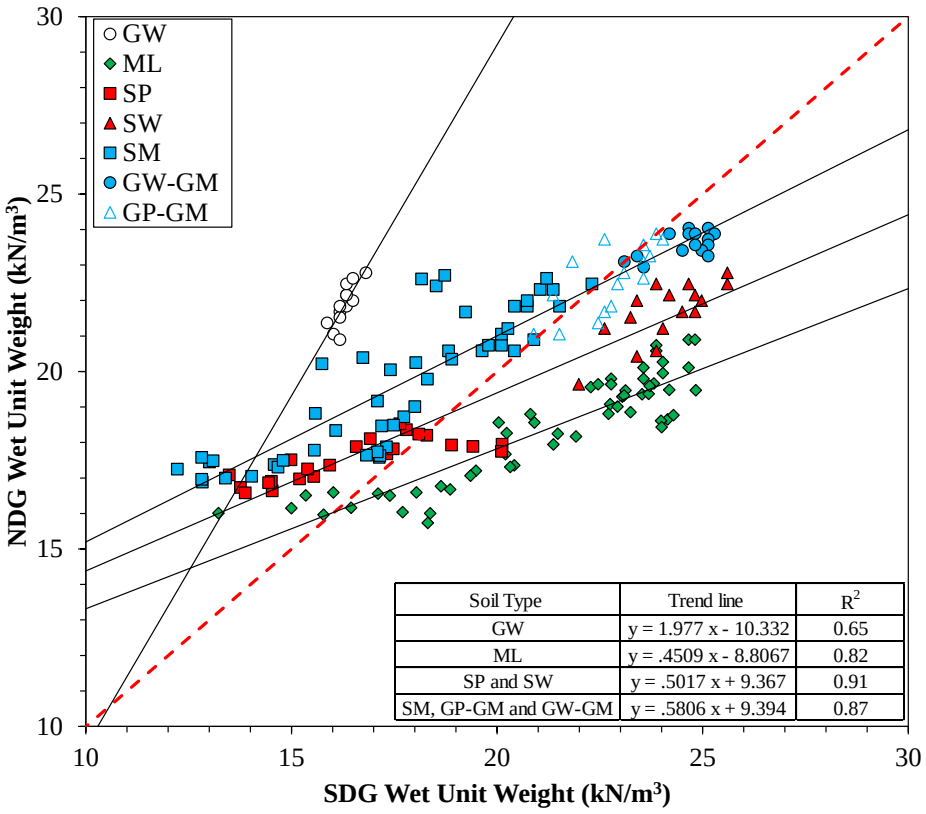

Figure 5.7: SDG wet unit weight versus NDG wet unit weight trend lines for combined non-plastic soil types

Also within Figure 5.7 are the trend line equations and R^2 values for each of the developed trend lines. The strongest R^2 was seen with the SP and SW combined soil types which had a value of 0.91. For the other soil types, R^2 were also high, each having R^2 values of 0.65 or above.

Like the non-plastic soils, trend lines were added to the plastic soils as well. Figure 5.8 shows these trend lines based on the adjusted USCS soil types. Also to stay consistent with the plasticity designations from the adjusted USCS, soil types were not combined based on slope similarities.

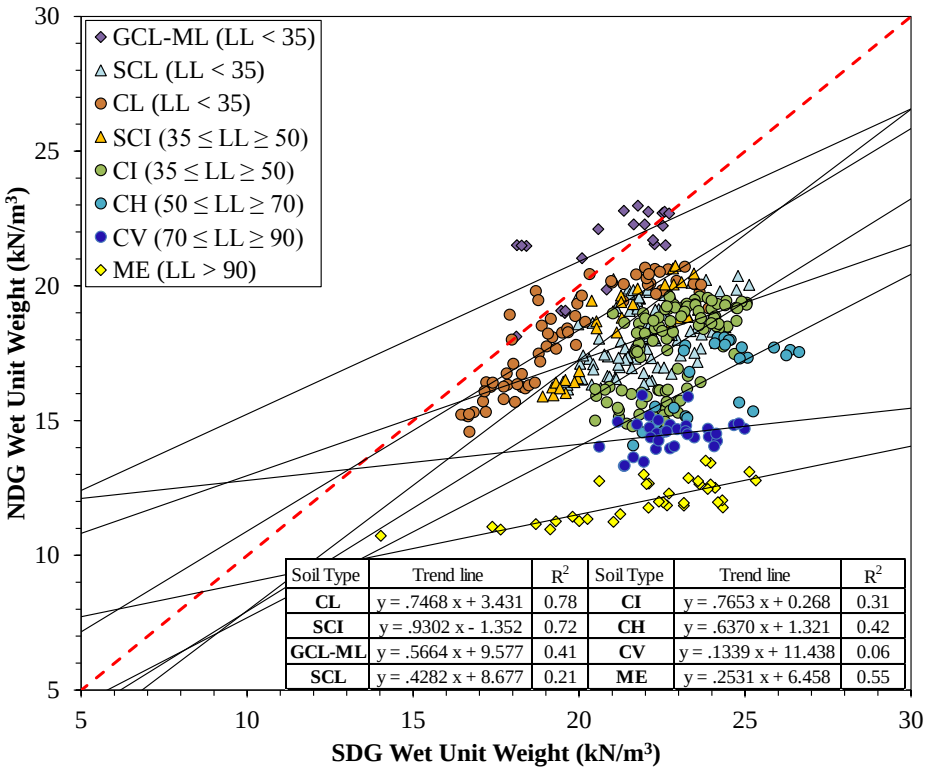

Soil Type	Trend line	R^2	Soil Type	Trend line	R^2
CL	y = .7468 x + 3.431	0.78	**CI**	y = .7653 x + 0.268	0.31
SCI	y = .9302 x - 1.352	0.72	**CH**	y = .6370 x + 1.321	0.42
GCL-ML	y = .5664 x + 9.577	0.41	**CV**	y = .1339 x + 11.438	0.06
SCL	y = .4282 x + 8.677	0.21	**ME**	y = .2531 x + 6.458	0.55

Figure 5.8: SDG wet unit weight versus NDG wet unit weight trend lines for plastic soil types

Also shown are the equations and R^2 values for each of the soil-specific trend lines. For soil types that had lower plasticity, the R^2 values tended to have a better correlation than that out of the higher plasticity soils. This was seen with the CV soil type that only had an R^2 value of 0.06. For soil types such as the CL and SCI, the correlations are much higher and experienced R^2 values as high as 0.78.

5.5.1 Obtaining Equivalent NDG Wet Unit Weights

The developed soil-specific trend lines, when all plotted together, could potentially cause confusion in choosing which soil specific trend line to use. To alleviate this concern, the 12 plastic and non-plastic soil specific trend lines were separated into four graphs based on similarities in slopes. Initial efforts to separate the trend lines into graphs based on their soil type such as CL, SCL and GML were unsuccessful. However, no matter the combination of the soil type, the slopes of the trend lines differentiated from each other too much. So it was decided that the trend lines should be separated based on their slopes as it can see in Figure 5.9.

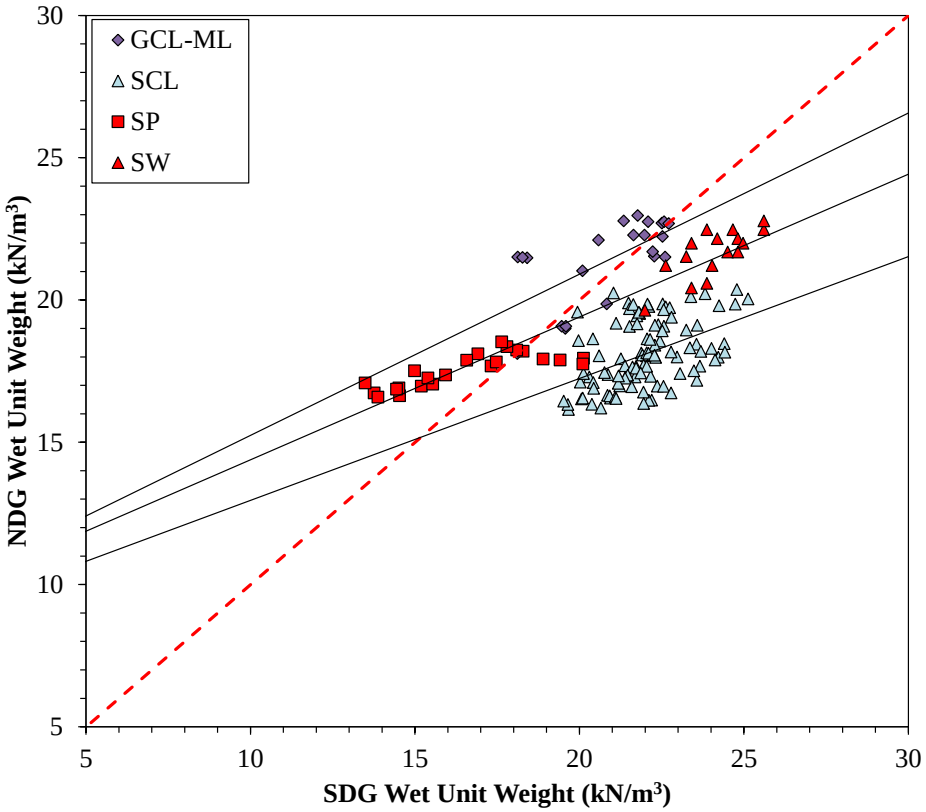

Figure 5.9: Soil-specific trend lines of GCL-ML, SCL, SP and SW soil types before removal of data

Figure 5.9 presents developed trends as fitted to the adjusted USCS soil type data. Each of the trend lines have similar slopes and are distinguishable from each other. After removal of the data, as seen in Figure 5.10, the trend lines were then labeled with the soil type that is specific its developed trend line. This process of separating the soils into graphs based on similar trend line slopes was done for every soil type and the remaining three graphs are presented in Appendix C.

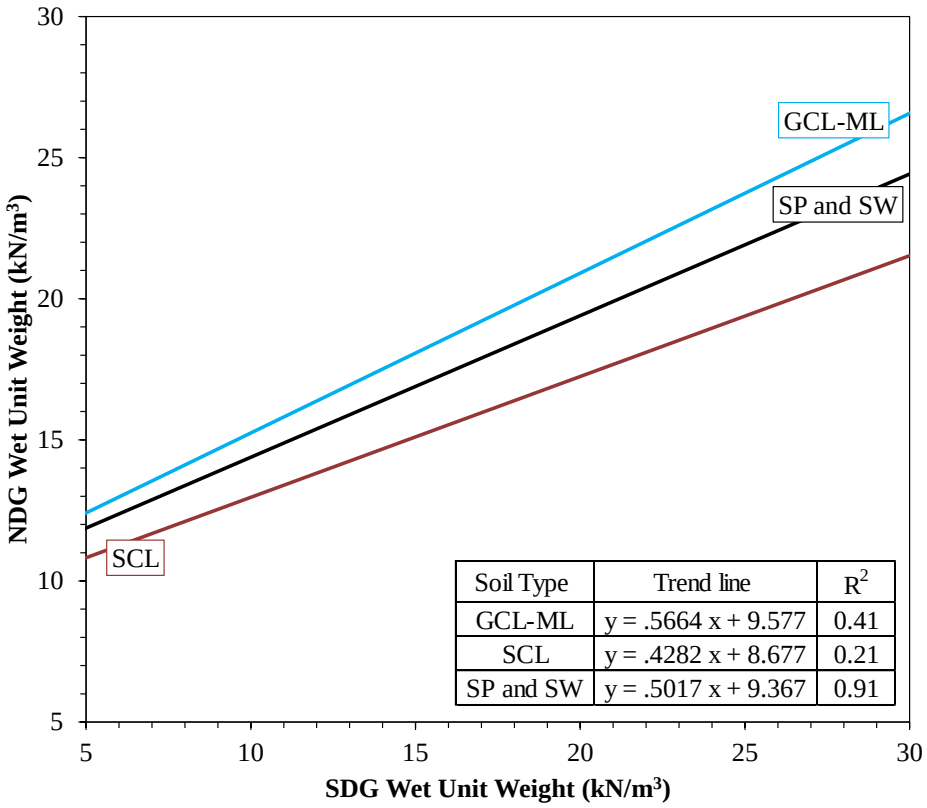

Figure 5.10: Soil-specific trend lines of GCL-ML, SCL, SP and SW soil types after removal of data

Figure 5.10 represents what would be used in the field while performing tests with the SDG. The operator would first know what soil type is going to be tested, then find the trend line that is specific for that soil type. After obtaining the outputted SDG wet unit weight, an equivalent NDG wet unit weight could then be obtained. This method does

not require a lengthy equation and it accounts each of the soils observed on an individual bases. To visually show this process of obtaining equivalent NDG wet unit weight, Figure 5.11 gives a step-by-step procedure of how to obtain NDG wet unit weight from the outputted SDG wet unit weight by the use of a graph.

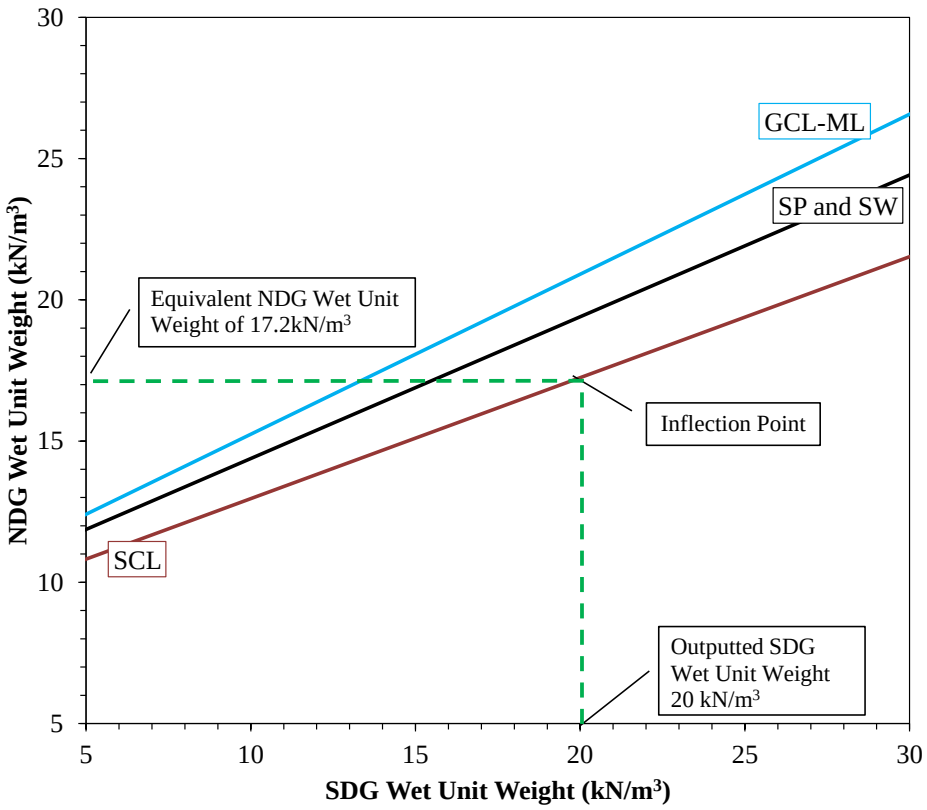

Figure 5.11: Example of obtaining equivalent NDG wet unit weights from outputted SDG values

The following steps show how the operator of the SDG would obtain an equivalent SDG wet unit weight by the use of the graph shown in Figure 5.11.

- Before field testing, the soil was confirmed to be a SCL in the laboratory through material testing and classified per the adjusted USCS
- Input the material properties into the SDG and perform a test to obtain a wet unit weight.

- After obtaining a SDG wet unit weight the value would be found on x-axis of graph. As an example the SDG outputted a wet unit weight of 20 kN/m^3, as seen in Figure 5.11.
- The operator would then go vertical and intersect the trend line corresponding to SCL.
- The operator would then go horizontally towards the y-axis, to obtain an equivalent NDG wet unit weight, which in this case, is roughly 17.2 kN/m^3.

This method shown above can be used for every soil specific trend line developed in this research for obtaining an equivalent NDG wet unit weight. However, there many variations in soils types that are not mentioned in this research. If this is the case, a new soil-specific trend line should be developed.

5.5.2 Reliability of Soil-specific Trend Lines

Because of the amount of data, a statistical analysis was performed to show the confidence and reliability of the developed soil-specific trend lines. Figure 5.12 shows graphical representations of 95% confidence intervals developed from the data collected and standard deviations of the data per trend line. Four of the 12 confidence interval graphs are shown and the remaining eight confidence interval graphs can be seen in Appendix C.

Within these graphs, the solid line represents the soil specific trend line applied to the data. Parallel to the black lines are two dashed lines that show the 95% confidence intervals that are above and below the soil specific trend line. So the closer the dashed lines are to the soil specific trend lines, the higher the confidence that later data will be plotted within one standard deviation shown on the graphs.

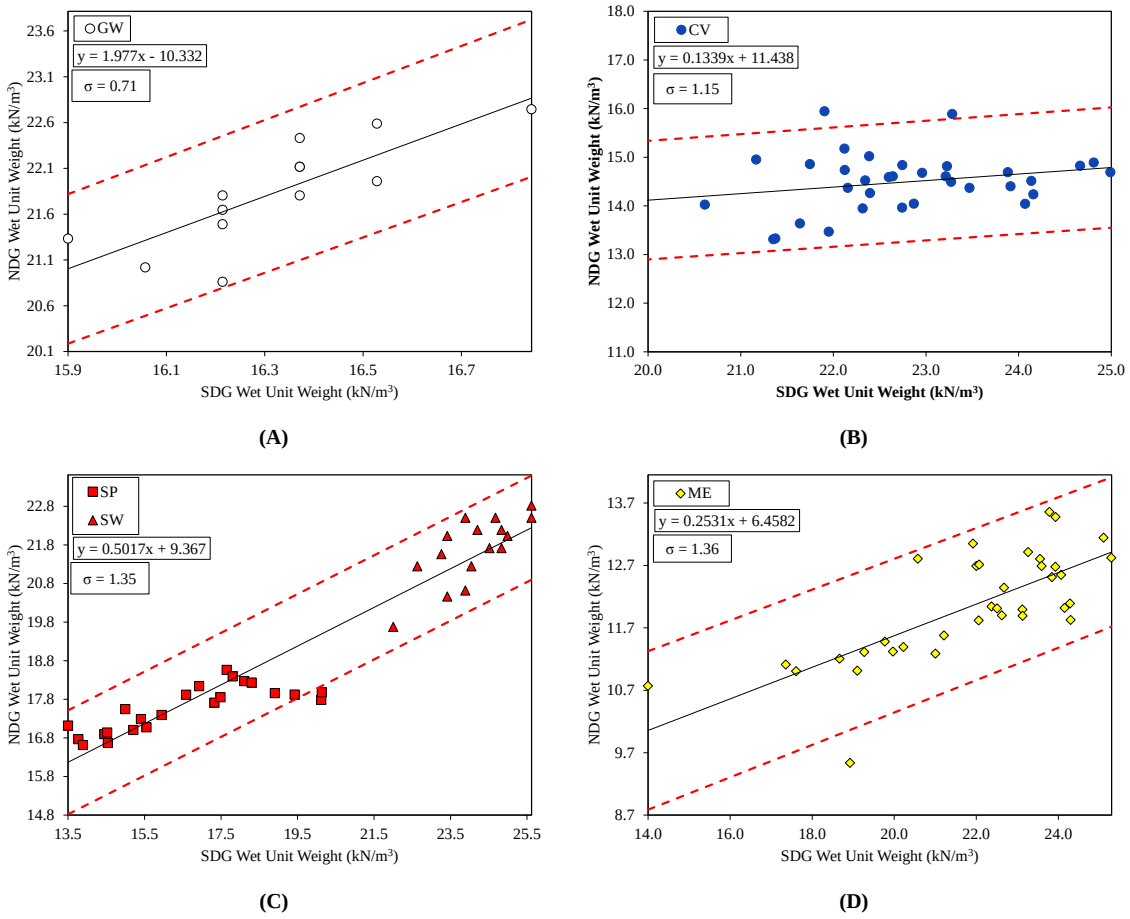

Figure 5.12: Confidence intervals and standard deviation of soil trend lines: (A) GW; (B) CV; (C) SP and SW; (D) ME

These four graphs show the soil types with the least amount of standard deviation and the tightest 95 % confidence intervals. Figure 5.12(A) shows the soil type of the well graded gravel GW, Figure 5.12(B) shows the soil type of a very plastic clay CV, Figure 5.12(C) shows the soil types of poorly and well graded sand SP and SW and Figure 5.12(D) shows the extremely plastic silt ME. Some of the data plotted outside of the 95% confidence intervals as seen in Figure 5.12(B,C and D). These lines represent where 95% of the data plotted, not all 100% of the data. Of the four graphs, the lowest standard deviation was seen in the well graded gravel GW as seen in Figure 5.12(A).

5.6 Development of Moisture Specific Trend Lines

Up to this point, it has been shown that gravimetric moisture contents can be obtained from volumetric moisture contents outputted by the moisture probes. This was done by developing general moisture content trend lines during the laboratory calibration procedures. What has also been shown is that through the use of soil-specific trend lines, the SDG can obtain equivalent NDG wet unit weights. As has been presented previously, the wet unit weights outputted by the SDG are comparable to the wet unit weights obtained by the NDG and sand cone devices.

However, the outputted SDG gravimetric moisture content and dry unit weight are both calculated values that are obtained from measurements of volumetric moisture contents and wet unit weights. So when irregularities are observed in outputted values of dry unit weight and gravimetric moisture content, it is most likely because of errors in determining the measured volumetric moisture content. Therefore, the most viable option for developing a reliable method for obtaining dry unit weight and gravimetric moisture content is by using the moisture probes and SDG together.

5.6.1 Obtaining Equivalent NDG Dry Unit Weights

An equivalent NDG dry unit weight can be obtained through the use of Equation 21

$$(\gamma_{dry})_{NDG} = \frac{(\gamma_{wet})_{NDG}}{1 + \frac{\omega_{oven}}{100}} \quad \textbf{(21)}$$

where $(\gamma_{dry})_{NDG}$ is the calculated NDG equivalent dry unit weight. $(\gamma_{wet})_{NDG}$ is the equivalent NDG wet unit weight found using the SDG outputted wet unit weight and soil specific trend lines and ω_{oven} is the equivalent gravimetric moisture content obtained using the general moisture content trend line calculations. In order to obtain this NDG

dry unit weight, the SDG and one of the moisture probes have to be used in tandem. Upon obtaining outputted values during testing, the equivalent NDG wet unit weight and gravimetric oven moisture content are inputted into the equation.

A graphical method for using the SDG and the moisture probes in tandem was also developed. As seen in Equation 21, the equation contains the variables $(\gamma_{wet})_{NDG}$ and ω_{oven} and both of which can be calculated through the use with a linear equation. The linear equation used to obtain a $(\gamma_{wet})_{NDG}$ can be seen in Equation 22

$$(\gamma_{wet})_{NDG} = m_1(\gamma_{wet})_{SDG} + b_1 \quad \textbf{(22)}$$

and the linear equation used to find ω_{oven} can be seen in Equation 23

$$\omega_{oven} = m_2(\theta)_{probe} + b_2 \quad \textbf{(23)}$$

to then be used together to form the expanded form of Equation 21 to retrieve Equation 24

$$(\gamma_{dry})_{NDG} = \frac{(m_1(\gamma_{wet})_{SDG} + b_1)}{1 + \frac{(m_2(\theta)_{probe} + b_2)}{100}} \quad \textbf{(24)}$$

where the variable m_1, m_2, b_1, and b_2 are coefficients that are unique to each linear line as seen in Table 5.2 and $(\gamma_{wet})_{SDG}$ and $(\theta)_{probe}$ are the outputted values that are obtained from the SDG and moisture probes during testing.

Table 5.2: Soil-specific and general moisture content trend line coefficients

Soil-Specific Trend Line Identification	Trend Line Coefficients		General Moisture Content Trend Line Identification	Trend Line Coefficients	
	m_1	b_1		m_2	b_2
CH	0.6370	1.321	Theta Probe	0.7124	-2.1953
CI	0.7653	0.268	Hydra Probe	0.4857	3.0687
CL	0.7468	3.431	Left Blank Intentionally		
CV	0.1339	11.438			
GCL-ML	0.5664	9.577			
GW	1.9770	-10.332			
ML	0.4509	8.806			
ME	0.2531	6.458			
SCI	0.9302	-1.352			
SCL	0.4282	8.677			
SM, GP-GM, GW-GM	0.5806	9.394			
SP and SW	0.5017	9.367			

An example is presented for using these equations to obtain a NDG dry unit weight using the SDG and Theta probe. For a soil that has been classified as a CH using the adjusted USCS, the operator would choose coefficients values for m_1 (0.637) and b_1 (1.321) coefficient values for m_2 (0.7124) and b_2 (-2.1953). Tests would then be performed with each of the devices to retrieve $(\gamma_{wet})_{SDG}$ and $(\theta)_{probe}$ values. These values would be input into Equation 19 to obtain an equivalent NDG dry unit weight.

This process can also be performed graphically. By using Equation 24, a graph can be developed that relates a SDG wet unit weight to a NDG dry unit weight. This is achieved by holding the outputted volumetric moisture content $(\theta)_{probe}$ constant while changing the SDG wet unit weight $(\gamma_{wet})_{SDG}$. A line is then produced that is linear and unique to the current volumetric moisture content. These moisture specific lines are also unique to each different soil type. Figure 5.13 shows the graph that can be used to obtain a NDG dry unit weight from a SDG wet unit weight by the use of a moisture specific trend line. This graph gives an example of the developed moisture specific trend lines that are for the soil type GML.

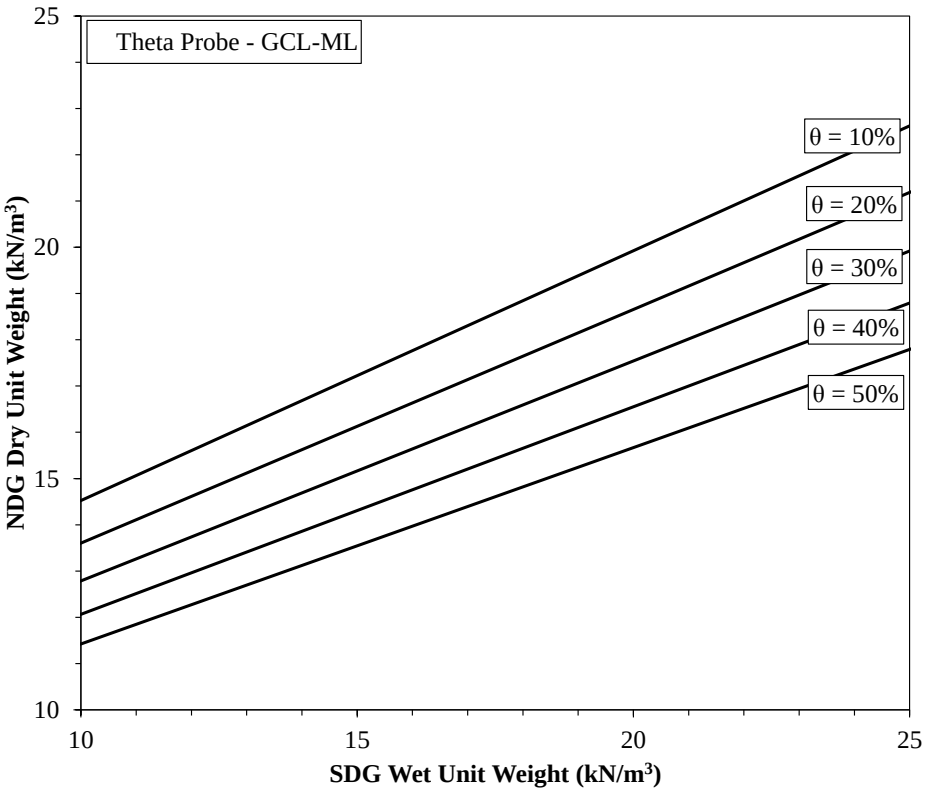

Figure 5.13: Moisture Specific Trend lines to Obtain Equivalent NDG Dry Unit Weights

The graph in Figure 5.13 is for one soil type and the multiple lines represent different outputted volumetric moisture contents that would obtained from the moisture probes. These graphs were constructed for all twelve soil types and for each moisture probe. In all, 24 different graphs were constructed and the Theta Probe specific graphs can be seen in Appendix A and the Hydra Probe specific graphs can be seen in Appendix B.

It is also assumed that because Equation 23 is linear, interpolation can be used when volumetric moisture contents fall in between the moisture displayed on the graph. Figure 5.14 presents an example of interpolating between the moisture content trend lines.

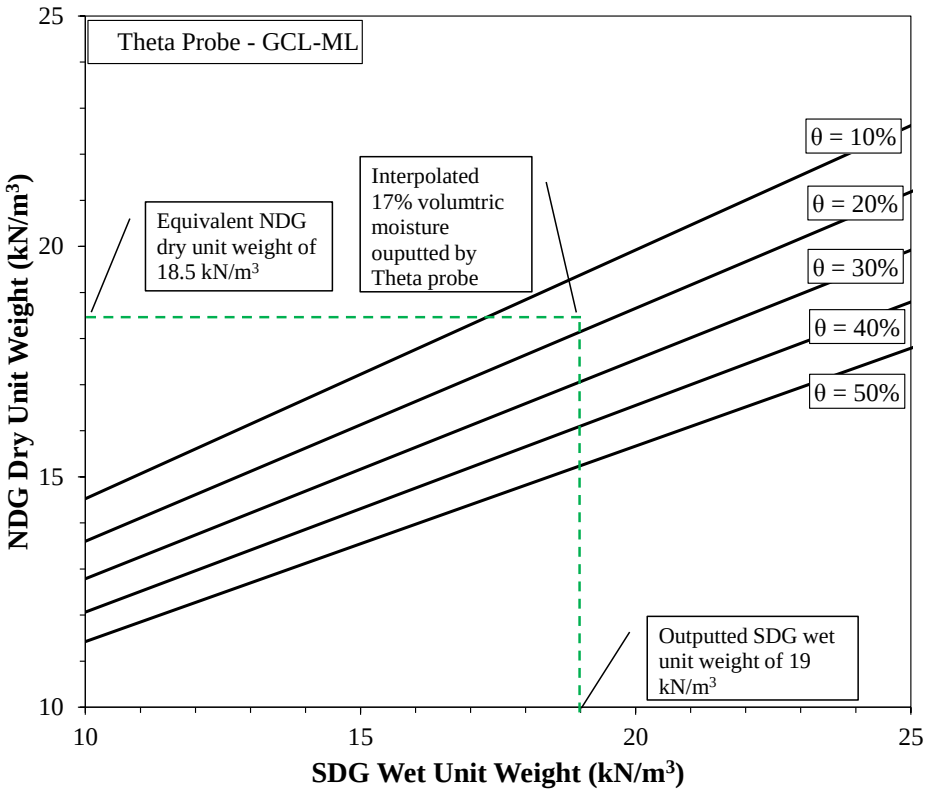

Figure 5.14: Interpolating NDG dry unit weight from the SDG and moisture probe outputted values

As an example, an operator measures an outputted SDG wet unit weight of 19 kN/m^3 and a Theta Probe outputted volumetric moisture content of 17%. But since there is not a moisture specific line for 17%, interpolation would have to be done. As seen in Figure 5.14, the SDG outputted a wet unit weight of 19 kN/m^3. The interpolated 17% volumetric moisture would be between the 10% and 20% moisture specific trend lines. After interpolation of the 17% mark, the operator would then go horizontally, to obtain a NDG dry unit weight of 18.5 kN/m^3.

The coefficients for the 2nd order polynomial general moisture content trend lines are shown as well in Appendix D. The 2nd order polynomial lines were not used to develop the SDG wet unit weight to NDG dry unit weight comparison. The reason for is that the

curvature of the trend lines makes it difficult to interpolate between lower moisture contents.

CHAPTER 6

6 Performance of Calibration Methods

6.1 Calibration Methods

Up to this point, this study has presented that by either using a general moisture content trend line or trend line equations, equivalent gravimetric moisture content can be obtained from volumetric moisture contents outputted by the moisture probes. To validate the reliability of the developed trend lines to obtain equivalent gravimetric moisture contents, field data were plotted with fitted linear and 2nd order polynomial trend lines. The data were then adjusted to observe predicted gravimetric moisture contents versus gravimetric oven moisture contents. Since the same evaluation was performed on both probes, a discussion of results from the Theta Probe will only be shown. All the graphs presented with the Theta Probe were also constructed for the Hydra Probe and can be seen in Appendix D.

This study has also presented that when SDG and a moisture probe are used in tandem a method to obtain equivalent NDG dry unit weights can be performed by the use of a graph. Along with the methods presented in this study, there are also other calibration methods that have been presented in other studies. Rose (2013) presented 1-Point and 3-Point calibration methods and Mejias-Santiago et al. (2013) presented a general equation. To show how the calibration methods presented in this study compared to these other methods,

6.2 General Moisture Content Trend Line Equations

The Theta Probe was tested at the Kiddville Rd., Ramp D Silt and Messer sites. The soil conditions at Kiddville Rd. and Ramp D Silt were compacted roadways and the soil at Messer was being compacted for future foundation use of an apartment complex. To

adjust the validation field data to obtain predicted gravimetric oven moisture contents, the outputted volumetric moisture contents from the Theta Probe were inputted into both the developed linear and 2nd order polynomial trend line equations. The predicted oven moisture contents were then related to the actual gravimetric moisture contents as seen in Figure 6.1.

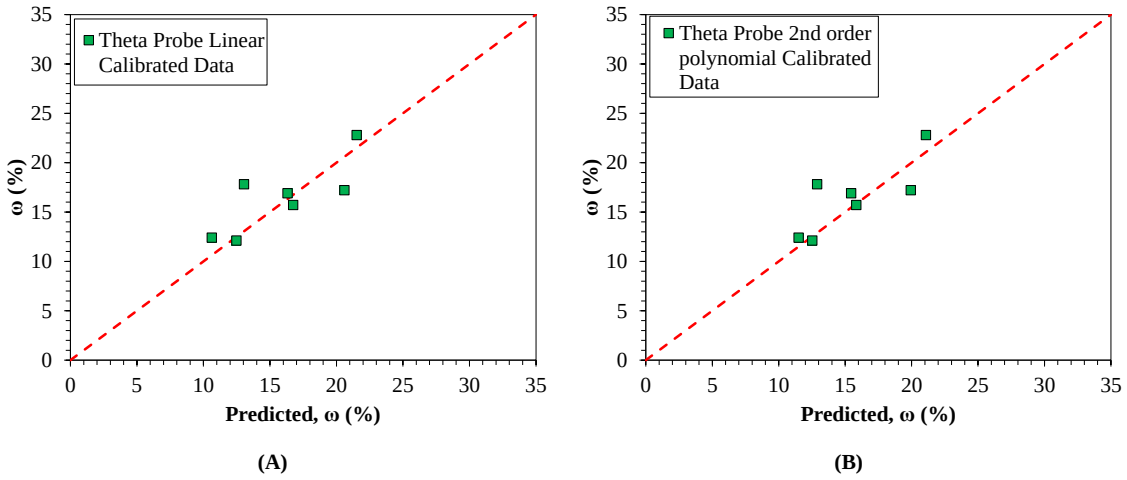

Figure 6.1: Predicted gravimetric moisture content versus actual gravimetric moisture content; (A) Linear trend line calibrated data; (B) 2nd order polynomial trend line calibrated data.

Figure 6.1(A) shows the predicted oven moisture contents related to the actual oven moistures after being inputted into the developed linear equation. The Theta Probe was able to predict the actual oven moisture contents fairly well. Of the seven data points, five were able to able to predict actual oven moisture content relative to the line-of-unity while two deviated. Figure 6.1(B) is the same as Figure 6.1(A), but the field validation data were inputted into the developed 2nd order polynomial equation. As it can be seen, there were improvements to the Theta Probe predictions of actual moisture contents. The same five data points plotted the same, if not a slightly closer to the line-of-unity.

A percent error analysis was also performed to graphically show how well the validation field data were able to predict gravimetric moisture contents. Figure 6.2 shows a relationship regarding the predicted oven moisture content ω percent error versus oven moisture content for the Theta probe.

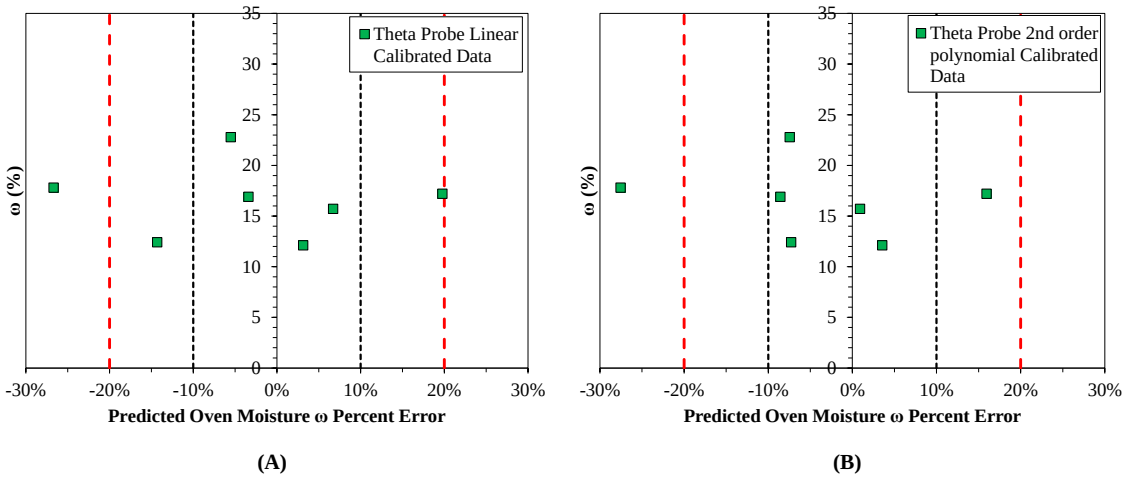

Figure 6.2: Percent error graphs of predicted versus actual moisture content; (A) Linear calibrated data; (B) 2nd order polynomial calibrated data.

The dashed red and black lines vertical lines are the boundaries of ±20% and ±10% error, respectively, that represent the probes ability to predict oven moisture contents within those limits. For the data plotted in Figure 6.2(A), six of the seven data points were able to predict gravimetric oven moisture contents with ±20% accuracy while four of those points plotted within ±10%. Likewise, the percent errors were plotted for the 2nd order polynomial calibration trend line and an improvement of the data were achieved in that five of the seven data points were able to plot within ±10%. The other two points fell outside of the ±10% intervals with one being outside of the ±20% error mark. Validation data were plotted alongside the trend lines and error analysis showed that most of the data reliably plotted within the ±10% error mark. Through the use of either the linear or 2nd order polynomial equations developed from the trend lines or by interpolation from

graphs, an equivalent gravimetric can be obtained from the relationships of outputted volumetric to oven gravimetric moisture contents.

6.3 SDG Calibration Methods

Data from the field study was applied to the calibration method presented in this study to show the reliability of the method when the devices were used in tandem. The test site soils of Band Stoll Field, Wild Cat Den, Jane Lane and Messer soils were reclassified as CI using the adjusted USCS which changed the original classification of CL. Also, tests with the Hydra Probe were performed at each of the sites while the Theta Probe was only available during the Messer site testing. The test sites of Kiddville Rd. and Ramp D Silt, under the adjusted USCS, were reclassified as Intermediate Silt (MI) so they could not be evaluated. Out of the 12 graphs that were developed to obtain an equivalent NDG dry unit weight based on soil type; a graph for an intermediate silt soil was not available because testing on this soil type had not been performed before. Table 6.1 shows the outputted values from the SDG and moisture probes that were obtained at each site.

Table 6.1: Outputted values from devices needed to perform graphical interpolation

Test Site	Adjusted USCS	Hydra Probe θ	Theta Probe θ	SDG γ_{wet}
Wild Cat Den	CI	37.7	-	18.1
Band Stoll Field	CI	42.5	-	19.2
Messer	CI	40.3	33.3	17.6
Jane Lane	CI	36.0	-	18.7

The outputted values were then applied to the calibration method presented in this study was compared to the dry unit weights obtained from a sand cone apparatus at each site.

Figure 6.3 shows the predicted NDG dry unit weights compared to measured values of dry unit weights.

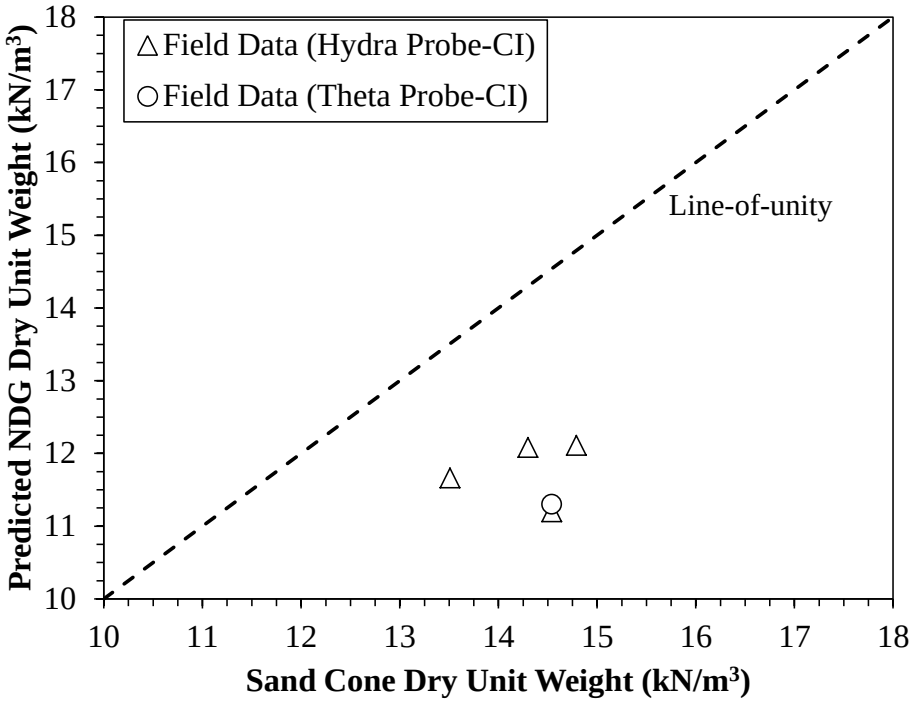

Figure 6.3: Sand cone dry unit weight compared to predicted NDG dry unit weight

As shown in Figure 6.3, the predicted NDG dry unit weights while using both the Hydra Probe and Theta Probe were less than the dry unit weights obtained from the sand cone test. Altun et al. (2008) also experienced sand cone dry unit weights being greater than NDG dry unit weights while performing tests in a silty sand. On average, the sand cone dry unit weights tended to be slightly greater than the NDG dry unit weights and during a few tests the sand cone dry unit weights were as high as 10% greater than the NDG dry unit weight. This data could have possibly been improved if the predicted NDG dry unit weights were compared to actual NDG readings. More testing is going to be needed to fully examine if the calibration method presented in this study has the ability to predict reliable dry unit weights.

Comparisons to the calibration methods presented by Rose (2013) and Mejias-Santiago et al. (2013) wanted to be made to the calibration method presented in this study, but could not be performed. The Rose (2013) method requires multiple readings at an individual site to be made and for the four sites evaluated in this study; only one test with the soil actual material properties was performed. The other tests performed with the SDG were material property error adjustment tests, so the 1-Point and 3-Point calibration procedure could not be applied to the outputted data. The Mejias-Santiago et al. (2013) calibration method requires an outputted SDG dry unit weight value to be inputted into the presented equation. This value was not recorded during testing in this study because outputted SDG values wet unit weight and gravimetric moisture content were only recorded. Since the dry unit weight was not recorded at each site, the calibration equation could not be plotted alongside the data presented in Figure 6.3. Also, the method presented in this study could be applied to the data from the Mejias-Santiago et al. (2013) and Rose (2013) data because moisture probes were not used in conjunction with the SDG during the testing.

CHAPTER 7

7 Conclusions

This research has focused on Tran Tech's SDG 200, Delta-T's Theta Probe ML2x and Stevens Water Hydra Probe. This research has shown the SDG has the ability, through moisture specific trend line, to reliably obtain an equivalent NDG dry unit weight. Also in conjunction with the SDG, two moisture probes were able to obtain gravimetric moisture contents through the use of a general moisture content trend line from outputted volumetric moisture contents.

Based on laboratory calibrations, field testing and interpretation of data through case studies this research concludes the following:

- The SDG has the capability of becoming a viable QC device. However, inconsistencies are occurring when trying to accurately obtain SDG moisture contents and dry/wet unit weights when compared to oven moisture contents and NDG unit weights, respectively. Calibration equations and procedures were implemented in trying to correct these inconsistencies but the device needs more research in order to become reliable QC device.
- Researchers such as Rose (2013) and Mejias-Santiago et al. (2013) implemented calibrations for the SDG by partially focusing on the material properties inputted into the device. Mejias-Santiago et al. (2013) presented a general equation that took into consideration most of the material properties that are inputted into the SDG. Rose (2013) separated soils into sub-categories such as fines and coarse grained materials and applied a 1-point and 3-point calibration to the outputted

SDG. By doing this R^2 values became higher and SDG outputted values were more reliable when compared to known values.

- A calibration procedure that involved the Theta and Hydra probe showed that there is a relationship between the outputted volumetric contents of the devices and gravimetric oven moisture contents. Through the use of a proctor mold, the devices were calibrated to nine soil types that were compacted at standard energy following. After plotting outputted volumetric versus gravimetric moisture contents, the data were treated as one soil type and a linear and 2^{nd} order polynomial trend line was plotted through the data. General moisture content trend lines were developed and field data validated that the developed trend lines were reliable in obtaining equivalent gravimetric oven moisture contents.
- During a field evaluation, the SDG outputted data were compared to sand cone wet unit weights and oven moisture contents and evaluated for performance. The wet unit weights outputted by the SDG showed inconsistencies when compared to the sand cone but were able to plot data in groupings of soil types. When evaluating the outputted moisture contents, the SDG was not able to distinguish between moisture contents and outputted a moisture content of 21% regardless of the actual moisture.
- Through an error adjustment analysis of the material properties inputted into the SDG, it was shown that the device could possibly have constraints. By referencing the USCS plasticity index chart, depending on the difference between the LL and PL of the soil, the device gave inconsistencies for the wet

unit weight and moisture content. This constraint was seen when there was a PI of seven or less. When the PI was equal to 8 and greater, the output values did not deviate from the outputted value from the first test ran with the actual material properties. Seeing that the inputted material properties could have an effect on the calculations of the device, it was then decided to break soils into an adjusted USCS classification based on the plasticity of the soil.

- Through gathering data from case studies the adjusted USCS classification was applied to the soil types. From each project a SDG moisture content vs oven moisture content and SDG wet unit weight vs NDG wet unit weight, graphs were developed to show trends based on soil types. The moisture content relationship showed that for the non-plastic soils, a calibration procedure could be applied to the data to correct the under-predicted or over-predicted moisture contents from the SDG. However, for the plastic soil the outputted moisture contents ranged form 18% to 26% regardless of the actual moisture that ranged from 5% to 75%. Further research is going to have to be performed to make a conclusive reasoning to why this is happening to the plastic soils
- For the wet unit weight relationships it was shown when classifying soils to adjusted USCS soil trends did appear when compared to the NDG. Soils were separated based on plasticity and trend lines were plotted through each of the grouped soils. These trend lines showed that soils were being separated based on the adjusted USCS classification given to each soil.
- To further implement the soil specific trend lines, graphs were developed that could relate outputted SDG wet unit weights to NDG dry unit weights. This was

performed by using the general moisture content trend lines developed through the calibration process with the moisture probes. By using the equations from the universal moisture trend lines and the soil specific trend lines, graphs were then developed that related the outputted SDG wet unit weight to NDG dry unit weight per soil type and through moisture specific trend lines.

- The calibration methods presented by Rose (2013), Mejias-Santiago et al. (2013) and the method presented in this study, all have potential of reliably obtaining outputted values from the SDG. The 1-Point and 3-Point calibrations not only showed improvements in data in the Rose (2013) data but the Mejias-Santiago et al. (2013) data as well. However, a sand cone or NDG reference data point is needed in order to perform the calibration. The general equation presented by Mejias-Santiago et al. (2013) also improved correlations in data, however the developed equation requires a lot of variable values to be inputted into the equation to obtain a NDG dry unit weight. The method presented in this study, does not require a reference data from the NDG or sand cone, nor does it require a lengthy equation. To determine if the method presented in this study is as reliable as the other methods presented by Rose (2013) and Mejias-Santaigo (2013) further field testing is needed.

QC through proper compaction of a soil subgrade is vital to ensure longevity, structural stability and performance. To ensure proper QC, devices such as the NDG, have performed well in years past but recently there has been concerns regarding the nuclear source that the NDG uses to obtain its outputted values. So to alleviate these concerns, researchers have been testing NNDG's such as the SDG to be a possible alternative to the

NDG. However, the SDG seems to have some inefficiency in obtaining reliable moisture contents so two alternative moisture probes were studying as well to be used along the SDG to obtain moisture contents. Through this research it has been shown that the SDG has the capability to obtain reliable wet unit weights and the moisture probes show promise in obtain equivalent gravimetric moisture contents. When these devices are used together, they then can obtain equivalent NDG dry unit weights and gravimetric moisture contents which are both equally important in QC in roadway construction.

7.1 Recommendations for Further Research

- More performance testing with the SDG and moisture probes alongside a NDG, should be performed to examine if the calibration procedures presented in this study are able to predict reliable NDG dry unit weights.
- The calibration procedure using the general moisture content trend line to obtain equivalent gravimetric moisture contents should be further evaluated through field testing.
- Using similar procedures as presented by Mejias-Santiago et al. (2013), more soil types should be tested to allow for new developments of soil-specific trend lines to obtain equivalent NDG wet unit weights and dry unit weights.
- After evaluating the SDG ability to predict a NDG dry unit weight through the calibration procedure presented in this study, a comparison between the calibration methods presented by Rose (2013) and Mejias-Santiago et al. (2013) should be performed. After doing so, comments regarding reliability of the methods should be made.

- A smart-phone app should be developed that automatically computes NDG dry unit weights from outputted SDG wet unit weights and moisture probe volumetric moisture contents.

Appendix A

Graphs to Obtain Equivalent NDG Dry Unit Weights using the Theta Probe

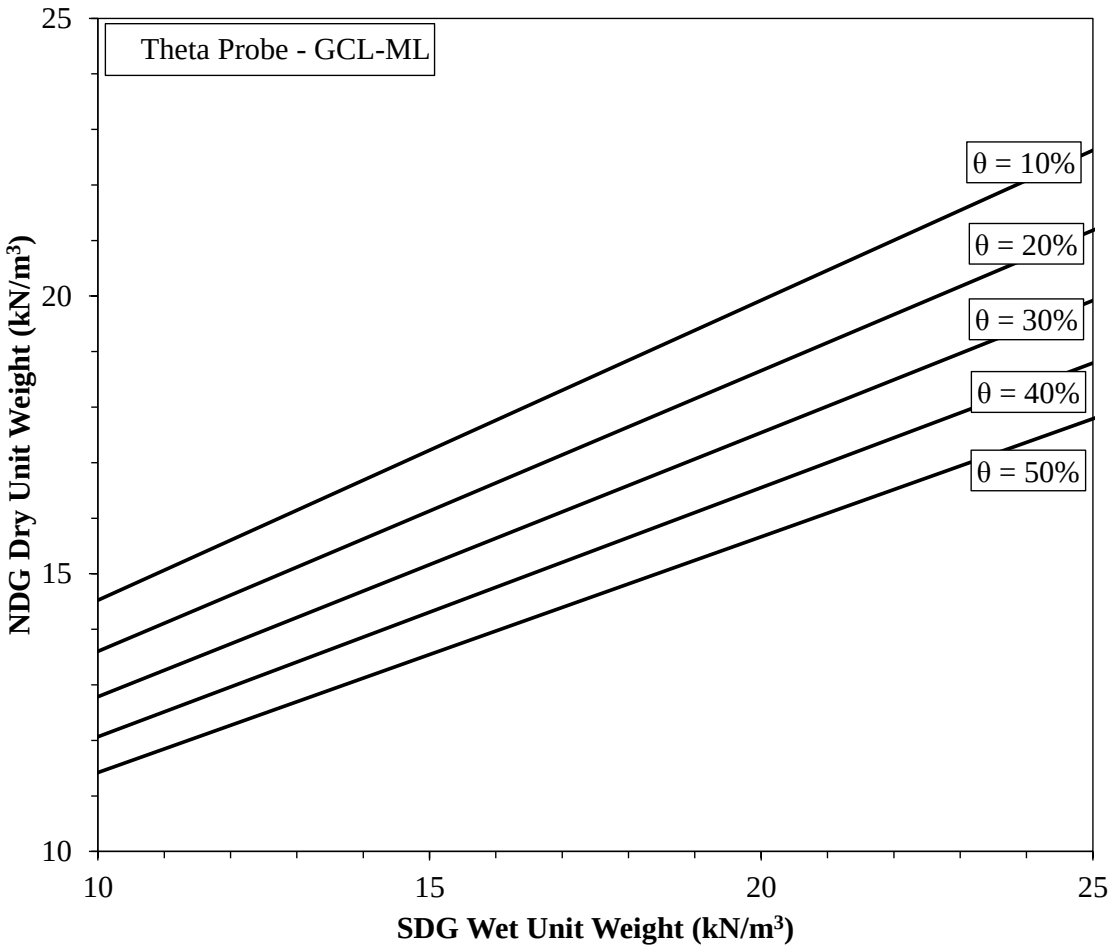

Figure A.1: Graph to obtain an NDG dry unit weight: Theta Probe – GCL-ML

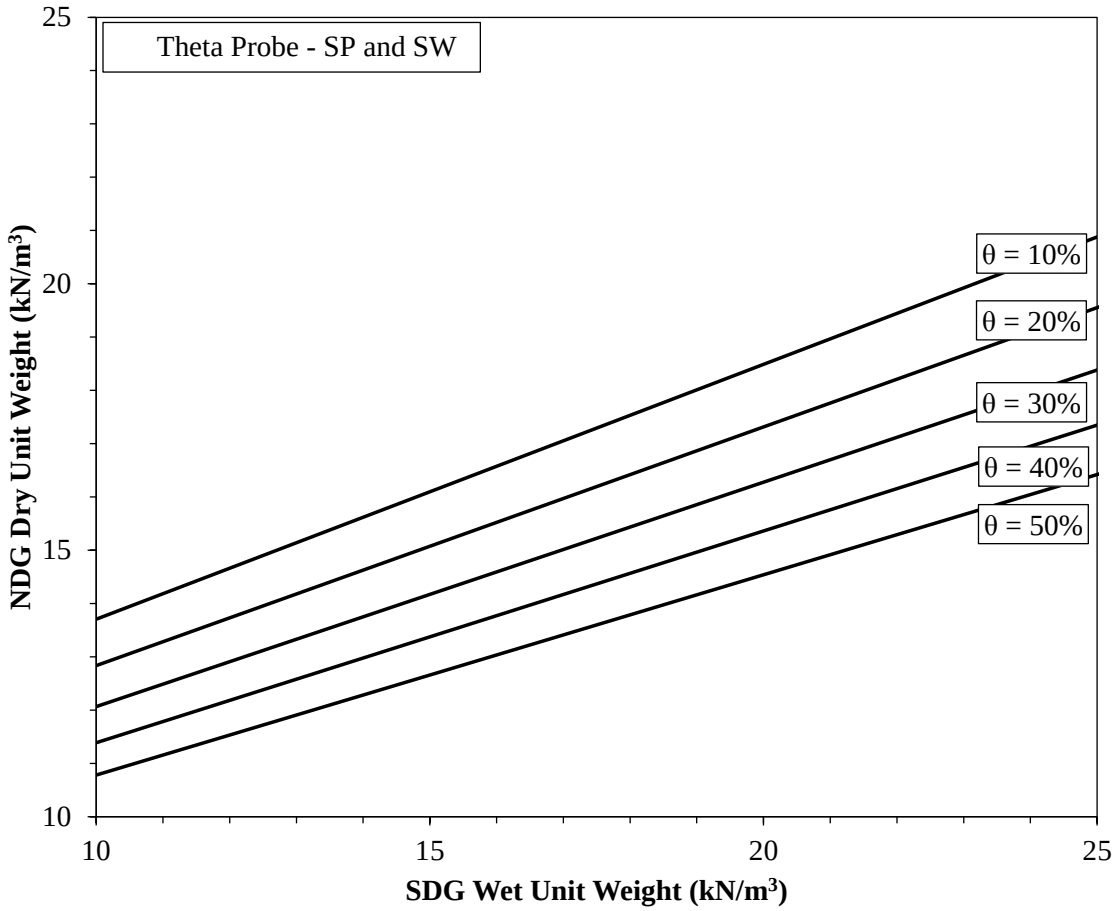

Figure A.2: Graph to obtain an NDG dry unit weight: Theta Probe – SP and SW

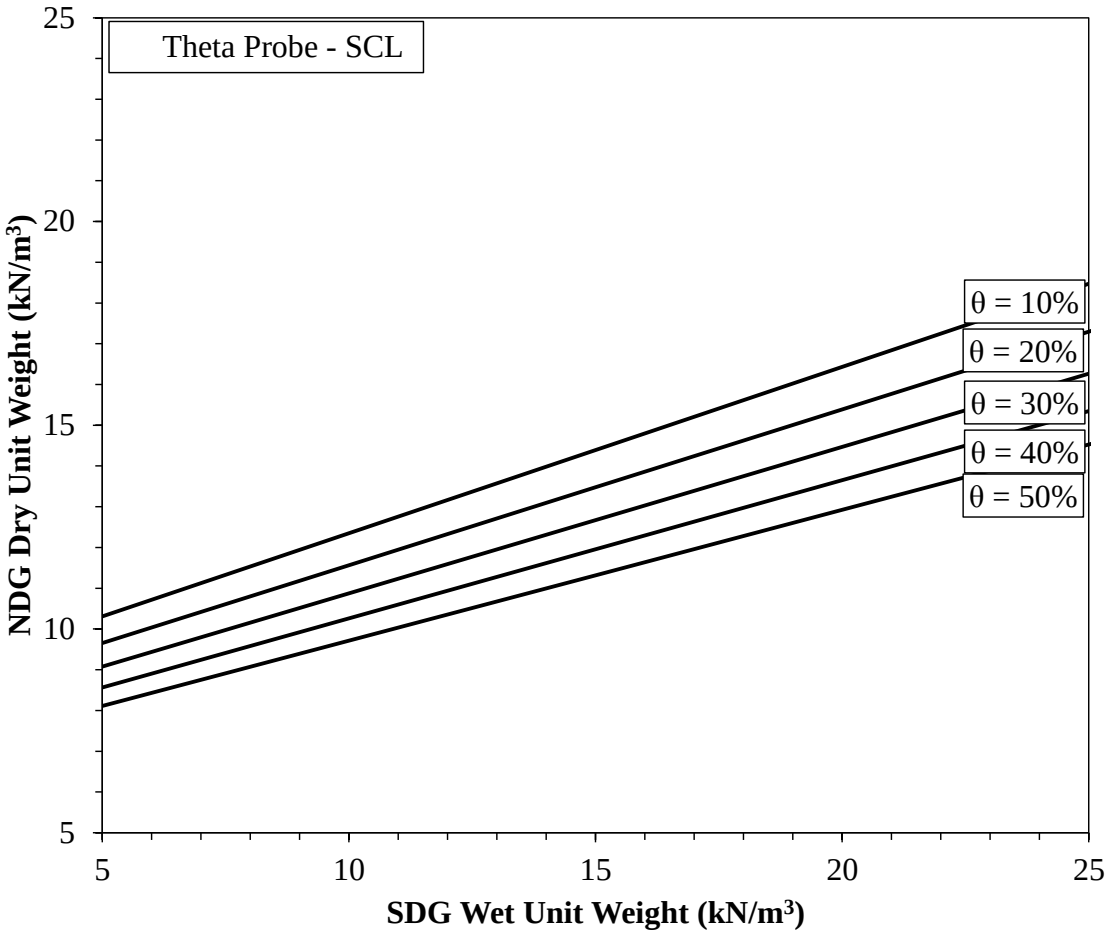

Figure A.3: Graph to obtain an NDG dry unit weight: Theta Probe – SCL

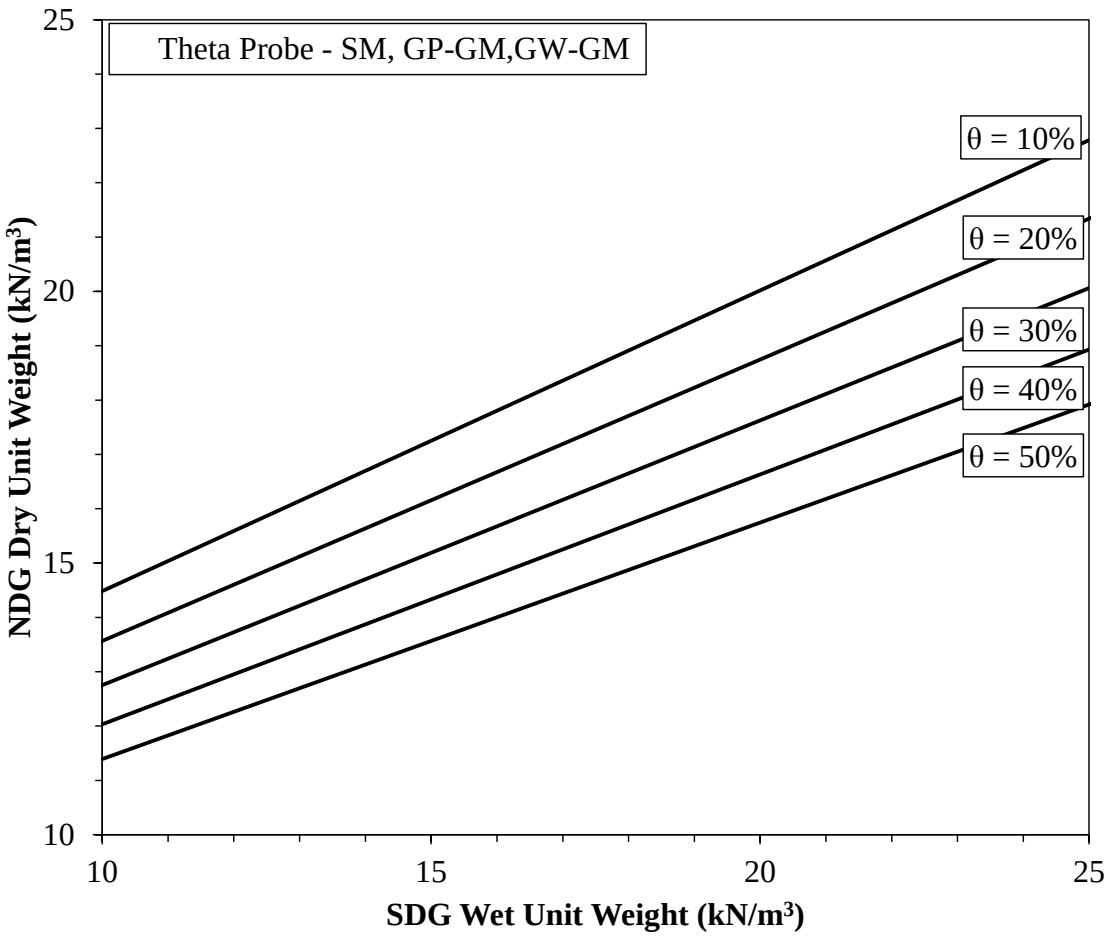

Figure A.4: Graph to obtain an NDG dry unit weight: Theta Probe – SM, GP-GM, GW-GM

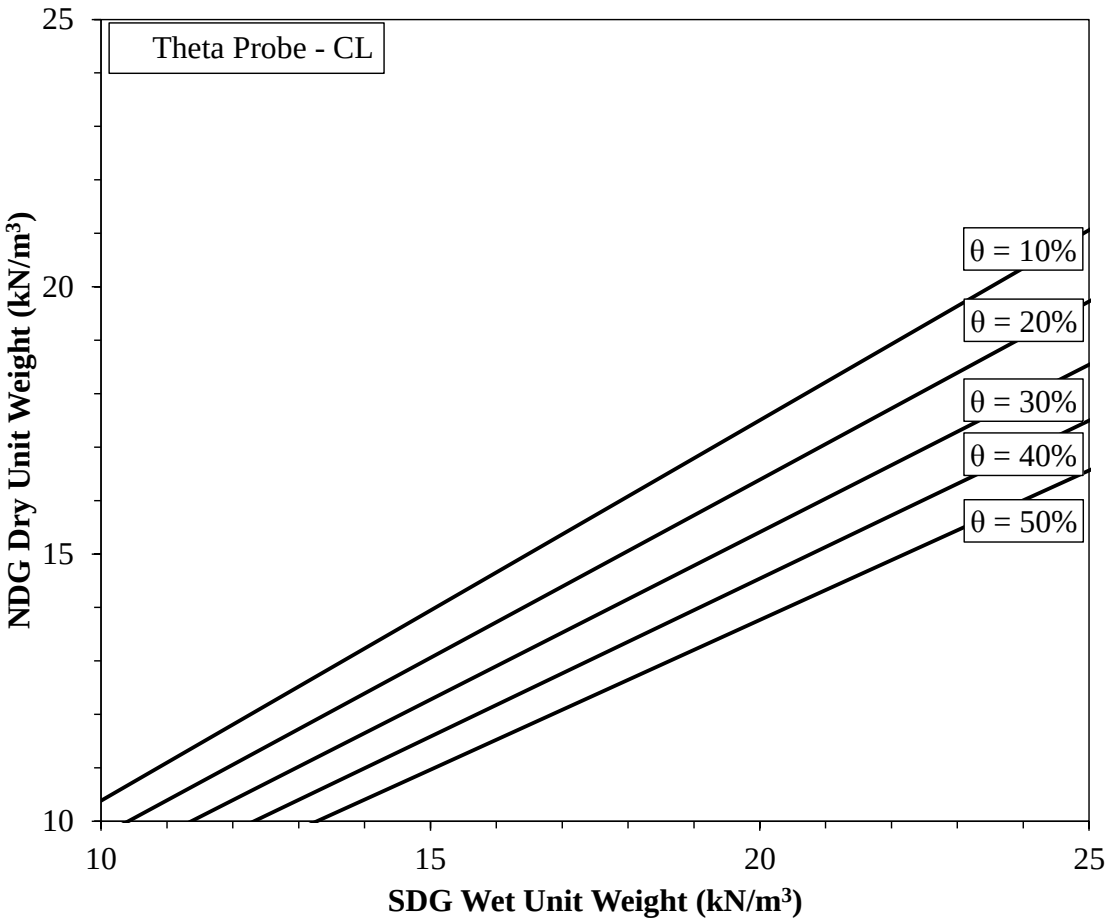

Figure A.5: Graph to obtain an NDG dry unit weight: Theta Probe – CL

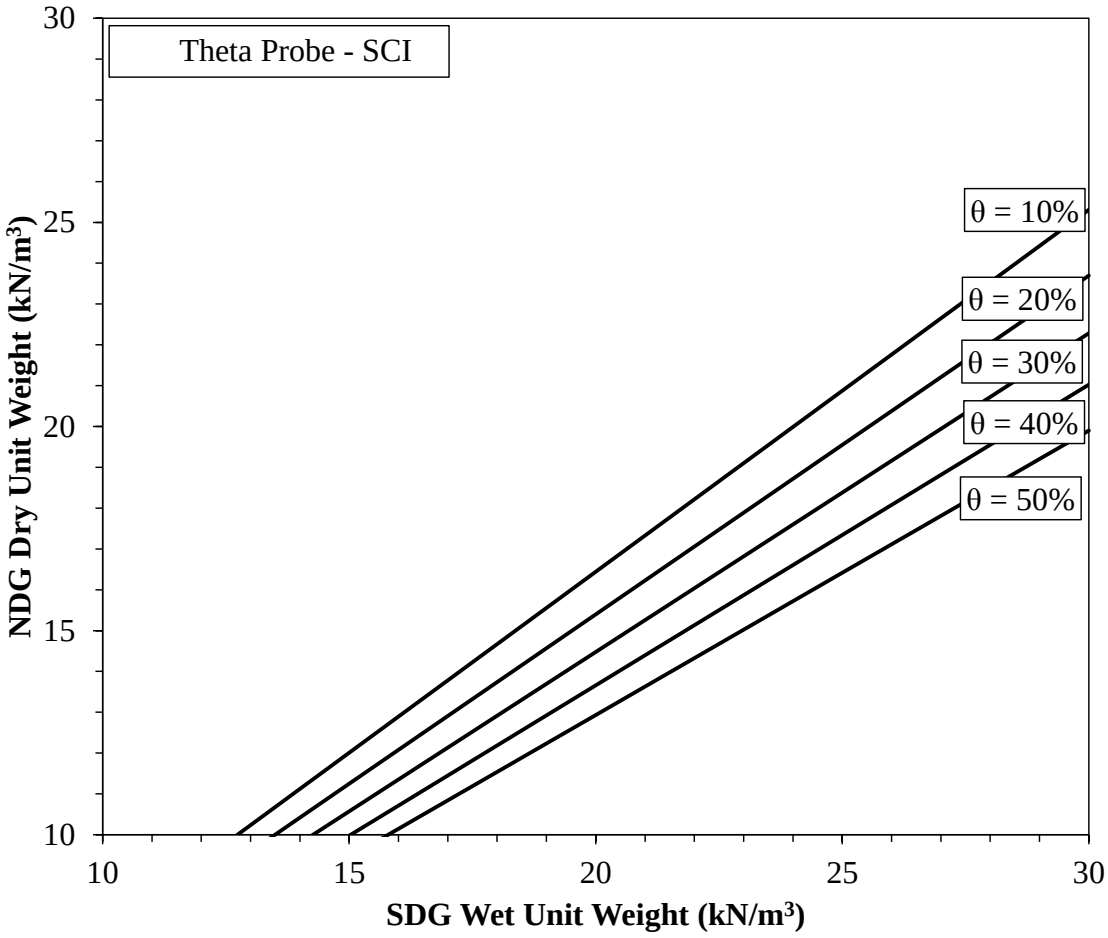

Figure A.6: Graph to obtain an NDG dry unit weight: Theta Probe – SCI

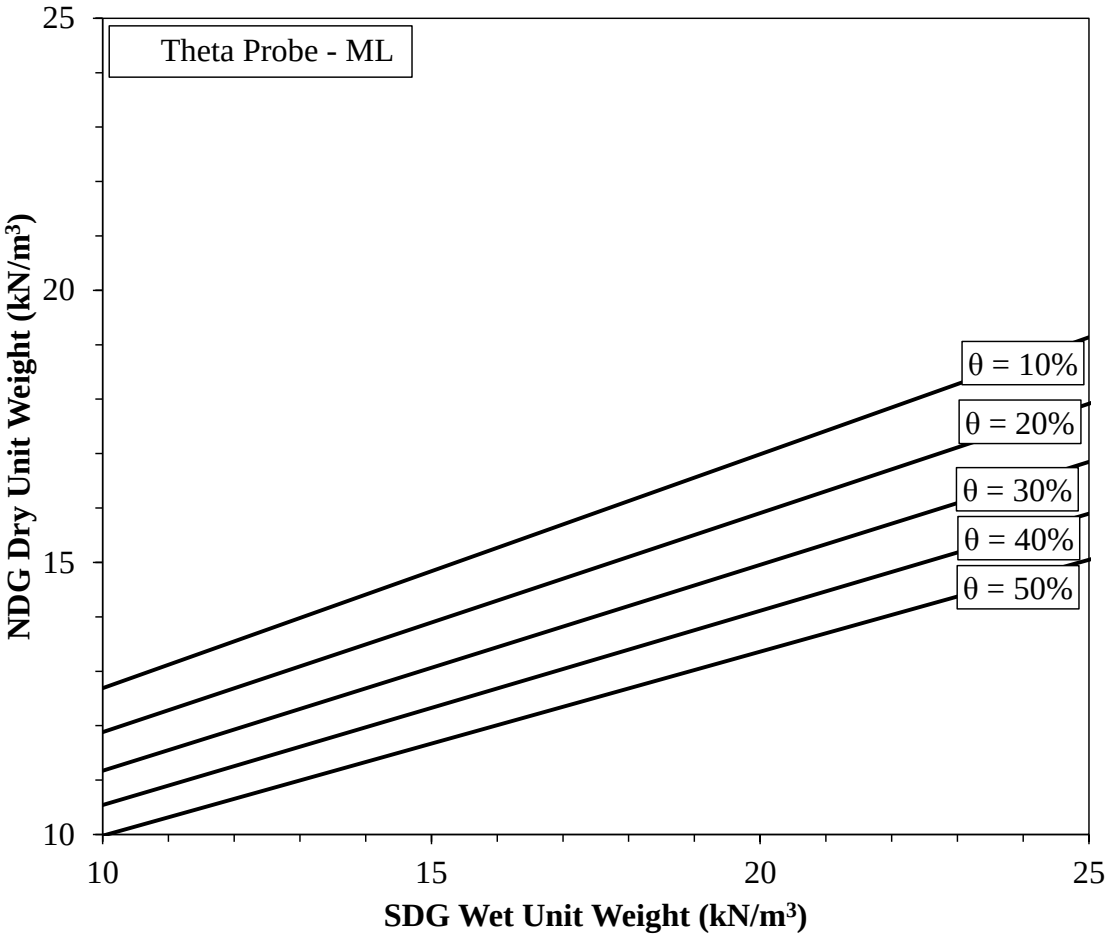

Figure A.7: Graph to obtain an NDG dry unit weight: Theta Probe – ML

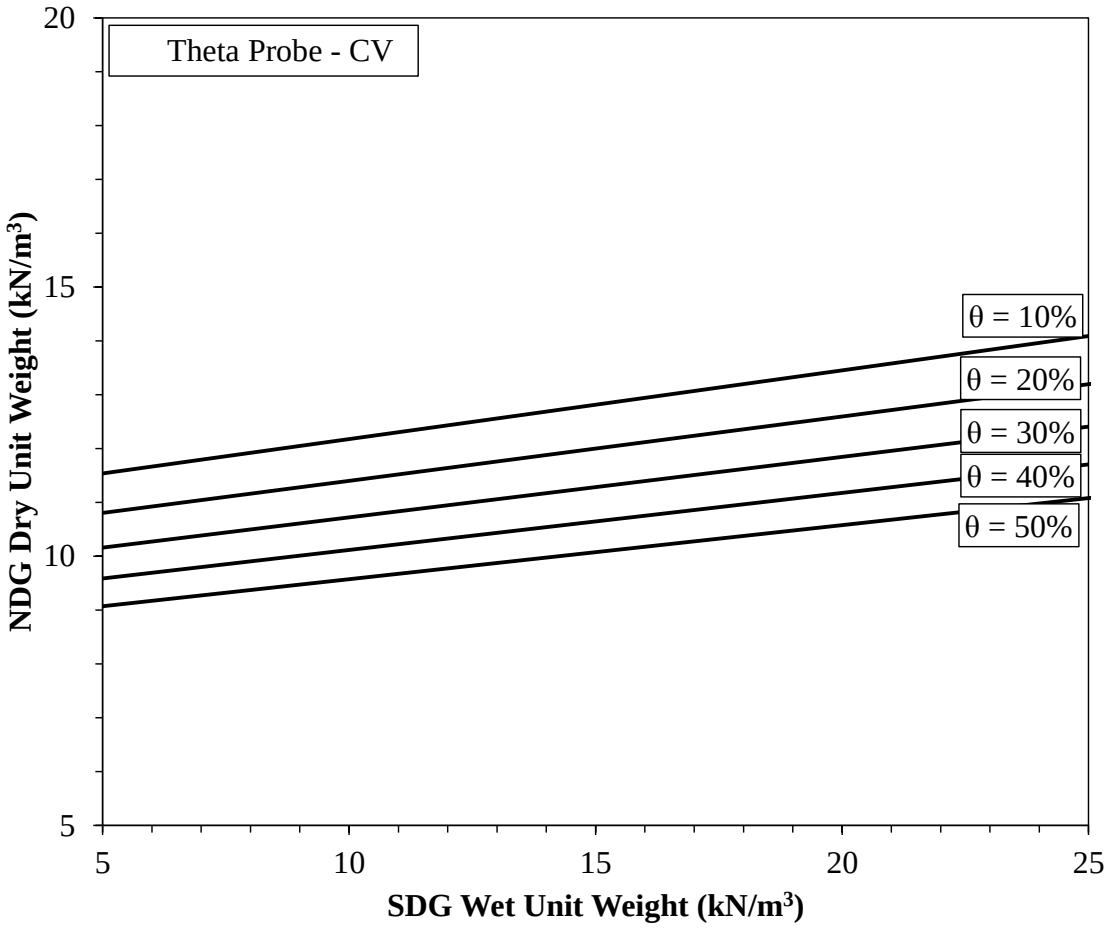

Figure A.8: Graph to obtain an NDG dry unit weight: Theta Probe – CV

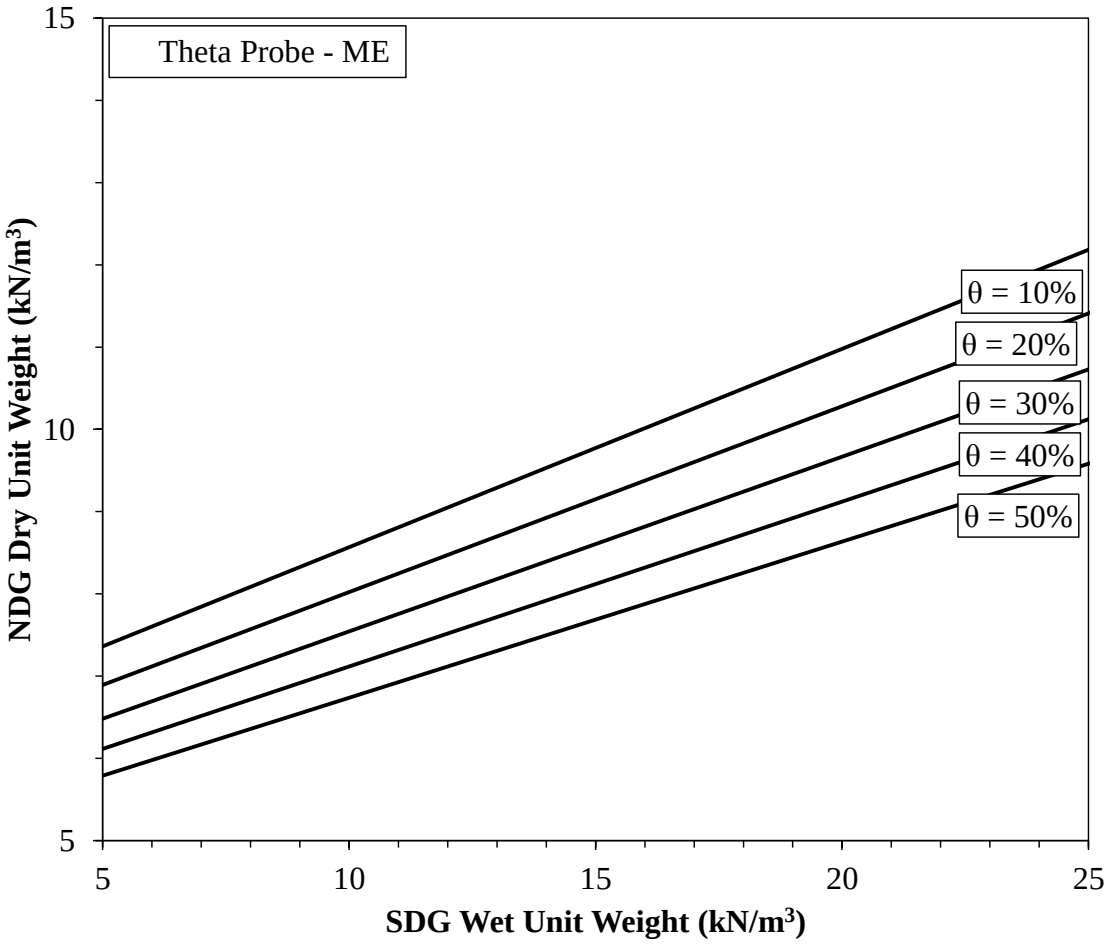

Figure A.9: Graph to obtain an NDG dry unit weight: Theta Probe – ME

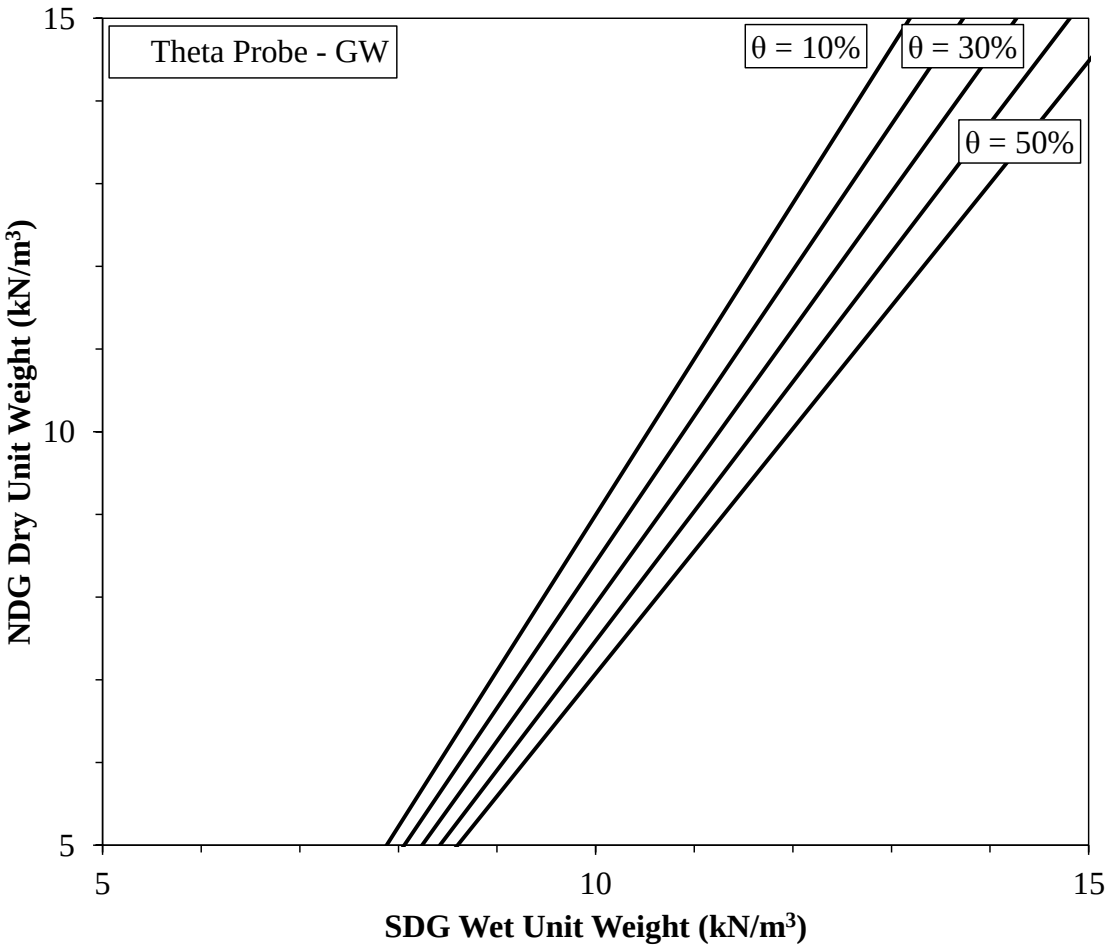

Figure A.10: Graph to obtain an NDG dry unit weight: Theta Probe – GW

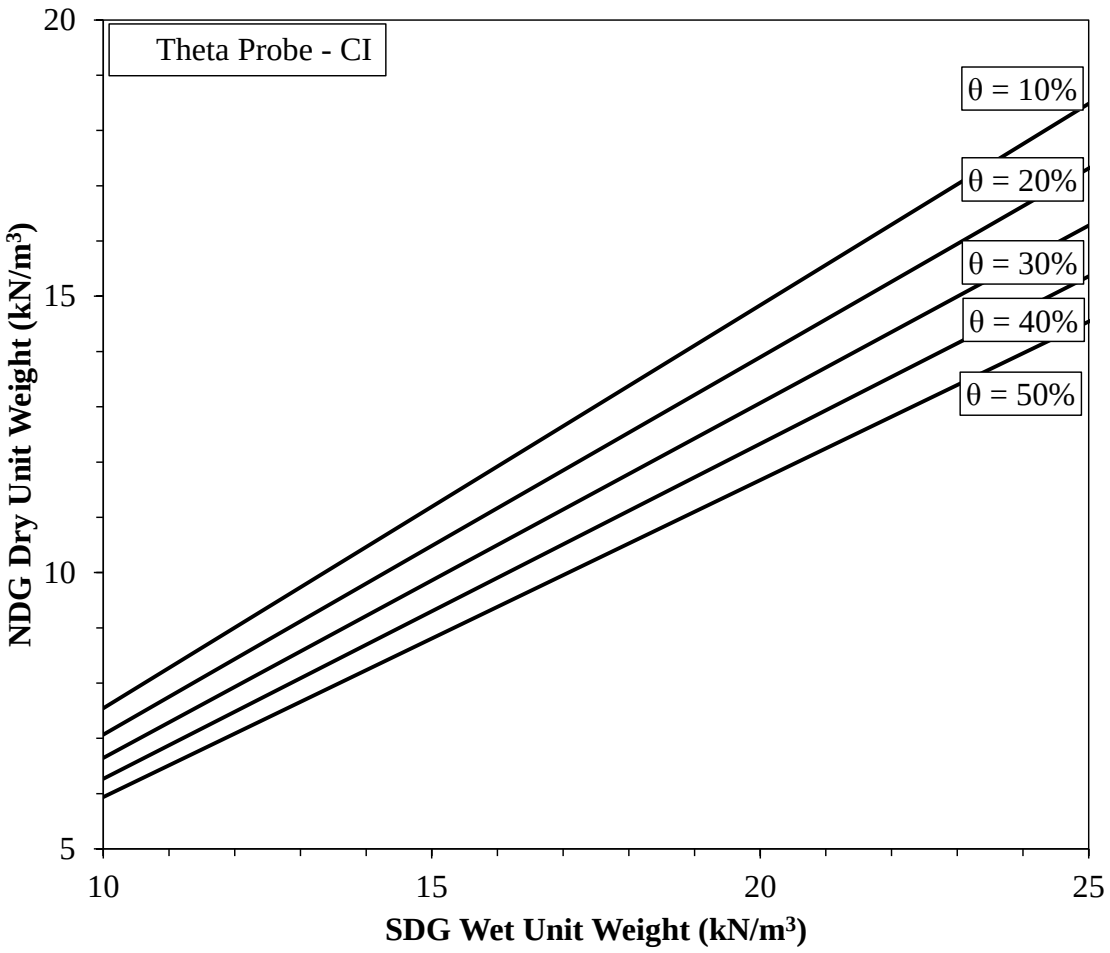

Figure A.11: Graph to obtain an NDG dry unit weight: Theta Probe – CI

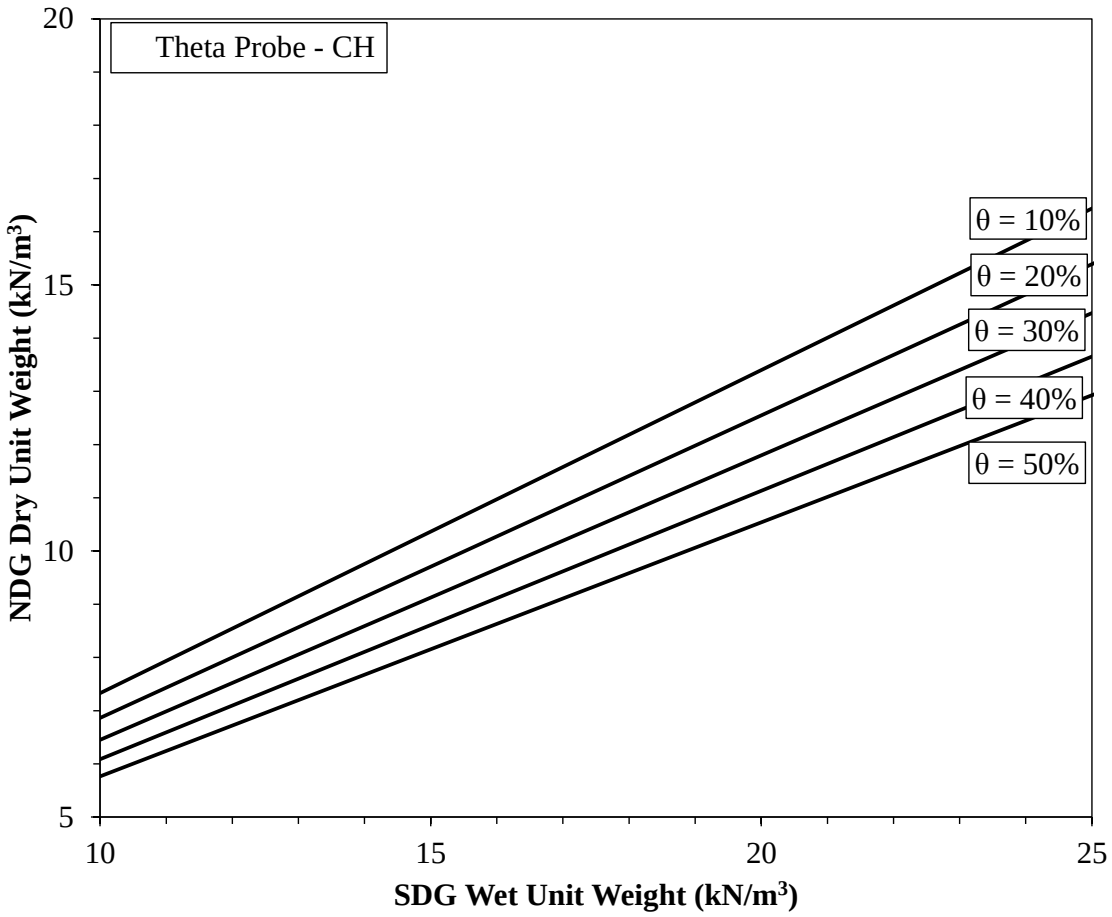

Figure A.12: Graph to obtain an NDG dry unit weight: Theta Probe – CH

Appendix B

Graphs to Obtain Equivalent NDG Dry Unit Weights using the Hydra Probe

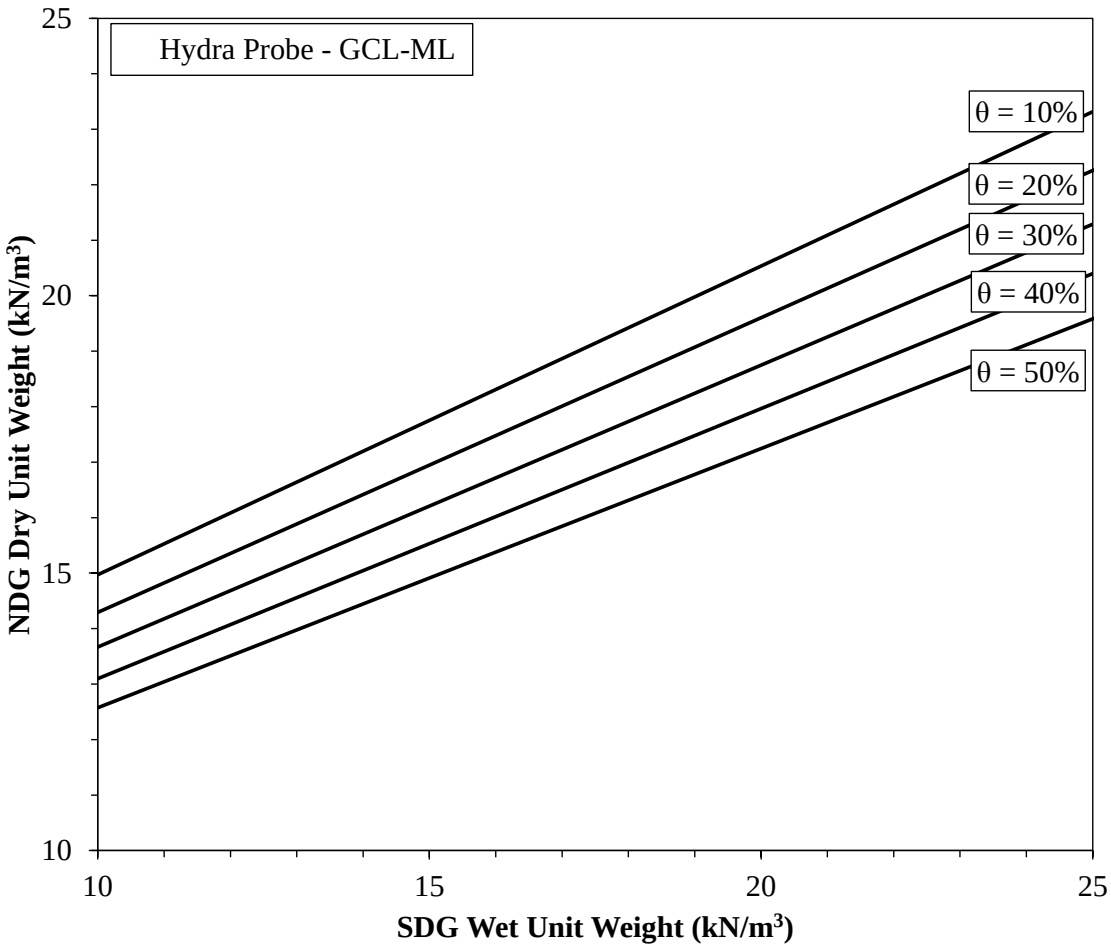

Figure B.1: Graph to obtain an NDG dry unit weight: Theta Probe – GCL-ML

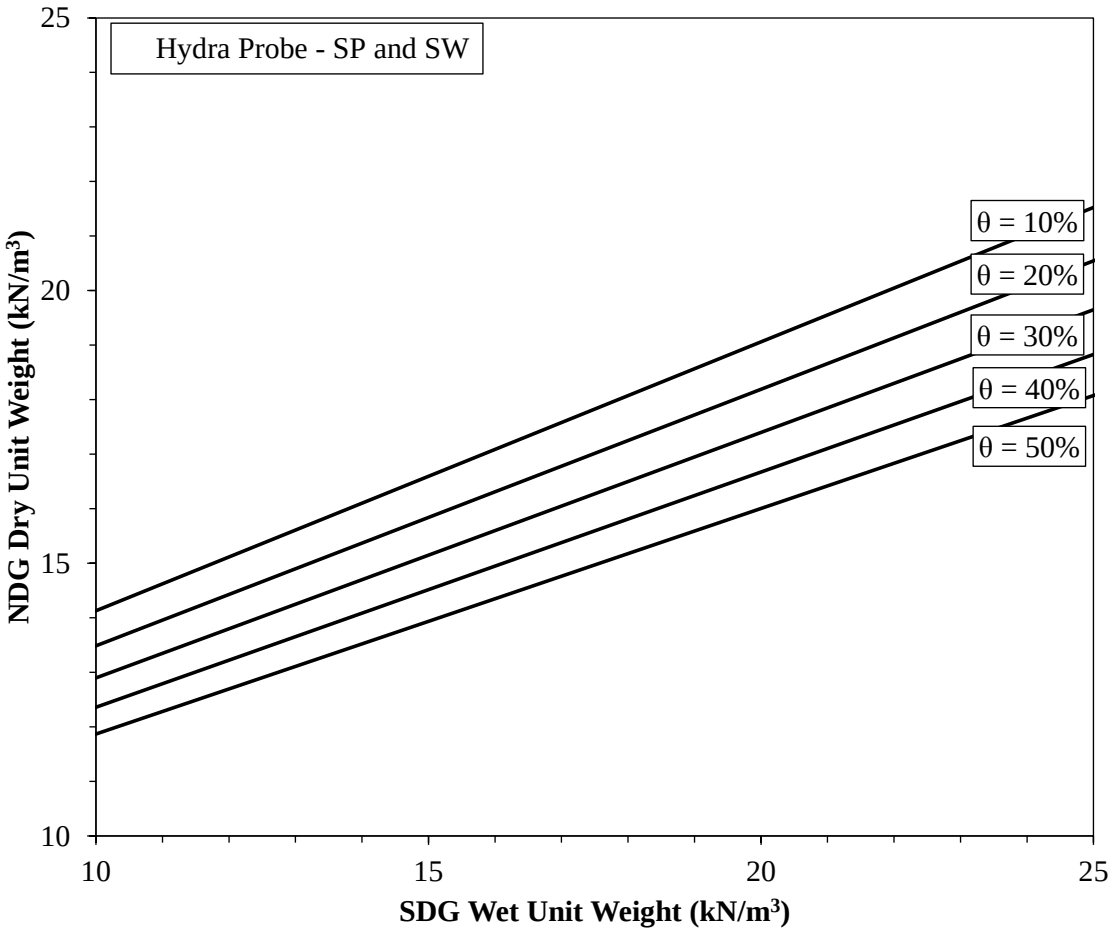

Figure B.2: Graph to obtain an NDG dry unit weight: Theta Probe – SP and SW

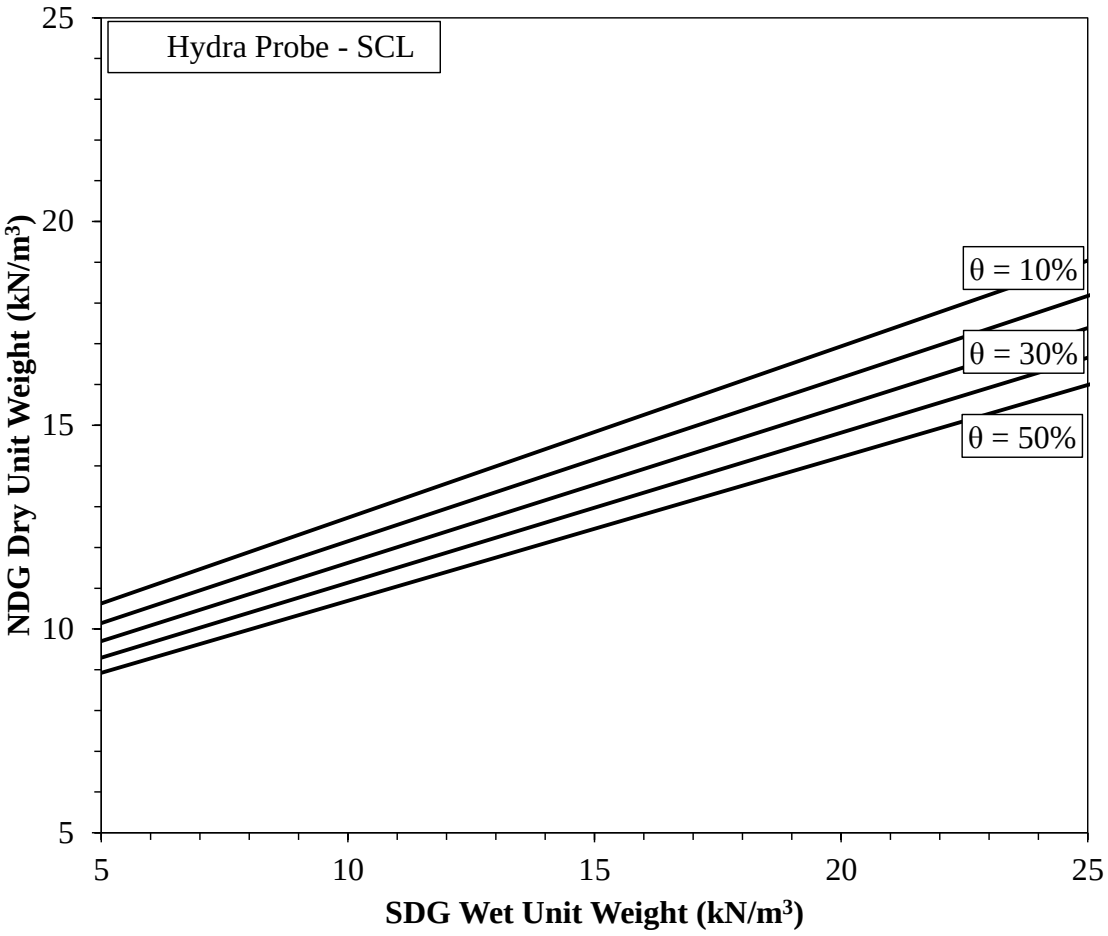

Figure B.3: Graph to obtain an NDG dry unit weight: Theta Probe – SCL

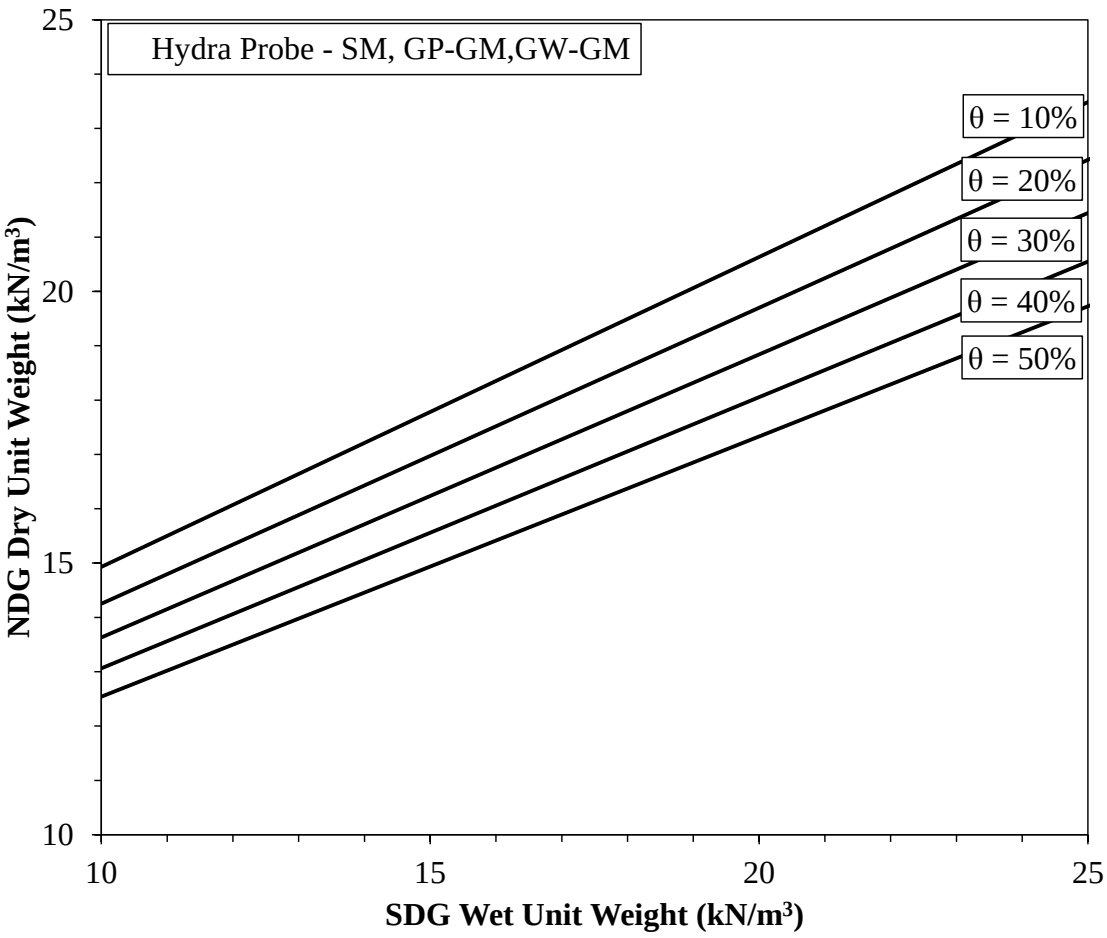

Figure B.4: Graph to obtain an NDG dry unit weight: Theta Probe – SM, GP-GM, GW-GM

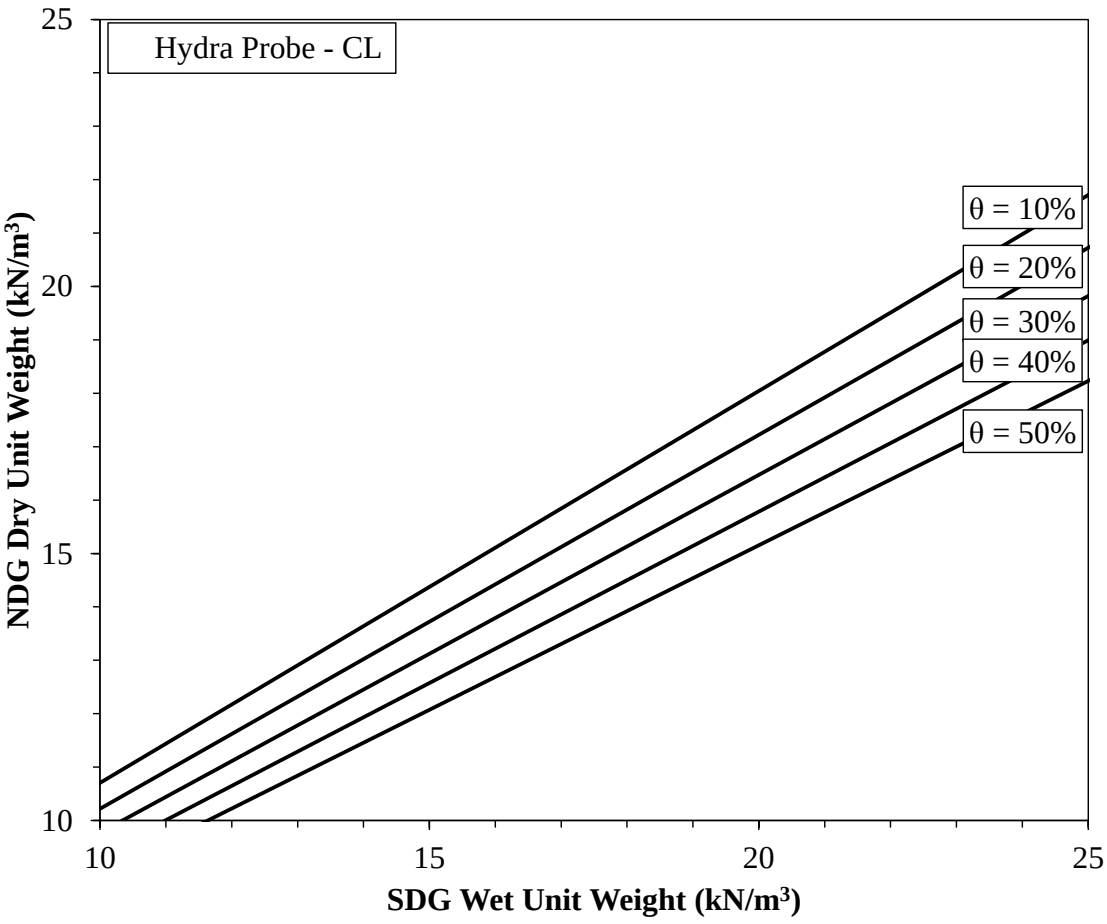

Figure B.5: Graph to obtain an NDG dry unit weight: Theta Probe – CL

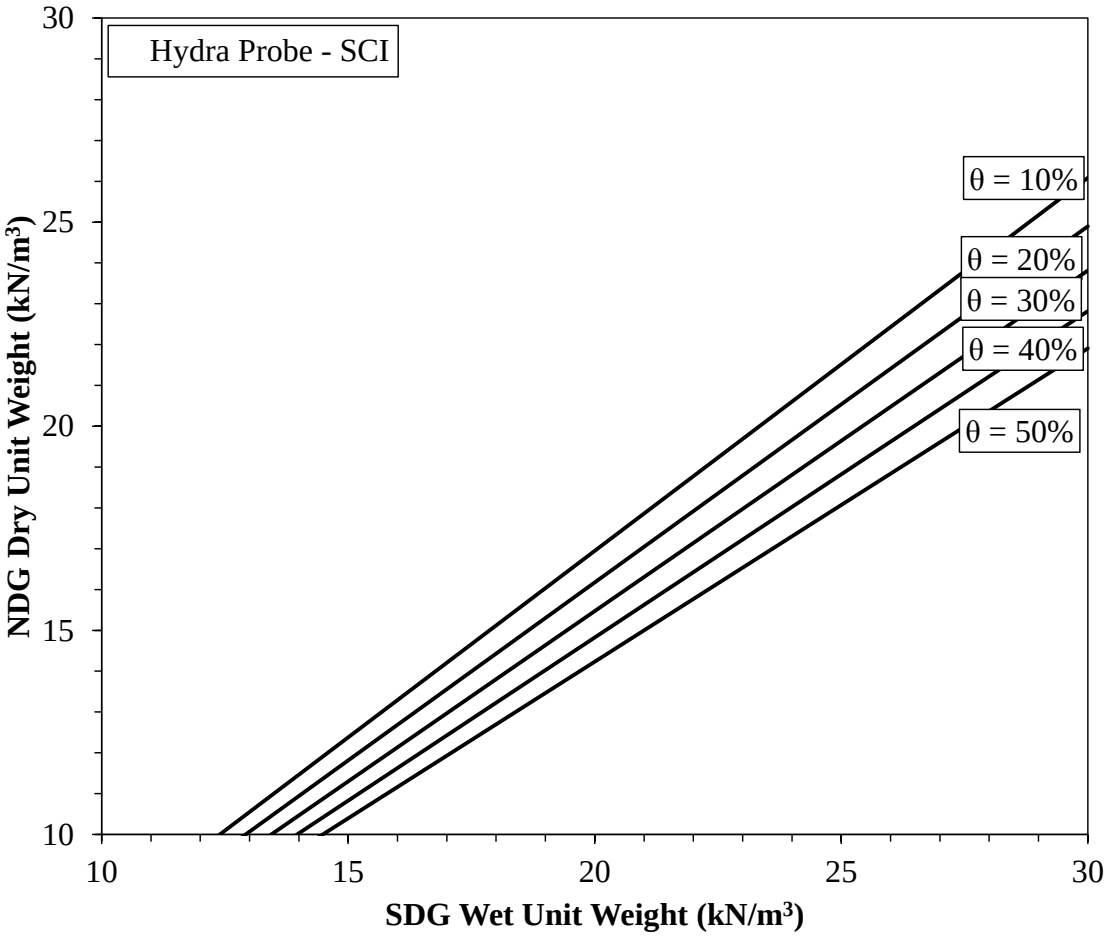

Figure B.6: Graph to obtain an NDG dry unit weight: Theta Probe – SCI

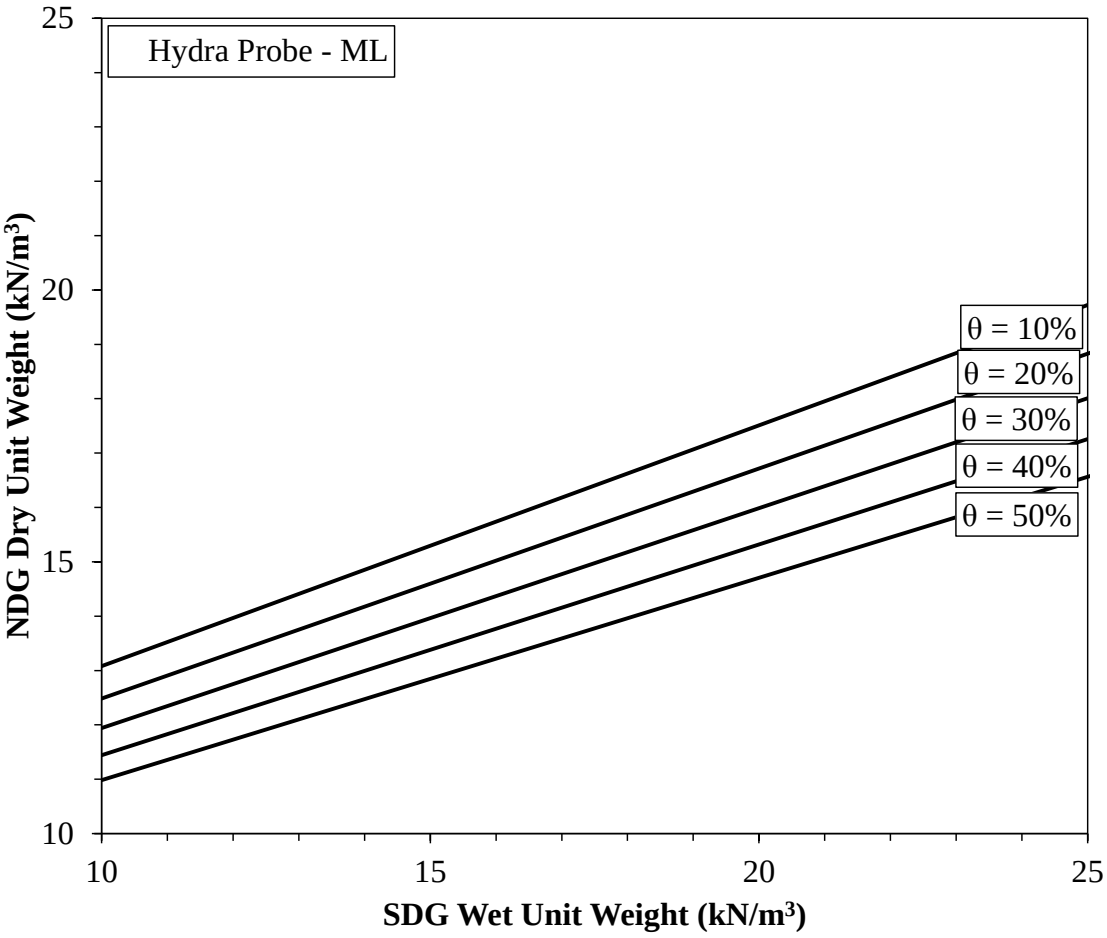

Figure B.7: Graph to obtain an NDG dry unit weight: Theta Probe – ML

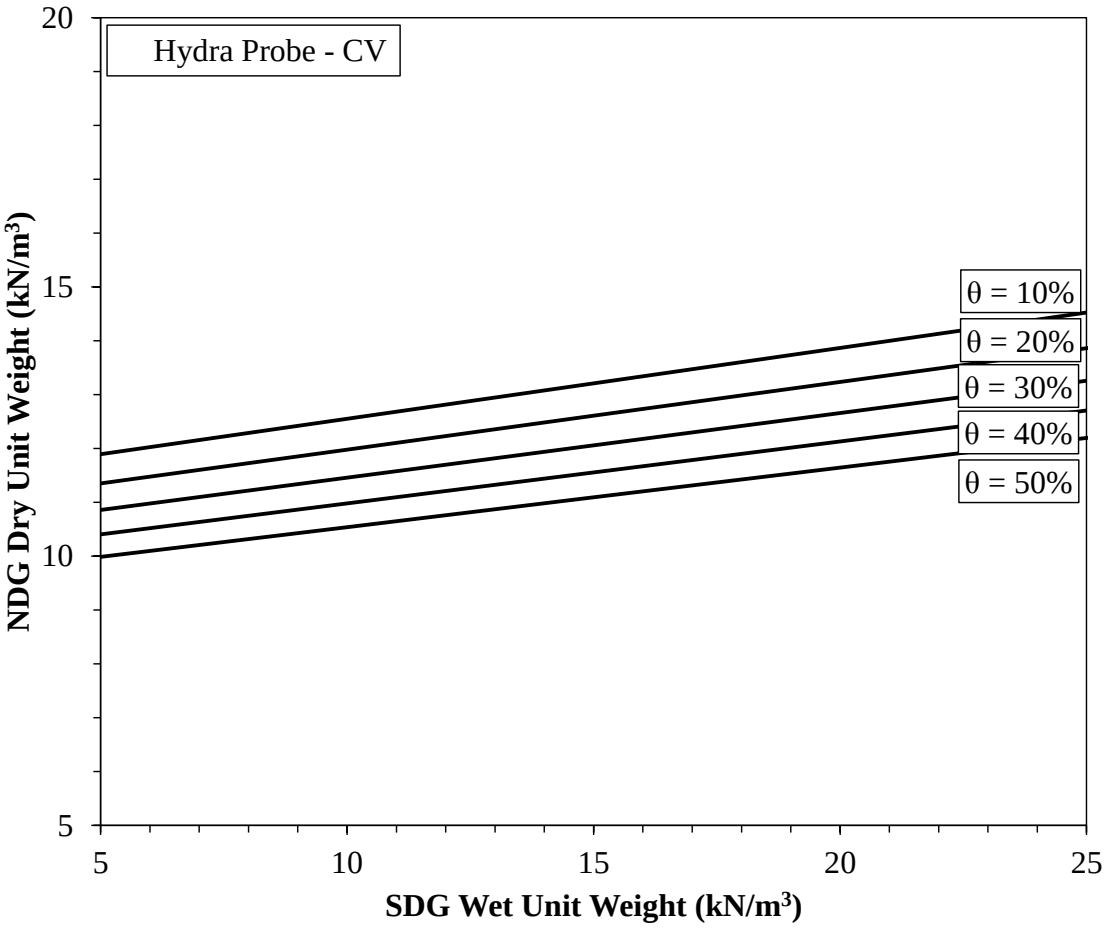

Figure B.8: Graph to obtain an NDG dry unit weight: Theta Probe – CV

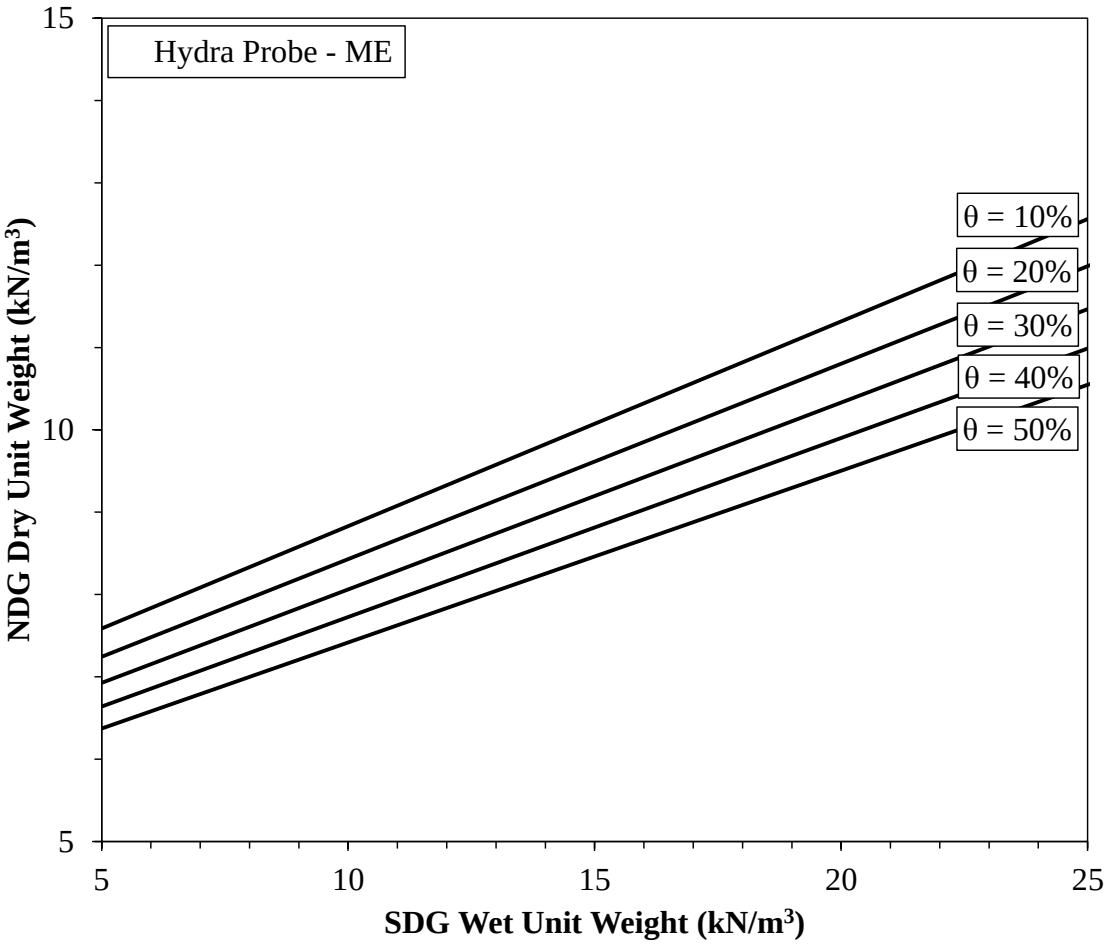

Figure B.9: Graph to obtain an NDG dry unit weight: Theta Probe – ME

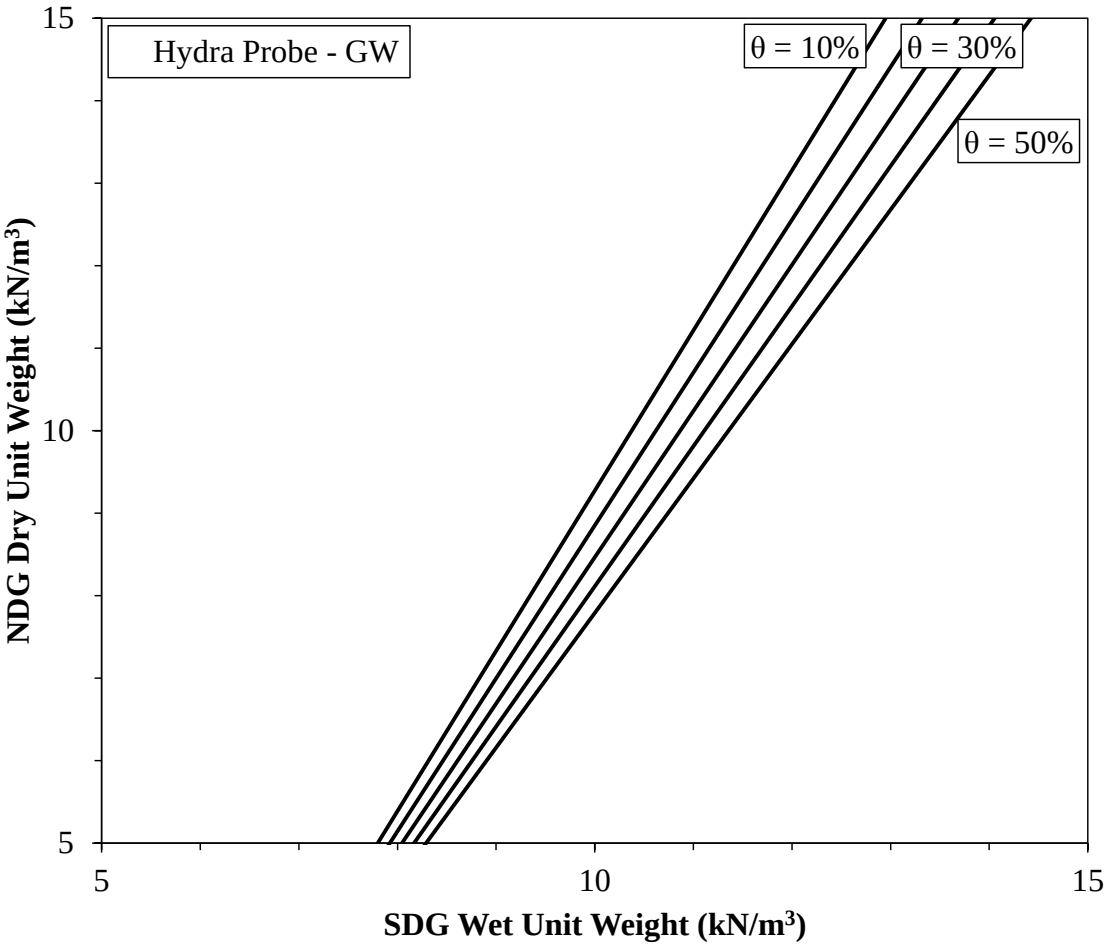

Figure B.10: Graph to obtain an NDG dry unit weight: Theta Probe – GW

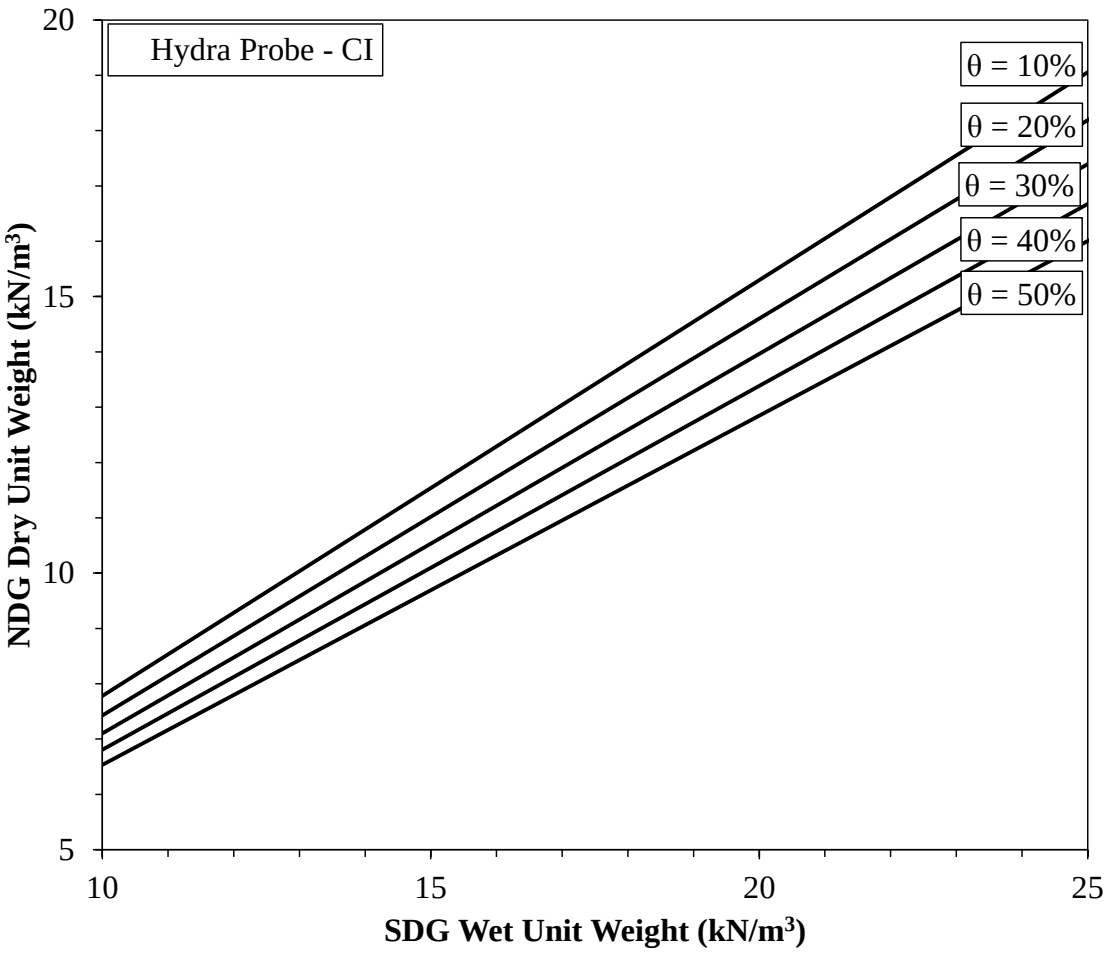

Figure B.11: Graph to obtain an NDG dry unit weight: Theta Probe – CI

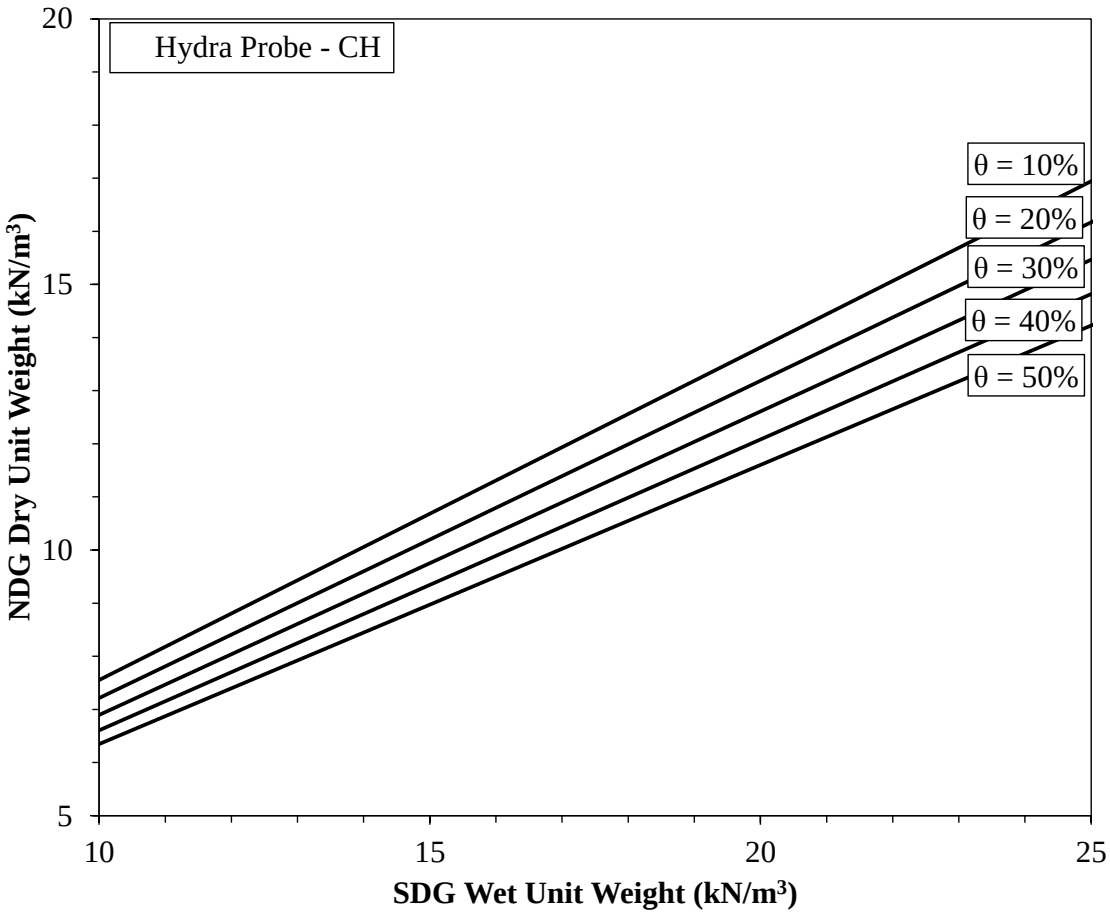

Figure B.12: Graph to obtain an NDG dry unit weight: Theta Probe – CH

Appendix C

Graphs to Obtain Equivalent NDG Wet Unit Weights from outputted SDG Wet Unit Weights along with Confidence Interval Graphs.

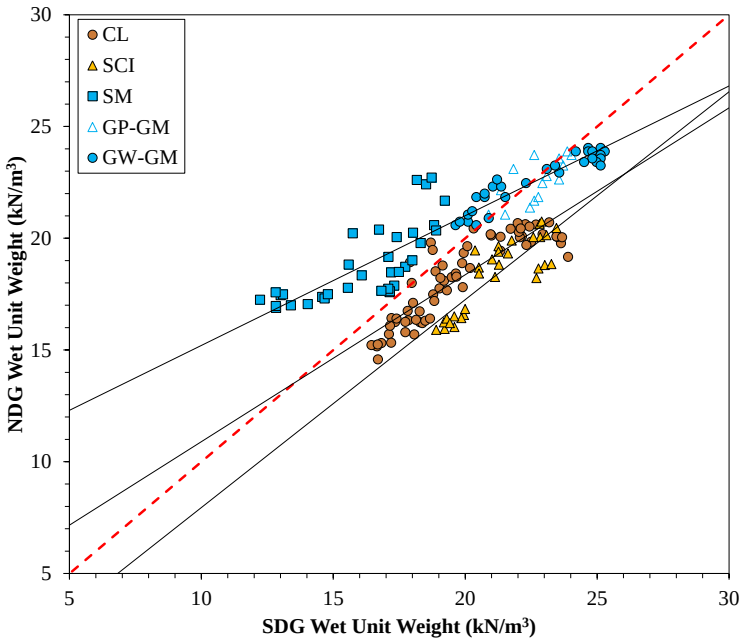

Figure C.1: Soil-specific trend lines of soil types CL, SCI, SM, GP-GM and GW-GM

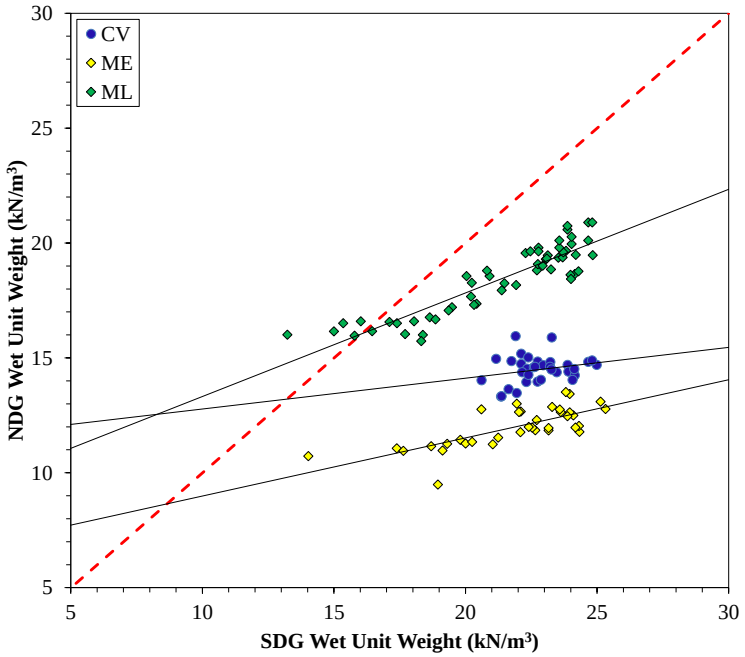

Figure C.2: Soil-specific trend lines for soil types CV, ME and ML

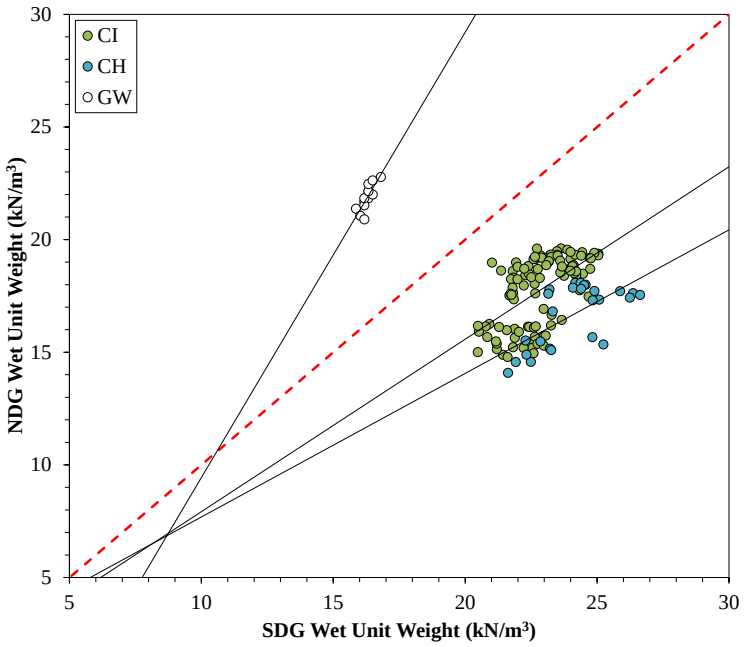

Figure C.3: Soil-specific trend lines for soil types CI, CH and GW

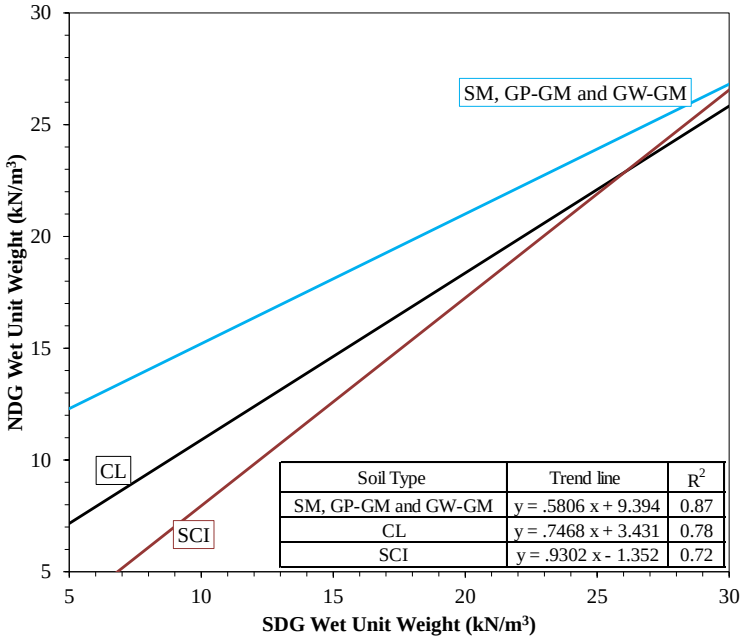

Figure C.4: Graph to obtain equivalent NDG wet unit weights from SDG wet unit weights; SM, GP-GM, GW-GM, CL, SCI

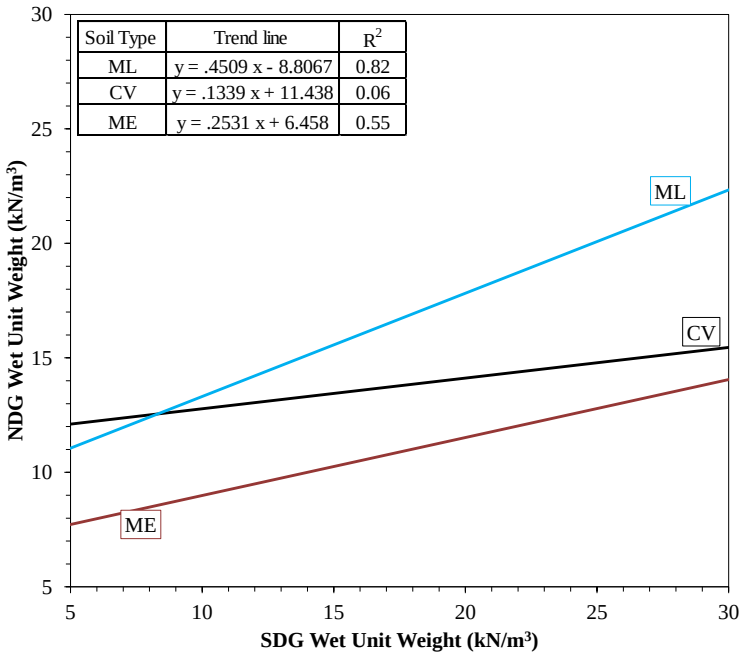

Figure C.5: Graph to obtain equivalent NDG wet unit weights from SDG wet unit weights; M, CV, ME

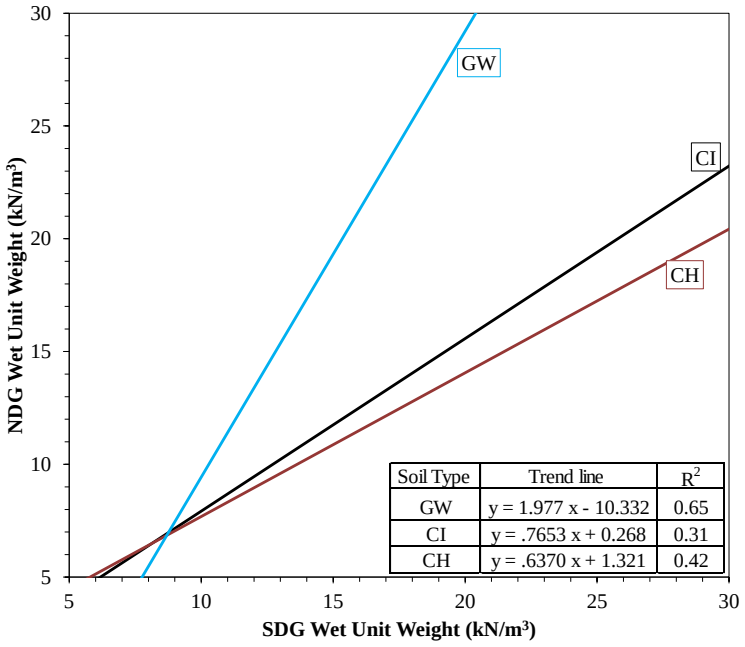

Figure C.6: Graph to obtain equivalent NDG wet unit weights from SDG wet unit weights; GW, CI, CH

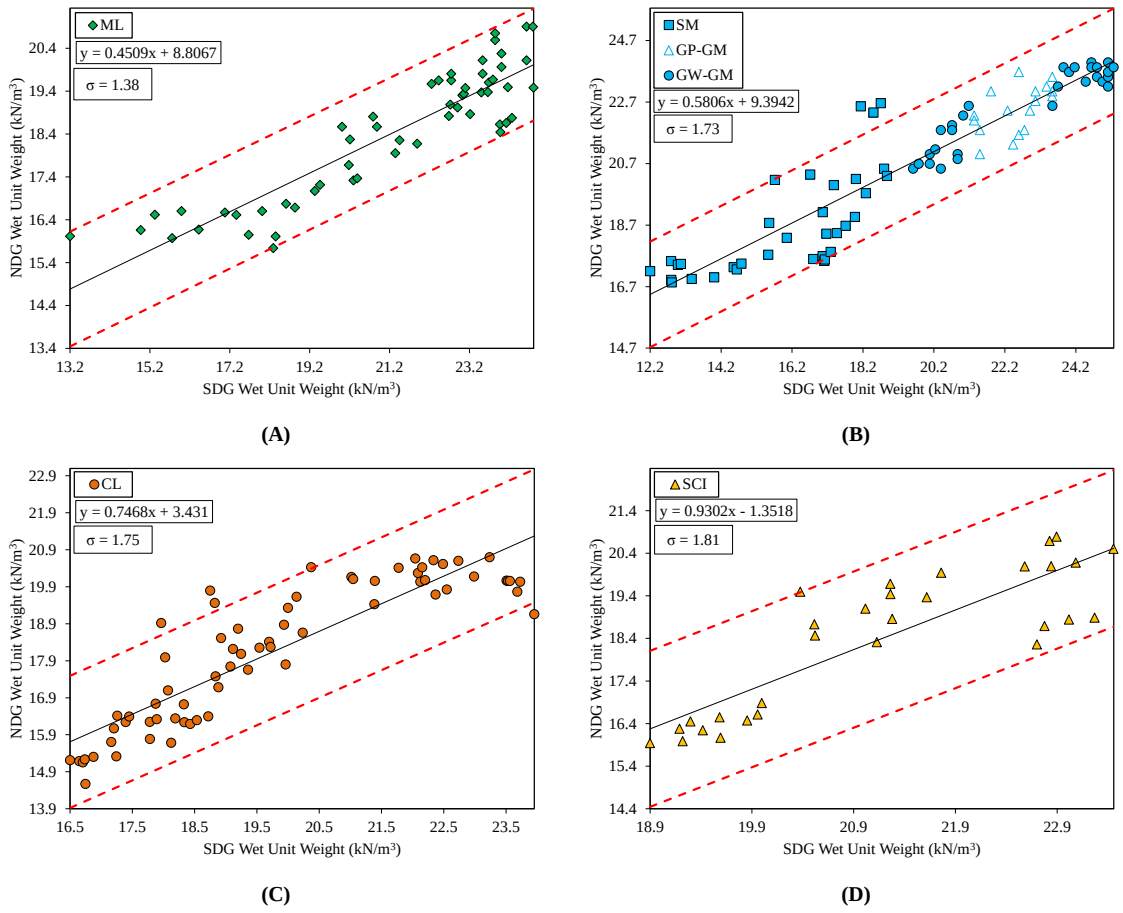

Figure C.7: 95% confidence interval graphs: (A) M; (B) SM, GP-GM, GW-GM; (C) CL; (D) SCI

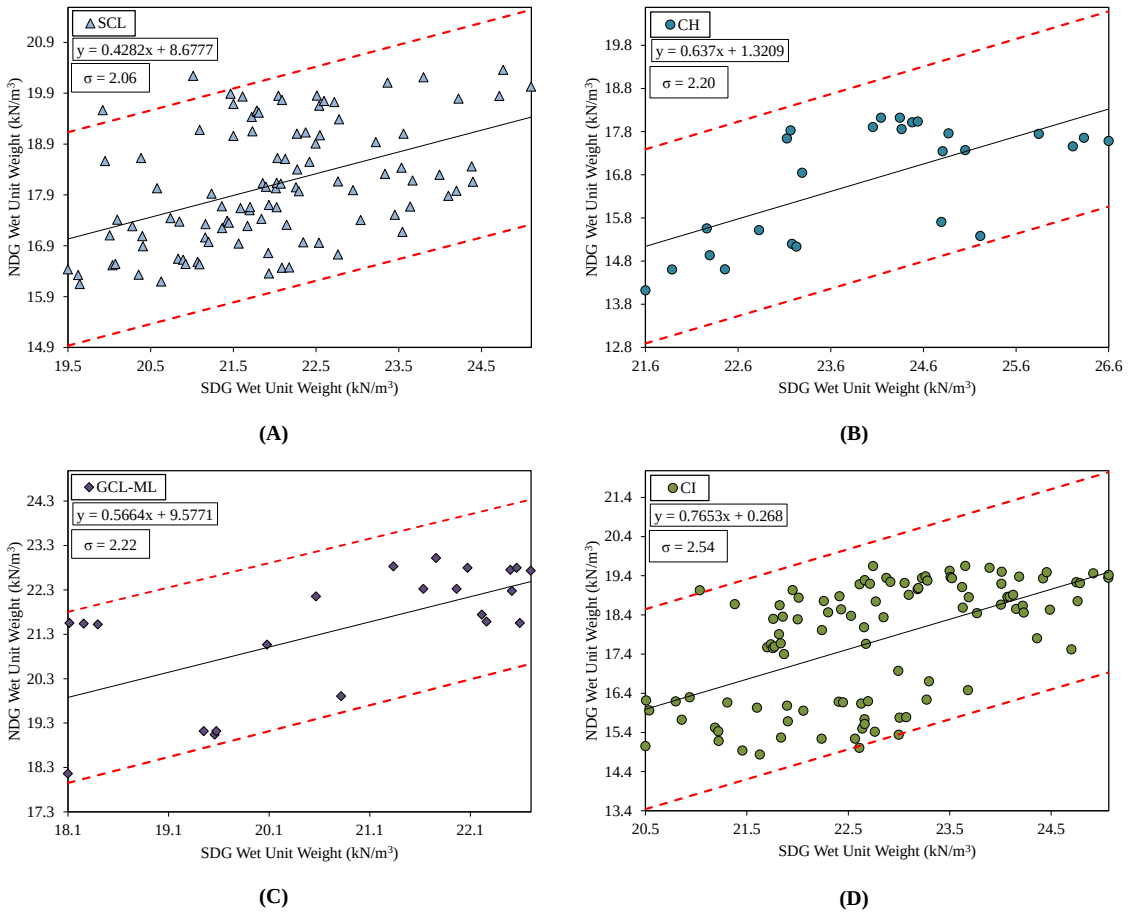

Figure C.8: 95% confidence interval graphs: (A) SCL; (B) CH; (C) GCL-ML; (D) CI

Appendix D

Moisture Probe Laboratory Calibration Data

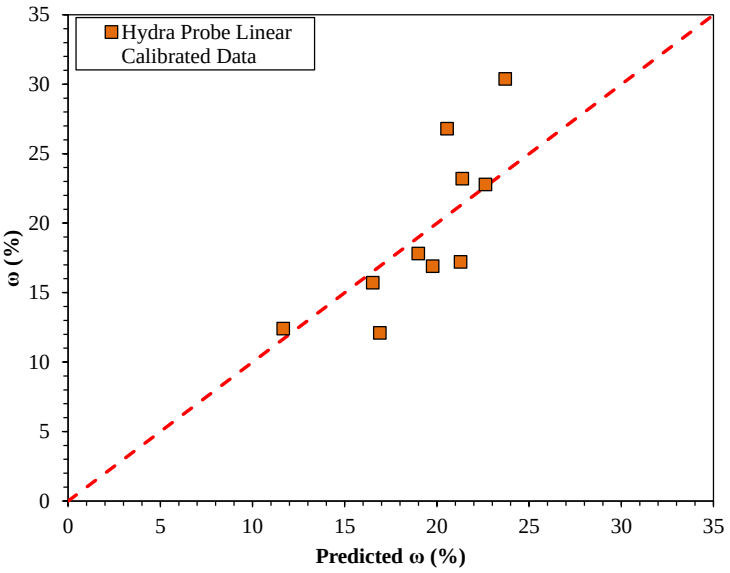

Figure D.1: Hydra Probe predicted gravimetric moisture content using linear equation

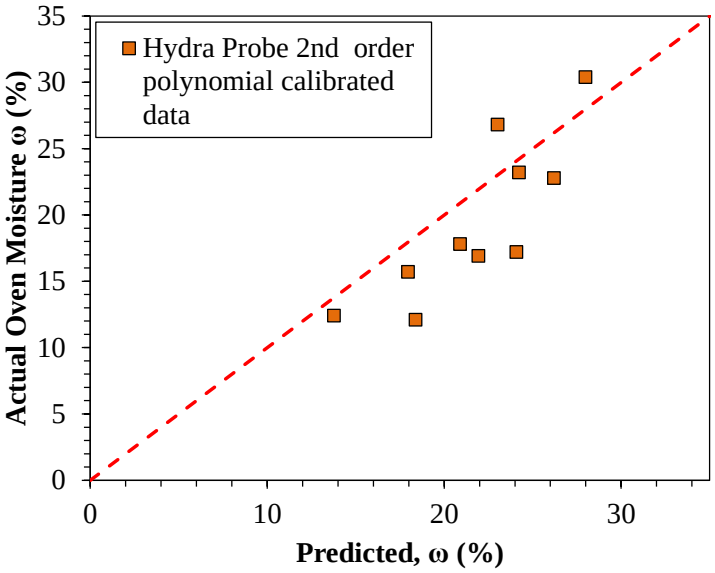

Figure D.2: Hydra Probe predicted gravimetric moisture content using 2nd order polynomial equation

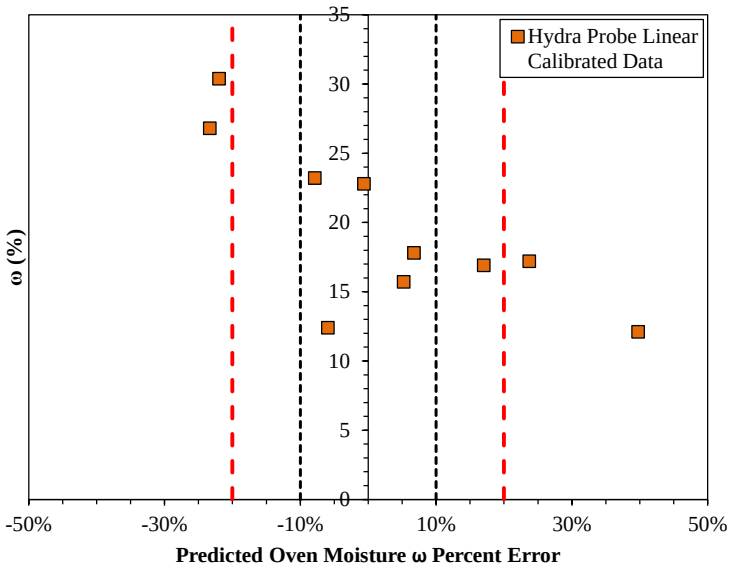

Figure D.3: Hydra Probe percent error graph of predicted gravimetric moisture content using linear equation

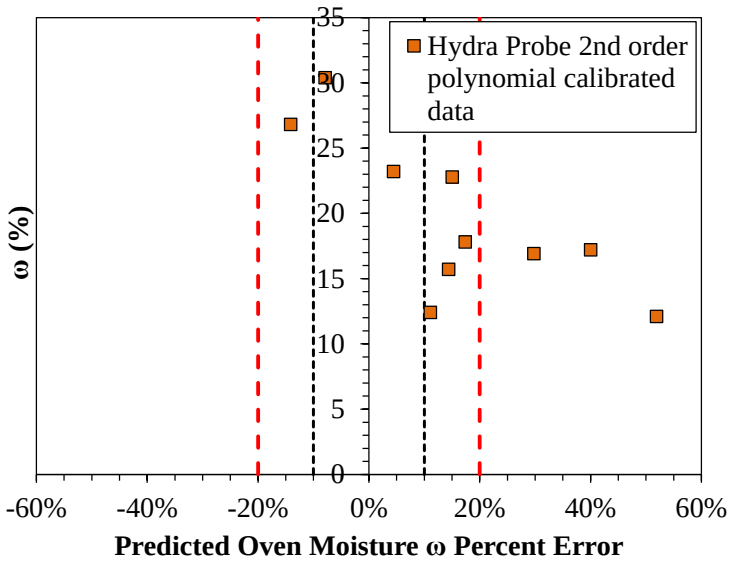

Figure D.4: Hydra Probe percent error graph of predicted gravimetric moisture content using 2nd order polynomial equation

Table D.1: 2nd order polynomial coefficients

Probe	2nd order polynomial		
	A_3	B_3	C_3
Theta Probe	0.0181	-0.3019	11.069
Hydra Probe	0.0091	-0.0495	10.006

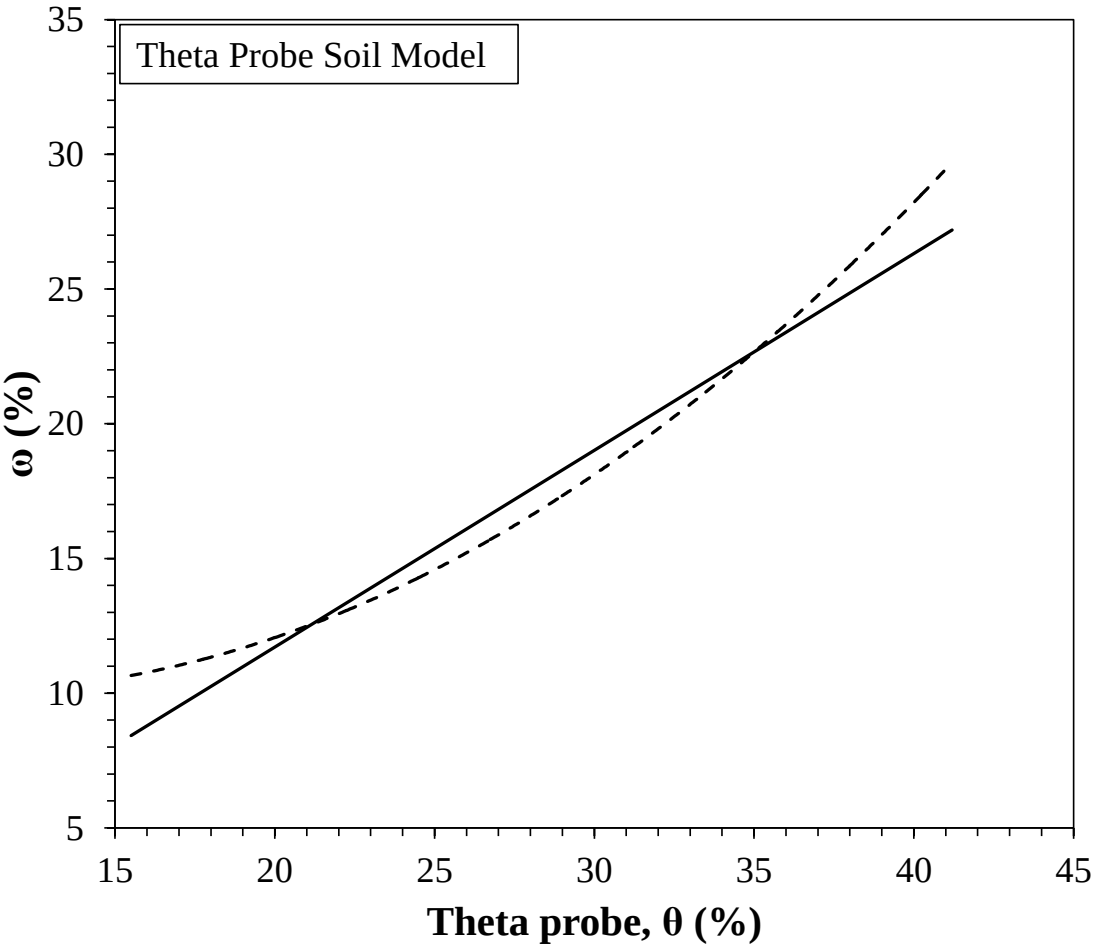

Figure D.5: General Moisture Content Trend Line for the Theta Probe

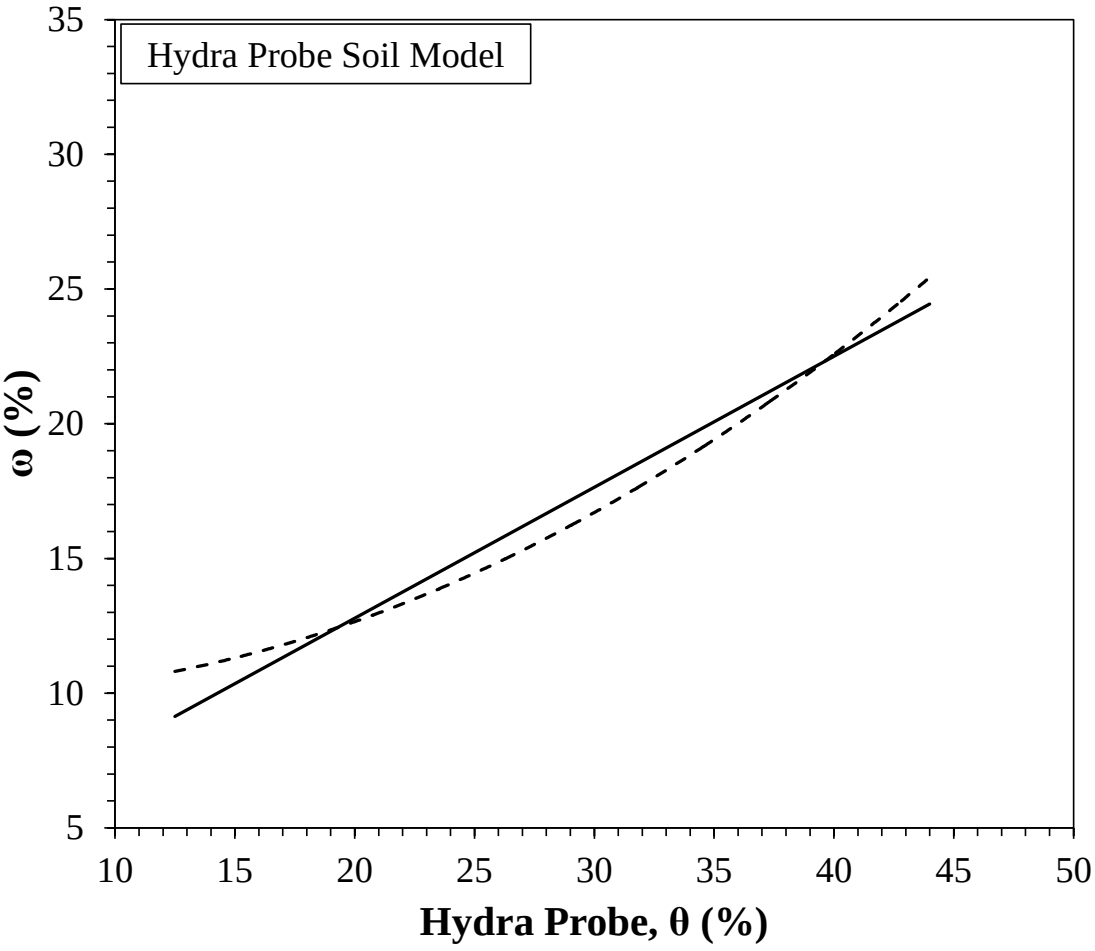

Figure D.6: General Moisture Content Trend Line for the Hydra Probe

Appendix E

Soil Material Property Calculations

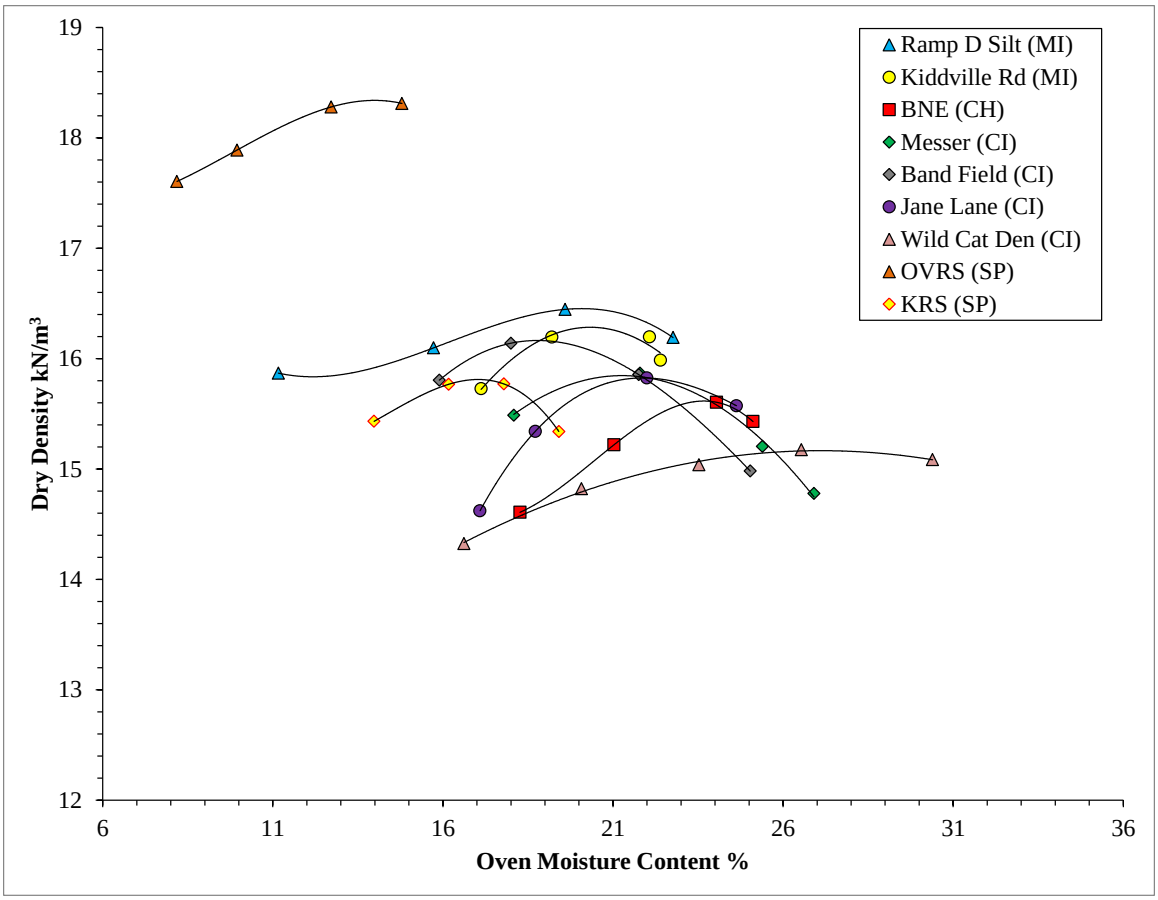

Figure E.1: Proctor point data for each of the laboratory tested soils

	Wild Cat Den Plasticity Index
Soil Source:	Sample for the Research of Joshua Wells
Sample Location:	Test Site #2 On Campus
Soil Sample Description:	Greyish Brown Clay

Plastic Limit (PL)

	Trial 1	Trial 2	Trial 3
Weight of Tin	31.98	32.51	
Weight of Tin + Wet Soil	42.93	43.86	
Weight of Tin + Dry Soil	41.3	42.1	
Weight of Water	1.63	1.76	
Weight of Solids	9.32	9.59	
Water Content	17.5%	18.4%	

PL = 18%

Liquid Limit (LL)

Blow Count	14	36	28
Weight of Tin	31.89	32.08	31.98
Weight of Tin + Wet Soil	56.84	57.89	56.28
Weight of Tin + Dry Soil	50	51.3	49.7
Weight of Water	6.84	6.59	6.58
Weight of Solids	18.11	19.22	17.72
Water Content	37.8%	34.3%	37.1%

LL = 36%

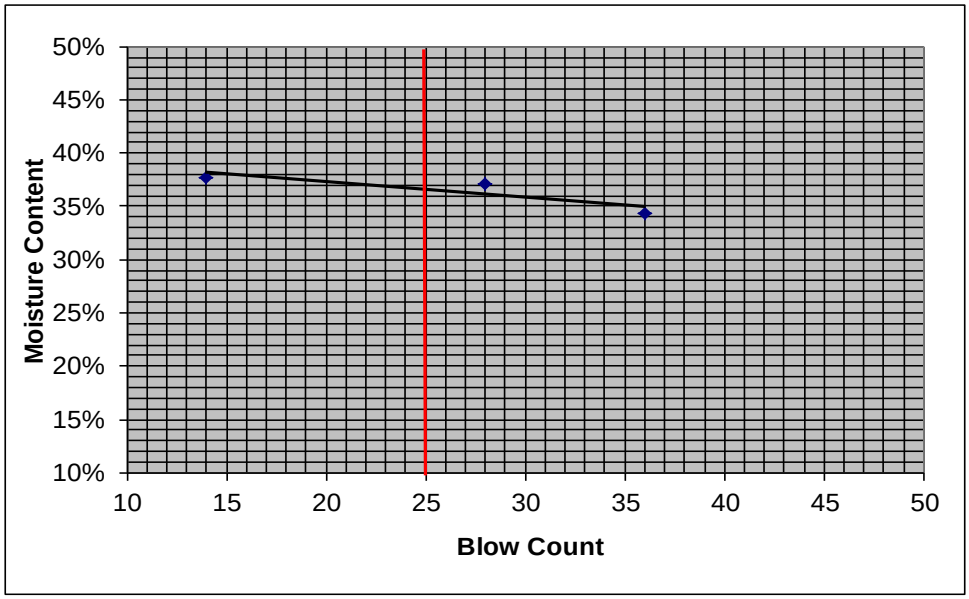

Plasticity Index = LL - PL = **18**

Figure E.2: Atterberg limit test for Wild Cat Den

	Band (Stoll) Field Plasticity Index
Soil Source:	Sample for the Research of Joshua Wells
Sample Location:	Test Site #1 On Campus
Soil Sample Description:	Greyish Brown Clay

Plastic Limit (PL)

	Trial 1	Trial 2	Trial 3
Weight of Tin	32.04	32.52	
Weight of Tin + Wet Soil	45.95	44.45	
Weight of Tin + Dry Soil	43.3	42.1	
Weight of Water	2.65	2.35	
Weight of Solids	11.26	9.58	
Water Content	23.5%	24.5%	

PL = 24%

Liquid Limit (LL)

Blow Count	35	16	24
Weight of Tin	32.54	32.31	32
Weight of Tin + Wet Soil	61.32	53.08	57.55
Weight of Tin + Dry Soil	53.8	47.4	50.6
Weight of Water	7.52	5.68	6.95
Weight of Solids	21.26	15.09	18.6
Water Content	35.4%	37.6%	37.4%

LL = 37%

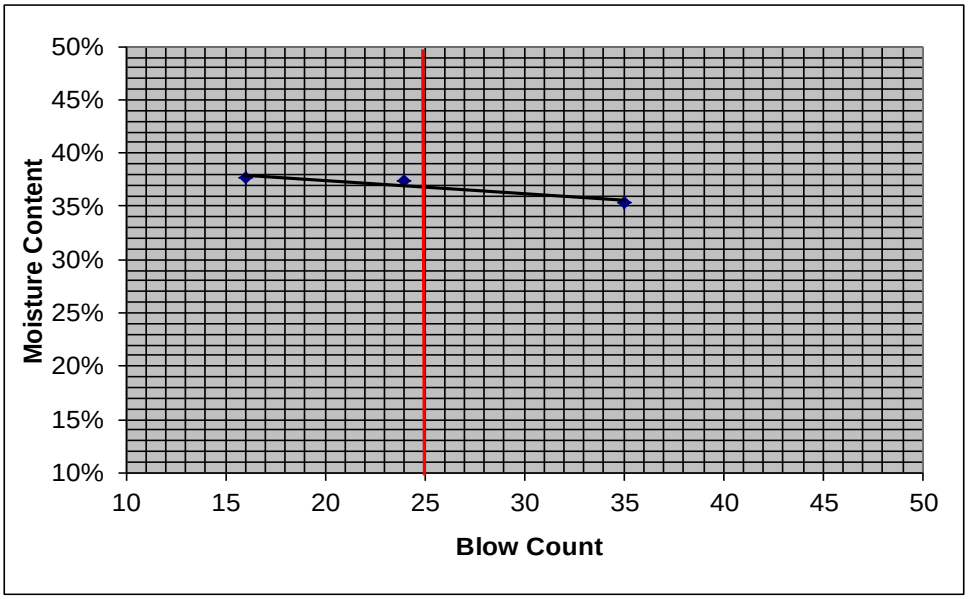

Plasticity Index = LL - PL = **13**

Figure E.3: Atterberg limit test for Band Stoll Field

	Jane Lane Elementary Plasticity Index
Soil Source:	Sample for the Research of Joshua Wells
Sample Location:	Test Site #2
Soil Sample Description:	Greyish Brown Clay

Plastic Limit (PL)

	Trial 1	Trial 2	Trial 3
Weight of Tin	32.38	32	31.8
Weight of Tin + Wet Soil	41.91	39.06	39.56
Weight of Tin + Dry Soil	40.14	37.79	38.13
Weight of Water	1.77	1.27	1.43
Weight of Solids	7.76	5.79	6.33
Water Content	22.8%	21.9%	22.6%

PL = 22%

Liquid Limit (LL)

Blow Count	34	19	10
Weight of Tin	32.36	31.81	31.7
Weight of Tin + Wet Soil	46.71	51.18	52.77
Weight of Tin + Dry Soil	42.78	45.44	46.33
Weight of Water	3.93	5.74	6.44
Weight of Solids	10.42	13.63	14.63
Water Content	37.7%	42.1%	44.0%

LL = 41%

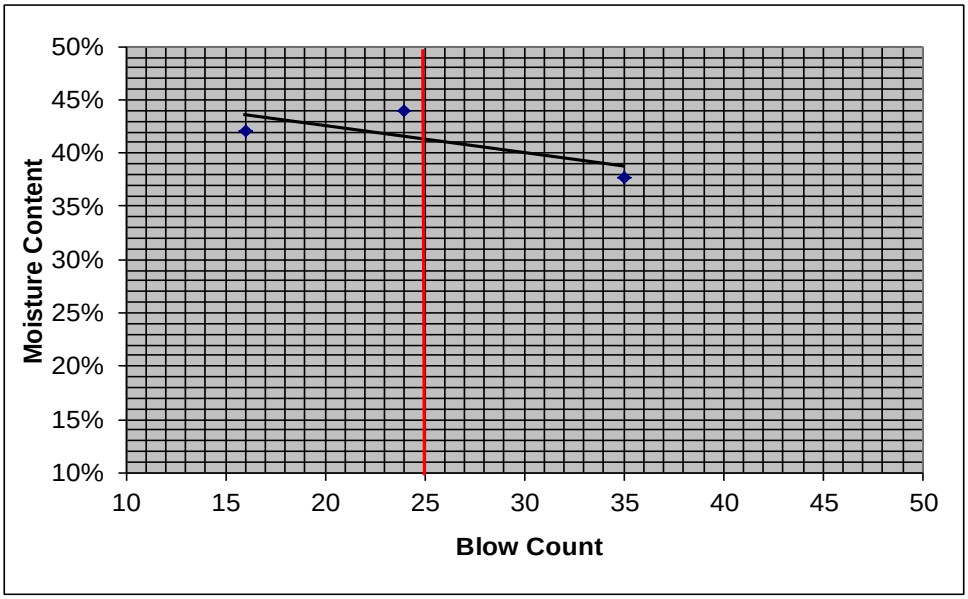

Plasticity Index = LL - PL = **19**

Figure E.4: Atterberg limit test for Jane Lane

	Ramp D Silt Plasticity Index
Soil Source:	Sample for the Research of Joshua Wells
Sample Location:	Test Site #2
Soil Sample Description:	Greenish Grey Silt

Plastic Limit (PL)

10 w 11

	Trial 1	Trial 2	Trial 3
Weight of Tin	32.55	18.18	24.76
Weight of Tin + Wet Soil	40.54	26.92	33.98
Weight of Tin + Dry Soil	38.7	24.92	31.9
Weight of Water	1.84	2	2.08
Weight of Solids	6.15	6.74	7.14
Water Content	29.9%	29.7%	29.1%

PL = 30%

Liquid Limit (LL)

GR ASH 145

Blow Count	34	21	15
Weight of Tin	31.72	31.76	31.81
Weight of Tin + Wet Soil	47.1	48.39	49.07
Weight of Tin + Dry Soil	42.3	42.94	43.23
Weight of Water	4.8	5.45	5.84
Weight of Solids	10.58	11.18	11.42
Water Content	45.4%	48.7%	51.1%

LL = 48%

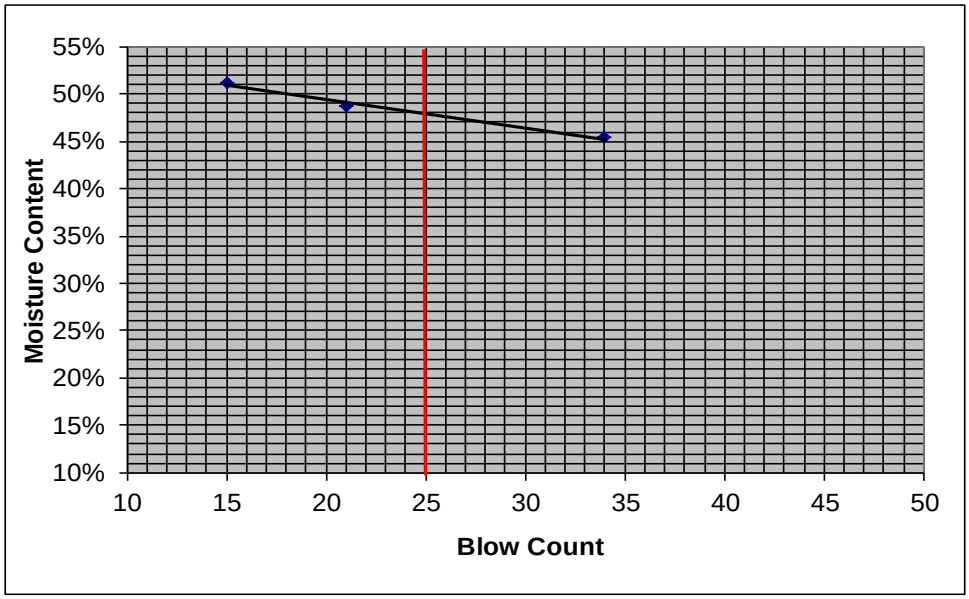

Plasticity Index = LL - PL = **19**

Figure E.5: Atterberg limit test for Ramp D Silt

	Kiddville Rd. Plasticity Index
Soil Source:	Sample for the Research of Joshua Wells
Sample Location:	Test Site #2
Soil Sample Description:	Greyish Brown Clay

Plastic Limit (PL)

	23	81 B1	
	Trial 1	Trial 2	Trial 3
Weight of Tin	31.8	31.74	33.15
Weight of Tin + Wet Soil	41.83	42.8	41.17
Weight of Tin + Dry Soil	39.9	40.59	39.56
Weight of Water	1.98	2.21	1.61
Weight of Solids	8.1	8.85	6.41
Water Content	24.4%	25.0%	25.1%

PL = 25%

Liquid Limit (LL)

	9 D		
Blow Count	35	19	
Weight of Tin	32.86	32.65	
Weight of Tin + Wet Soil	48.44	52.44	
Weight of Tin + Dry Soil	44.48	47.1	
Weight of Water	3.96	5.34	0
Weight of Solids	11.62	14.45	0
Water Content	34.1%	37.0%	#DIV/0!

LL = 36%

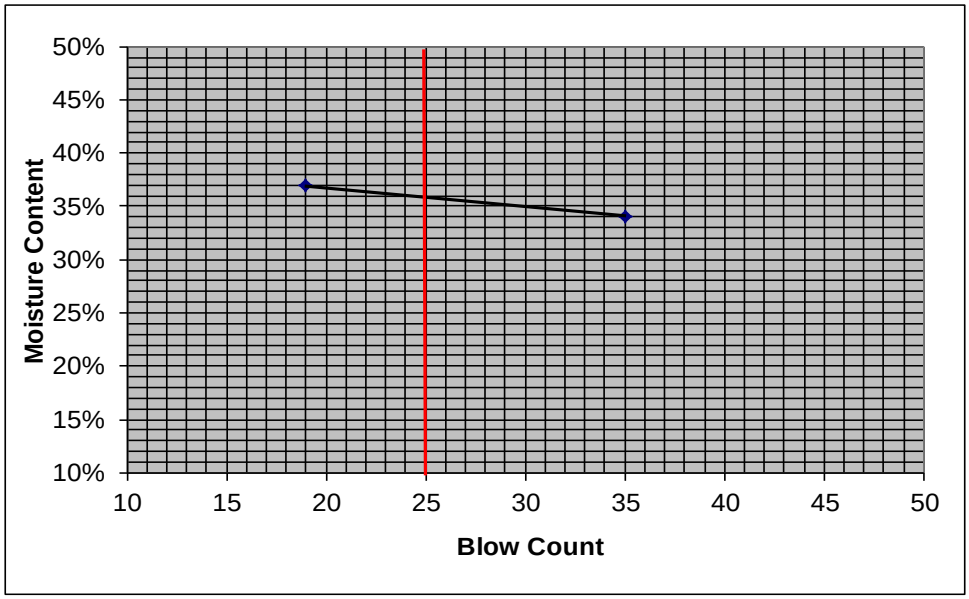

Plasticity Index = LL - PL = **11**

Figure E.6: Atterberg limit test for Kiddville Road

	BNE Plasticity Index
Soil Source:	Sample for the Research of Joshua Wells
Sample Location:	Test Site #2
Soil Sample Description:	Greyish Brown Clay

Plastic Limit (PL)

10 81 B1

	Trial 1	Trial 2	Trial 3
Weight of Tin	32.55	31.74	33.15
Weight of Tin + Wet Soil	41.86	42.86	43.12
Weight of Tin + Dry Soil	39.78	40.34	40.91
Weight of Water	2.08	2.52	2.21
Weight of Solids	7.23	8.6	7.76
Water Content	28.8%	29.3%	28.5%

PL = 29%

Liquid Limit (LL)

9 D 145

Blow Count	34	24	15
Weight of Tin	32.86	32.65	31.81
Weight of Tin + Wet Soil	46.22	49.33	51.22
Weight of Tin + Dry Soil	41.39	43.26	44.08
Weight of Water	4.83	6.07	7.14
Weight of Solids	8.53	10.61	12.27
Water Content	56.6%	57.2%	58.2%

LL = 57%

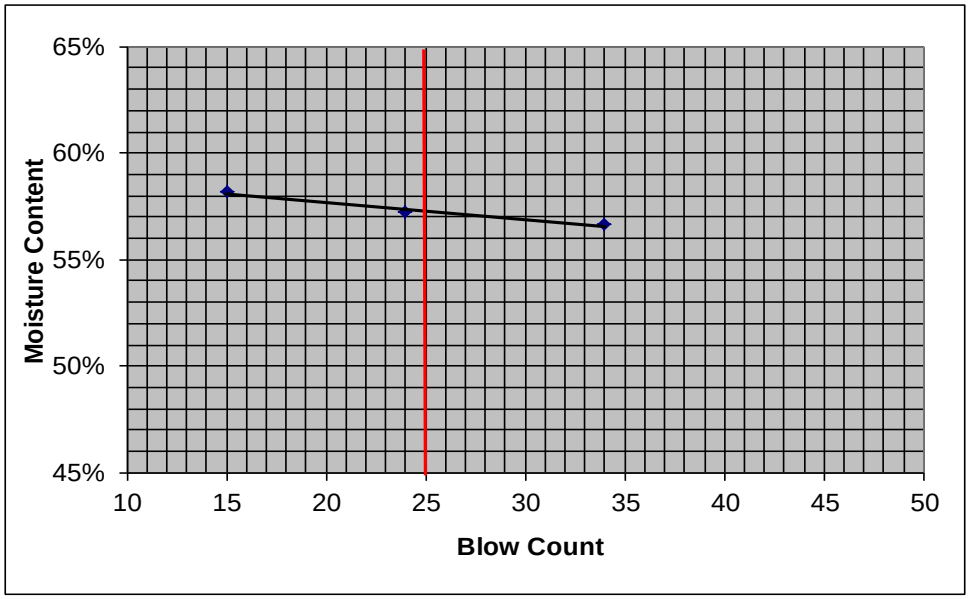

Plasticity Index = LL - PL = **28**

Figure E.7: Atterberg limit test for BNE

	Messer Plasticity Index
Soil Source:	Sample for the Research of Joshua Wells
Sample Location:	Test Site #2
Soil Sample Description:	Greyish Brown Clay

Plastic Limit (PL)

23 B1 11

	Trial 1	Trial 2	Trial 3
Weight of Tin	31.8	33.15	24.76
Weight of Tin + Wet Soil	39.56	38.99	39.2
Weight of Tin + Dry Soil	37.9	37.75	36.2
Weight of Water	1.66	1.24	3
Weight of Solids	6.1	4.6	11.44
Water Content	27.2%	27.0%	26.2%

PL = 27%

Liquid Limit (LL)

GR ASH D

Blow Count	37	26	16
Weight of Tin	31.72	31.76	32.65
Weight of Tin + Wet Soil	48.25	46.22	47.16
Weight of Tin + Dry Soil	43.25	41.6	42.4
Weight of Water	5	4.62	4.76
Weight of Solids	11.53	9.84	9.75
Water Content	43.4%	47.0%	48.8%

LL = 46%

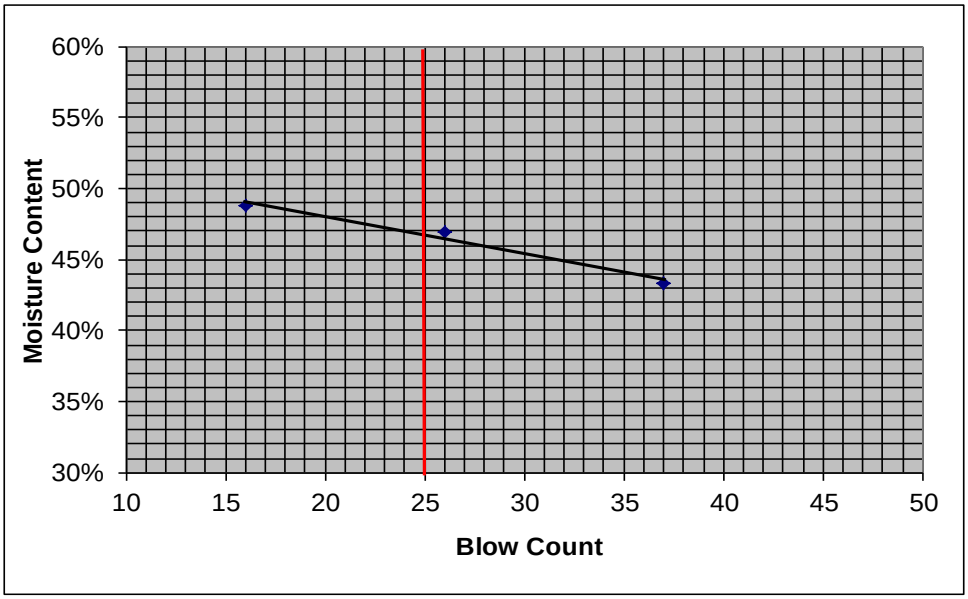

Plasticity Index = LL - PL = **20**

Figure E.8: Atterberg limit test for Messer

Table E.1: Specific gravity test for Wild Cat Den

Specific Gravity							
Soil Description	Wild Cat Den		Wild Cat Den		Wild Cat Den		
Pecometer Number	1		2		3		
Nominal Pycometer Volume	500	ml	500	ml	500	ml	
Oven Dry Weight of Soil	53.69	g	54.6	g	56.42	g	
Weight of Pycometer+ Water	663.7	g	659.7	g	661.4	g	2.82
Weight of Pycometer+ Water+Soil	698.34	g	694.71	g	698.14	g	
Temperature	21	deg. Cels	21	deg. Cels	21	deg. Cels	
Correction Factor K	0.998		0.998		0.998		
Specific Gravity	2.81		2.78		2.86		
Time							

Table E.2: Specific gravity test for Band Stoll Field

Specific Gravity							
Soil Description	Stoll Field		Stoll Field		Stoll Field		
Pecometer Number	1		2		3		
Nominal Pycometer Volume	500	ml	500	ml	500	ml	
Oven Dry Weight of Soil	50.9	g	51.8	g	53.28	g	
Weight of Pycometer+ Water	663.7	g	659.7	g	661.4	g	2.68
Weight of Pycometer+ Water+Soil	695.78	g	692.24	g	694.65	g	
Temperature	21	deg. Cels	21	deg. Cels	21	deg. Cels	
Correction Factor K	0.998		0.998		0.998		
Specific Gravity	2.70		2.68		2.65		
Time							

Table E.3: Specific gravity test for Jane Lane

Specific Gravity											
Soil Description	Jane Lane		Jane Lane		Jane Lane		Jane Lane		Jane Lane		
Pecometer Number	1		2		3		2		3		
Nominal Pycometer Volume	500	ml	500	ml	500	ml	500	ml	500	ml	
Oven Dry Weight of Soil	22.56	g	23.98	g	24.6	g	53.67	g	52.5	g	
Weight of Pycometer+ Wat	663.7	g	659.7	g	661.4	g	659.7	g	661.4	g	2.68
Weight of Pycometer+ Wat	677.77	g	674.69	g	676.7	g	693.63	g	694.59	g	
Temperature	21	deg. Ce	21	deg. Ce	21	deg. Ce	21	deg. Ce	21	deg. Ce	
Correction Factor K	0.998		0.998		0.998		0.998		0.998		
Specific Gravity	2.65		2.66		2.64		2.71		2.71		
Time											

Table E.4: Specific gravity test for Ramp D Silt

Specific Gravity						
Soil Description	Ramp D Silt		Ramp D Silt		Ramp D Silt	
Pecometer Number	A		B		5	
Nominal Pycometer Volume	500	ml	500	ml	500	ml
Oven Dry Weight of Soil	53.1	g	51.25	g	51.8	g
Weight of Pycometer+ Water	679.75	g	679.26	g	679.22	g
Weight of Pycometer+ Water+Soi	713.86	g	712.42	g	712.6	g
Temperature	21	deg. Cels	21	deg. Cels	21	deg. Cels
Correction Factor K	0.998		0.998		0.998	
Specific Gravity	2.79		2.83		2.81	
Time						

2.81

Table E.5: Specific gravity test for Kiddville Road

Specific Gravity						
Soil Description	Kiddville Rd.		Kiddville Rd.		Kiddville Rd.	
Pecometer Number	A		B		5	
Nominal Pycometer Volume	500	ml	500	ml	500	ml
Oven Dry Weight of Soil	56.2	g	51.72	g	55.01	g
Weight of Pycometer+ Water	679.75	g	679.26	g	679.22	g
Weight of Pycometer+ Water+Soi	715.38	g	712.26	g	714.15	g
Temperature	21	deg. Cels	21	deg. Cels	21	deg. Cels
Correction Factor K	0.998		0.998		0.998	
Specific Gravity	2.73		2.76		2.73	
Time						

2.74

Table E.6: Specific gravity test for BNE

Specific Gravity						
Soil Description	BNE		BNE		BNE	
Pecometer Number	A		B		5	
Nominal Pycometer Volume	500	ml	500	ml	500	ml
Oven Dry Weight of Soil	50.8	g	51.82	g	46.63	g
Weight of Pycometer+ Water	679.75	g	679.26	g	679.22	g
Weight of Pycometer+ Water+Soi	712.23	g	712.36	g	708.83	g
Temperature	20	deg. Cels	20	deg. Cels	20	deg. Cels
Correction Factor K	1		1		1	
Specific Gravity	2.77		2.77		2.74	
Time						

2.76

Table E.7: Specific gravity test for Messer

Specific Gravity							
Soil Description	Messer		Messer		Messer		
Pecometer Number	1		2		3		
Nominal Pycometer Volume	500	ml	500	ml	500	ml	
Oven Dry Weight of Soil	50.19	g	49.99	g	50.83	g	
Weight of Pycometer+ Water	663.7	g	659.7	g	661.4	g	2.77
Weight of Pycometer+ Water+Soil	695.67	g	691.76	g	693.99	g	
Temperature	21	deg. Cels	21	deg. Cels	21	deg. Cels	
Correction Factor K	0.998		0.998		0.998		
Specific Gravity	2.75		2.78		2.78		
Time							

Table E.8: Specific gravity test for OVRS

Specific Gravity									
Soil Description	OVRS		OVRS		OVRS		OVRS		
Pecometer Number	2		3		4		5		
Nominal Pycometer Volume	500	ml	500	ml	500	ml	500	ml	
Oven Dry Weight of Soil	27.3	g	28.5	g	76.3	g	51.4	g	
Weight of Pycometer+ Water	677	g	671.1	g	677	g	677	g	2.73
Weight of Pycometer+ Water+Soil	694.4	g	689.2	g	724.9	g	709.7	g	
Temperature	20.8	deg. Cels	20.9	deg. Cels	20	deg. Cels	20	deg. Cels	
Correction Factor K	0.999		0.999		0.9999		0.999		
Specific Gravity	2.75		2.74		2.69		2.75		
Time									

Table E.9: Specific gravity test for KRS

Specific Gravity							
Soil Description	KRS		KRS		KRS		
Pecometer Number	1		2		3		
Nominal Pycometer Volume	500	ml	500	ml	500	ml	
Oven Dry Weight of Soil	99.5	g	96.3	g	88.7	g	
Weight of Pycometer+ Water	665	g	660.7	g	662.6	g	2.69
Weight of Pycometer+ Water+Soil	727.4	g	721.1	g	718.4	g	
Temperature	20	deg. Cels	20	deg. Cels	20	deg. Cels	
Correction Factor K	1		1		1		
Specific Gravity	2.68		2.68		2.70		
Time							

Table E.10: Hydrometer analysis for Wild Cat Den

Soil	Wild Cat Den
Location of Project	Lexington
Descripton	Silt
Tested By	Joshua Wells

Hydrometer Analysis

Hydrometer Type	H-4242		Zero Correction		-1.2	Meniscus	2
Dispersing Agent	Hexametaphosphate		Amount Used		4% & 125 ml		
Specific Gravity	2.85		Cf a=	0.9592	ω	-	%
Mass of Soil (dry)	50	g	% Finer	75	Sieve no.	200	

Time of Reading	Elapsed time, min	Temp C°	Actual Hydro Reading R_a	Corr. Hydro Reading R_c	Act/Adj % Finer	% Finer adjusted	L from Table 6-5	L/t	K from table 6-4	D, mm
7:30	0	First Reading Not Shown								
7:32	2	21	26.8	28	40.3	60.4299	9.3	4.65	0.0134	0.0289
7:34	4	21	25.5	26.7	38.4	57.6242	9.55	2.3875	0.0134	0.02071
7:38	8	21	24.5	25.7	37.0	55.466	9.85	1.23125	0.0134	0.01487
7:46	16	21	22.9	24.1	34.7	52.0129	10.22	0.63875	0.0134	0.01071
8:00	30	21	21	22.2	31.9	47.9123	10.7	0.35667	0.0134	0.008
8:30	60	21	19.9	21.1	30.4	45.5382	11	0.18333	0.0134	0.00574
9:30	120	21	19	20.2	29.1	43.5958	11.3	0.09417	0.0134	0.00411
	2.00									
12:30	300	21	17.5	18.7	26.9	40.3585	11.65	0.03883	0.0133	0.00262
	5									
4:00	510	21	17	18.2	26.2	39.2794	11.8	0.02314	0.0133	0.00202
	8.5									
11:00	1650	21	16.5	17.7	25.5	38.2003	11.75	0.00712	0.0133	0.00112
	27.5									
10:30	3030	21	16	17.2	24.7	37.1212	11.95	0.00394	0.0133	0.00084
	50.5									

Table E.11: Hydrometer analysis for Band Stoll Field

Soil	Stoll Field
Location of Project	Lexington
Descripton	Silt
Tested By	Joshua Wells

Hydrometer Analysis

Hydrometer Type	H-4242		Zero Correction		-1.2	Meniscus	2
Dispersing Agent	Hexametaphosphate		Amount Used		4% & 125 ml		
Specific Gravity	2.68		Cf a=	0.99326	ω	-	%
Mass of Soil (dry)	50	g	% Finer	87.5	Sieve no.	200	

Time of Reading	Elapsed time, min	Temp C°	Actual Hydro Reading R_a	Corr. Hydro Reading R_c	Act/Adj % Finer	% Finer adjusted	L from Table 6-5	L/t	K from table 6-4	D, mm
7:35	0	First Reading Not Shown								
7:37	2	21	28.8	30.2	52.5	91.8643	8.7	4.35	0.0134	0.02795
7:39	4	21	27	28.2	49.0	85.7805	9.2	2.3	0.0134	0.02032
7:43	8	21	25	26.2	45.5	79.6968	9.7	1.2125	0.0134	0.01476
7:51	16	21	21.5	22.7	39.5	69.0503	10.6	0.6625	0.0134	0.01091
8:05	30	21	19	20.2	35.1	61.4456	11.3	0.37667	0.0134	0.00822
8:35	60	21	16	17.2	29.9	52.32	12.1	0.20167	0.0134	0.00602
9:35	120	21	14.8	16	27.8	48.6698	12.4	0.10333	0.0134	0.00431
	2.00									
12:35	300	21	13	14.2	24.7	43.1945	12.9	0.043	0.0133	0.00276
	5									
4:35	540	21	12	13.2	22.9	40.1526	13.1	0.02426	0.0133	0.00207
	9									
9:35	1560	21	11	12.2	21.2	37.1107	13.4	0.00859	0.0133	0.00123
	26									
7:35	2850	21	10	11.2	19.5	34.0689	13.7	0.00481	0.0133	0.00092
	47.5									

Table E.12: Hydrometer analysis for Jane Lane

Soil	Jane Lane Elementary
Location of Project	Lexington
Descripton	Lean Clay
Tested By	Joshua Wells

Hydrometer Analysis

Hydrometer Type	H-4242		Zero Correction		-1.2	Meniscus	2	
Dispersing Agent	Hexametaphosphate		Amount Used		4% & 125 ml			
Specific Gravity	2.69		Cf a=	0.99107	ω	-	%	
Mass of Soil (dry)	50	g	% Finer	80.5	Sieve no.	200		

Time of Reading	Elapsed time, min	Temp C°	Actual Hydro Reading R_a	Corr. Hydro Reading R_c	Act/Adj % Finer	% Finer adjusted	L from Table 6-5	L/t	K from table 6-4	D, mm
9:45	0	First Reading Not Shown								
9:47	2	20	29	30.2	48.2	77.5822	8.3	4.15	0.0138	0.02811
9:49	4	20	26.5	27.7	44.2	71.1599	9	2.25	0.0138	0.0207
9:53	8	19.8	24.2	25.4	40.5	65.2513	9.8	1.225	0.0138	0.01527
10:01	16	19.8	21.9	23.1	36.9	59.3427	10.2	0.6375	0.0138	0.01102
10:15	30	19.8	19.5	20.7	33.0	53.1772	10.9	0.3633	0.0138	0.00832
10:45	60	19.8	15.5	16.7	26.6	42.9014	11.9	0.1983	0.0138	0.00615
11:45	120	20	14.2	15.4	24.6	39.5618	12.2	0.1017	0.0138	0.0044
	2.00									
3:15	330	21	12.8	14.2	22.7	36.4791	12.5	0.0379	0.0136	0.00265
	5.5									
9:45	720	20.5	12	13.2	21.1	33.9101	12.8	0.0178	0.0136	0.00181
	12									
9:45	1440	20.5	10.9	12.1	19.3	31.0843	13.1	0.0091	0.0136	0.0013
	24									
10:15	2850	21	10	11.4	18.2	29.286	13.25	0.0046	0.0136	0.00093
	47.5									

Table E.13: Hydrometer analysis for Ramp D Silt

Soil	Ramp D Silt
Location of Projec	Winchester
Descripton	Lean Clay
Tested By	Joshua Wells

Hydrometer Analysis

Hydrometer Type	H-4242		Zero Correction		-1.2	Meniscus	1
Dispersing Agent	Hexametaphosphate		Amount Used		4% & 125 ml		
Specific Gravity	2.81		Cf a=	0.9666	ω	-	%
Mass of Soil (dry)	50	g	% Finer	79.5	Sieve no.	200	

Time of Reading	Elapsed time, min	Temp C°	Actual Hydro Reading R_a	Corr. Hydro Reading R_c	Act/Adj % Finer	% Finer adjusted	L from Table 6-5	L/t	K from table 6-4	D, mm
9:40	0	First Reading Not Shown								
9:42	2	20	31	32.2	49.5	78.6893	7.8	3.9	0.0131	0.02587
9:44	4	19.5	28.5	29.5	45.3	72.0912	8.5	2.125	0.0131	0.0191
9:48	8	20	27.5	28.7	44.1	70.1362	8.7	1.0875	0.0131	0.01366
9:56	16	20	25.8	27	41.5	65.9817	9.2	0.575	0.0131	0.00993
10:10	30	20	24	25.2	38.7	61.583	9.65	0.32167	0.0131	0.00743
10:40	60	19.8	22.5	23.55	36.2	57.5507	10.1	0.16833	0.0131	0.00537
11:40	120	20.5	18.6	19.8	30.4	48.3866	11.1	0.0925	0.0129	0.00392
	2.00									
3:10	330	21	16	17.4	26.7	42.5216	11.6	0.03515	0.0129	0.00242
	5.5									
9:40	720	20.5	14.2	15.4	23.7	37.634	12.5	0.01736	0.0129	0.0017
	12									
9:40	1440	20.5	12.8	14	21.5	34.2128	12.95	0.00899	0.0129	0.00122
	24									
10:10	2850	21	11.5	12.9	19.8	31.5246	13.2	0.00463	0.0129	0.00088
	47.5									

Table E.14: Hydrometer analysis for Kiddville Rd

Soil	Kiddville Rd
Location of Project	Lexington
Descripton	Silt
Tested By	Joshua Wells

Hydrometer Analysis

Hydrometer Type	H-4242		Zero Correction		-1.2	Meniscus	2
Dispersing Agent	Hexametaphosphate		Amount Used		4% & 125 ml		
Specific Gravity	2.74		Cf a=	0.98048	ω	-	%
Mass of Soil (dry)	50	g	% Finer	86.6	Sieve no.	200	

Time of Reading	Elapsed time, min	Temp C°	Actual Hydro Reading R_a	Corr. Hydro Reading R_c	Act/Adj % Finer	% Finer adjusted	L from Table 6-5	L/t	K from table 6-4	D, mm
7:35	0	First Reading Not Shown								
7:37	2	20	29	30.2	51.3	88.8264	8.3	4.15	0.0134	0.0273
7:39	4	20	27.9	29.1	49.4	85.591	8.6	2.15	0.0134	0.01965
7:43	8	20	26	27.2	46.2	80.0026	9.1	1.1375	0.0134	0.01429
7:51	16	20	23.8	25	42.5	73.5318	9.7	0.60625	0.0134	0.01043
8:05	30	20	21.9	23.1	39.2	67.9434	10.2	0.34	0.0134	0.00781
8:35	60	20.5	19.5	20.7	35.2	60.8843	10.8	0.18	0.0134	0.00569
9:35	120	20.5	16.1	17.3	29.4	50.884	12.1	0.10083	0.0134	0.00426
	2.00									
12:35	300	20.5	14.9	16.1	27.3	47.3545	12.3	0.041	0.0133	0.00269
	5									
4:35	540	21	13.5	14.9	25.3	43.8249	12.75	0.02361	0.0133	0.00204
	9									
9:35	1560	21	12	13.4	22.8	39.413	13.1	0.0084	0.0133	0.00122
	26									
7:35	2850	21	9.5	10.9	18.5	32.0599	13.5	0.00474	0.0133	0.00092
	47.5									

Table E.15: Hydrometer analysis for BNE

Soil	BNE
Location of Project	Lexington
Descripton	Fat Clay
Tested By	Joshua Wells

Hydrometer Analysis

Hydrometer Type	H-4242		Zero Correction		-1.2	Meniscus	1
Dispersing Agent	Hexametaphosphate		Amount Used		4% & 125 ml		
Specific Gravity	2.76		Cf a=	0.97642	ω	-	%
Mass of Soil (dry)	50	g	% Finer	89.25	Sieve no.	200	

Time of Reading	Elapsed time, min	Temp C°	Actual Hydro Reading R_a	Corr. Hydro Reading R_c	Act/Adj % Finer	% Finer adjusted	L from Table 6-5	L/t	K from table 6-4	D, mm
7:30	0	First Reading Not Shown								
7:32	2	20	27.8	29	50.5	90.2213	8.6	4.3	0.0133	0.02758
7:34	4	20	26.8	28	48.8	87.1102	8.9	2.225	0.0133	0.01984
7:38	8	20	25.4	26.6	46.4	82.7547	9.3	1.1625	0.0133	0.01434
7:46	16	20	23.9	25.1	43.7	78.0881	9.7	0.60625	0.0133	0.01036
8:00	30	20	22.6	23.8	41.5	74.0437	10.05	0.335	0.0133	0.0077
8:30	60	20.5	21.1	22.3	38.9	69.377	10.4	0.17333	0.0132	0.0055
9:30	120	20.5	19.8	21	36.6	65.3326	10.7	0.08917	0.0132	0.00394
	2.00									
12:30	300	20.5	18	19.2	33.5	59.7327	11.25	0.0375	0.0132	0.00256
	5									
4:30	540	21	16.8	18.2	31.7	56.6216	11.5	0.0213	0.0131	0.00191
	9									
9:30	1560	21	15.2	16.6	28.9	51.6439	12.25	0.00785	0.0131	0.00116
	26									
7:30	2850	21	14	15.4	26.8	47.9106	12.75	0.00447	0.0131	0.00088
	47.5									

Table E.16: Hydrometer analysis for Messer

Soil	Messer
Location of Project	Lexington
Descripton	Silt
Tested By	Joshua Wells

Hydrometer Analysis

Hydrometer Type	H-4242		Zero Correction		-1.2	Meniscus	2
Dispersing Agent	Hexametaphosphate		Amount Used		4% & 125 ml		
Specific Gravity	2.77		Cf a=	0.97442	ω	-	%
Mass of Soil (dry)	50	g	% Finer	74.01	Sieve no.	200	

Time of Reading	Elapsed time, min	Temp C°	Actual Hydro Reading R_a	Corr. Hydro Reading R_c	Act/Adj % Finer	% Finer adjusted	L from Table 6-5	L/t	K from table 6-4	D, mm
7:35	0	First Reading Not Shown								
7:37	2	21	30.2	31.4	45.3	78.4409	7.95	3.975	0.013	0.02592
7:39	4	21	28	29.2	42.1	72.945	8.9	2.225	0.013	0.01939
7:43	8	21	26.1	27.3	39.4	68.1986	9.4	1.175	0.013	0.01409
7:51	16	21	23.8	25	36.1	62.4529	10.05	0.62813	0.013	0.0103
8:05	30	21	21	22.2	32.0	55.4582	10.7	0.35667	0.013	0.00776
8:35	60	21	19.2	20.4	29.4	50.9616	11.28	0.188	0.013	0.00564
9:35	120	21	18	19.2	27.7	47.9639	11.5	0.09583	0.013	0.00402
	2.00									
12:35	300	21	16.5	17.7	25.5	44.2167	11.95	0.03983	0.013	0.00259
	5									
4:35	540	21	15	16.2	23.4	40.4695	12.3	0.02278	0.013	0.00196
	9									
10:35	1620	21	13.1	14.3	20.6	35.7231	12.88	0.00795	0.013	0.00116
	27									
10:35	3035	21	12.2	13.4	19.3	33.4748	13.4	0.00442	0.013	0.00086
	50.5833									

Table E.17: Particle size analysis and specific surface area for Wild Cat Den

Wild Cat Den Particle Size Analysis						Specific Surface Area			
Sieve Number	Opening (mm)	Weight Retained Each Sieve (g)	Weight of Soil Retained (g)	Weight of Soil Passed (g)	Percent Finer	Proportion of total by mass P %	Angularity factor f	Specific Surface mm^{-1}	$(P/100)*(S^2)*f$
1/2"	12.1	0.00	0.00	208.68	100.000				
3/8"	9.500	17.89	17.89	190.79	91.427	8.573	1	0.55962	0.0427
No. 4	4.750	36.71	54.60	154.08	73.836	17.592	1	0.89319	0.2232
No. 10	2.000	3.89	58.49	150.19	71.971	1.864	1	1.94666	0.11234
No. 20	0.850	8.55	67.04	141.64	67.874	4.097	1	4.60179	1.37986
No. 40	0.425	5.83	72.87	135.81	65.081	2.794	1	9.98268	4.4277
No. 60	0.250	2.23	75.10	133.58	64.012	1.069	1	18.4072	5.75829
No. 100	0.150	1.69	76.79	131.89	63.202	0.810	1	30.9839	12.3644
No. 140	0.106	0.80	77.59	131.09	62.819	0.383	1	47.5831	13.8042
No. 200	0.075	0.84	78.43	130.25	62.416	0.403	1	67.2927	28.9888
Pan	0.000	130.25	208.68	0.00	0.000				
	Total	208.68							
Hydrometer Reading	0.0289				60.4299	1.986	1	128.886	524.736
	0.02071				57.6242	2.806	1	245.3	2684.9
	0.01487				55.466	2.158	1	341.959	4013.63
	0.01071				52.0129	3.453	1	475.474	12415.5
	0.008				47.9123	4.101	1	648.109	27393
	0.00574				45.5382	2.374	1	885.463	29602.1
	0.00411				43.5958	1.942	1	1235.27	47136.3
	0.00262				40.3585	3.237	1	1827.67	171979
	0.00202				39.2794	1.079	1	2605.68	116520
	0.00112				38.2003	1.079	1	3981.83	272098
	0.00084				37.1212	1.079	1	6196.98	659051
						Total mm^{-2}			1343419

Table E.18: Particle size analysis and specific surface area for Band Stoll Field

Stoll Field Particle Size Analysis						Specific Surface Area			
Sieve Number	Opening (mm)	Weight Retained Each Sieve (g)	Weight of Soil Retained (g)	Weight of Soil Passed (g)	Percent Finer	Proportion of total by mass P %	Angularity factor f	Specific Surface mm^{-1}	$(P/100)*(S^2)*f$
3/8"	9.500	0.00	0.00	205.14	100.000				
No. 4	4.750	0.18	0.18	204.96	99.912	0.088	1	0.89319	0.00106
No. 10	2.000	1.12	1.30	203.84	99.366	0.546	1	1.94666	0.03138
No. 20	0.850	2.93	4.23	200.91	97.938	1.428	1	4.60179	0.45875
No. 40	0.425	2.96	7.19	197.95	96.495	1.443	1	9.98268	2.18095
No. 60	0.250	2.84	10.03	195.11	95.111	1.384	1	18.4072	7.11461
No. 100	0.150	3.56	13.59	191.55	93.375	1.735	1	30.9839	25.2686
No. 140	0.106	1.83	15.42	189.72	92.483	0.892	1	47.5831	30.6348
No. 200	0.075	1.69	17.11	188.03	91.659	0.824	1	67.2927	56.5824
Pan	0.000	188.03	205.14	0.00	0.000				
	Total	205.14							
Hydrometer Reading	0.02795				91.8643	0.205	1	131.053	53.3794
	0.02032				85.7805	6.084	1	251.763	5848.76
	0.01476				79.6968	6.084	1	346.493	11078.2
	0.01091				69.0503	10.647	1	472.966	36122.4
	0.00822				61.4456	7.605	1	633.521	46292.5
	0.00602				52.32	9.126	1	852.901	100686
	0.00431				48.6698	3.650	1	1178.5	76892.9
	0.00276				43.1945	5.475	1	1740.79	251659
	0.00207				40.1526	3.042	1	2510.23	290720
	0.00123				37.1107	3.042	1	3754.79	650458
	0.00092				34.0689	3.042	1	5627.76	1461236
						Total mm^{-2}			2931048

Table E.19: Particle size analysis and specific surface area for Jane Lane

Jane Lane Elementary Particle Size Analysis						Specific Surface Area			
Sieve Number	Opening (mm)	Weight Retained Each Sieve (g)	Weight of Soil Retained (g)	Weight of Soil Passed (g)	Percent Finer	Proportion of total by mass P %	Angularity factor f	Specific Surface mm^{-1}	(P/100)* (S^2)*f
3/8"	9.500	0.00	0.00	186.38	100.000				
No. 4	4.750	2.59	2.59	183.79	98.610	1.390	1	0.89319	0.01568
No. 10	2.000	9.58	12.17	174.21	93.470	5.140	1	1.94666	0.27545
No. 20	0.850	8.95	21.12	165.26	88.668	4.802	1	4.60179	1.43804
No. 40	0.425	6.01	27.13	159.25	85.444	3.225	1	9.98268	4.54427
No. 60	0.250	3.08	30.21	156.17	83.791	1.653	1	18.4072	7.91808
No. 100	0.150	2.85	33.06	153.32	82.262	1.529	1	30.9839	20.7592
No. 140	0.106	1.56	34.62	151.76	81.425	0.837	1	47.5831	26.7994
No. 200	0.075	1.56	36.18	150.20	80.588	0.837	1	67.2927	53.5988
Pan	0.032	150.20	186.38	0.00	0.000				
	Total	186.38							
Hydrometer Reading	0.02811				77.5822	3.006	1	130.668	725.76
	0.0207				71.1599	6.422	1	248.722	5618.48
	0.01527				65.2513	5.909	1	337.437	9514
	0.01102				59.3427	5.909	1	462.507	17873.7
	0.00832				53.1772	6.165	1	626.723	34246.2
	0.00615				42.9014	10.276	1	839.164	102330
	0.0044				39.5618	3.340	1	1153.79	62871
	0.00265				36.4791	3.083	1	1758.12	134750
	0.00181				33.9101	2.569	1	2738.7	272482
	0.0013				31.0843	2.826	1	3912.15	611610
	0.00093				29.286	1.798	1	5470.69	761085
						Total mm^{-2}			2013106

Table E.20: Particle size analysis and specific surface area for Ramp D Silt

Ramp D Silt Particle Size Analysis						Specific Surface Area			
Sieve Number	Opening (mm)	Weight Retained Each Sieve (g)	Weight of Soil Retained (g)	Weight of Soil Passed (g)	Percent Finer	Proportion of total by mass P %	Angularity factor f	Specific Surface mm^{-1}	$(P/100)*(S^2)*f$
3/8"	9.500	0.00	0.00	203.87	100.000				
No. 4	4.750	3.39	3.39	200.48	98.337	1.663	1	0.89319	0.01937
No. 10	2.000	7.97	11.36	192.51	94.428	3.909	1	1.94666	0.21635
No. 20	0.850	6.72	18.08	185.79	91.132	3.296	1	4.60179	1.01938
No. 40	0.425	5.16	23.24	180.63	88.601	2.531	1	9.98268	3.68346
No. 60	0.250	4.56	27.80	176.07	86.364	2.237	1	18.4072	11.0675
No. 100	0.150	5.66	33.46	170.41	83.588	2.776	1	30.9839	38.9224
No. 140	0.106	3.97	37.43	166.44	81.640	1.947	1	47.5831	64.3885
No. 200	0.075	3.87	41.30	162.57	79.742	1.898	1	67.2927	125.533
Pan	0.031	162.57	203.87	0.00	0.000				
	Total	203.87							
Hydrometer Reading	0.02587				78.6893	1.053	1	136.213	285.224
	0.0191				72.0912	6.598	1	269.944	7021.62
	0.01366				70.1362	1.955	1	371.478	3939.87
	0.00993				65.9817	4.154	1	515.057	16094.8
	0.00743				61.583	4.399	1	698.412	31334.4
	0.00537				57.5507	4.032	1	949.48	53086.2
	0.00392				48.3866	9.164	1	1306.6	228477
	0.00242				42.5216	5.865	1	1947.78	324950
	0.0017				37.634	4.888	1	2959.25	625054
	0.00122				34.2128	3.421	1	4160.93	865036
	0.00088				31.5246	2.688	1	5789.65	1315901
						Total mm^{-2}			3471181

Table E.21: Particle size analysis and specific surface area for Kiddville Rd

Kiddville Rd. Particle Size Analysis						Specific Surface Area			
Sieve Number	Opening (mm)	Weight Retained Each Sieve (g)	Weight of Soil Retained (g)	Weight of Soil Passed (g)	Percent Finer	Proportion of total by mass P %	Angularity factor f	Specific Surface mm^{-1}	$(P/100)*(S^2)*f$
3/8"	9.500	0.00	0.00	215.31	100.000				
No. 4	4.750	0.40	0.40	214.91	99.814	0.186	1	0.89319	0.00218
No. 10	2.000	5.78	6.18	209.13	97.130	2.685	1	1.94666	0.14973
No. 20	0.850	8.57	14.75	200.56	93.149	3.980	1	4.60179	1.24063
No. 40	0.425	6.08	20.83	194.48	90.326	2.824	1	9.98268	4.14198
No. 60	0.250	3.21	24.04	191.27	88.835	1.491	1	18.4072	7.43512
No. 100	0.150	2.42	26.46	188.85	87.711	1.124	1	30.9839	15.8817
No. 140	0.106	1.02	27.48	187.83	87.237	0.474	1	47.5831	15.7876
No. 200	0.075	1.01	28.49	186.82	86.768	0.469	1	67.2927	31.2656
Pan	0.000	186.82	215.31	0.00	0.000				
	Total	215.31							
Hydrometer Reading	0.0273				88.8264	2.058	1	132.604	532.764
	0.01965				85.591	3.235	1	259.075	3196.33
	0.01429				80.0026	5.588	1	358.054	10545.3
	0.01043				73.5318	6.471	1	491.355	22994.4
	0.00781				67.9434	5.588	1	664.529	36323.7
	0.00569				60.8843	7.059	1	900.241	84204.9
	0.00426				50.884	10.000	1	1219.91	219049
	0.00269				47.3545	3.530	1	1772.46	163208
	0.00204				43.8249	3.530	1	2557.55	339812
	0.00122				39.413	4.412	1	3801.75	938572
	0.00092				32.0599	7.353	1	5680.55	3492450
						Total mm^{-2}			5310889

Table E.22: Particle size analysis and specific surface area for BNE

BNE Particle Size Analysis						Specific Surface Area			
Sieve Number	Opening (mm)	Weight Retained Each Sieve (g)	Weight of Soil Retained (g)	Weight of Soil Passed (g)	Percent Finer	Proportion of total by mass P %	Angularity factor f	Specific Surface mm^{-1}	$(P/100)*(S^2)*f$
3/8"	9.500	0.00	0.00	203.32	100.000				
No. 4	4.750	0.84	0.84	202.48	99.587	0.413	1	0.89319	0.00633
No. 10	2.000	3.13	3.97	199.35	98.047	1.539	1	1.94666	0.11199
No. 20	0.850	4.61	8.58	194.74	95.780	2.267	1	4.60179	0.92178
No. 40	0.425	3.87	12.45	190.87	93.877	1.903	1	9.98268	3.64147
No. 60	0.250	2.69	15.14	188.18	92.554	1.323	1	18.4072	8.6059
No. 100	0.150	3.12	18.26	185.06	91.019	1.535	1	30.9839	28.2811
No. 140	0.106	1.82	20.08	183.24	90.124	0.895	1	47.5831	38.9088
No. 200	0.075	1.73	21.81	181.51	89.273	0.851	1	67.2927	73.9694
Pan	0.000	181.51	203.32	0.00	0.000				
	Total	203.32							
Hydrometer Reading	0.02758				90.2213	0.948	1	131.925	316.815
	0.01984				87.1102	3.111	1	256.507	3929.72
	0.01434				82.7547	4.356	1	355.729	10581
	0.01036				78.0881	4.667	1	492.366	21718.5
	0.0077				74.0437	4.044	1	672.01	35063.6
	0.0055				69.377	4.667	1	922.48	76237.1
	0.00394				65.3326	4.044	1	1289.16	129038
	0.00256				59.7327	5.600	1	1890.25	384124
	0.00191				56.6216	3.111	1	2714.22	439999
	0.00116				51.6439	4.978	1	4027.64	1550186
	0.00088				47.9106	3.733	1	5949.23	2536672
						Total mm^{-2}			5187865

Table E.23: Particle size analysis and specific surface area for Messer

Messer Construction Particle Size Analysis						Specific Surface Area			
Sieve Number	Opening (mm)	Weight Retained Each Sieve (g)	Weight of Soil Retained (g)	Weight of Soil Passed (g)	Percent Finer	Proportion of total by mass P %	Angularity factor f	Specific Surface mm^{-1}	$(P/100)*(S^2)*f$
3/8"	9.500	0.00	0.00	198.35	100.000				
No. 4	4.750	6.76	6.76	191.59	96.592	3.408	1	0.89319	0.04087
No. 10	2.000	13.65	20.41	177.94	89.710	6.882	1	1.94666	0.39201
No. 20	0.850	9.87	30.28	168.07	84.734	4.976	1	4.60179	1.58399
No. 40	0.425	7.20	37.48	160.87	81.104	3.630	1	9.98268	5.43762
No. 60	0.250	4.61	42.09	156.26	78.780	2.324	1	18.4072	11.8374
No. 100	0.150	4.38	46.47	151.88	76.572	2.208	1	30.9839	31.8659
No. 140	0.106	2.42	48.89	149.46	75.352	1.220	1	47.5831	41.5243
No. 200	0.075	2.37	51.26	147.09	74.157	1.195	1	67.2927	81.3327
Pan	0.000	147.09	198.35	0.00	0.000				
	Total	198.35							
Hydrometer Reading	0.02592				78.4409	4.284	1	136.086	1192.62
	0.01939				72.945	5.496	1	267.634	5917.41
	0.01409				68.1986	4.746	1	362.966	9399.66
	0.0103				62.4529	5.746	1	497.951	21415.5
	0.00776				55.4582	6.995	1	670.858	47320.1
	0.00564				50.9616	4.497	1	906.991	55603.8
	0.00402				47.9639	2.998	1	1259.76	71513.2
	0.00259				44.2167	3.747	1	1856.81	194201
	0.00196				40.4695	3.747	1	2659.31	398341
	0.00116				35.7231	4.746	1	3978.6	1129379
	0.00086				33.4748	2.248	1	5996.13	1215098
						Total mm^{-2}			3149381

Table E.24: Particle size analysis and specific surface area for OVRS

Ohio Valley River Sand						Specific Surface Area			
Sieve Number	Opening (mm)	Weight Retained Each Sieve (g)	Weight of Soil Retained (g)	Weight of Soil Passed (g)	Percent Finer	Proportion of total by mass P %	Angularity factor f	Specific Surface mm^{-1}	$(P/100)*(S^2)*f$
3/8"	9.500	0.00	0	498.7	100.000				
No. 4	4.750	7.60	7.6	491.1	98.476	1.524	1.25	0.89319	0.0152
No. 10	2.000	50.90	58.5	440.2	88.270	10.207	1.25	1.94666	0.48347
No. 20	0.850	114.50	173	325.7	65.310	22.960	1.25	4.60179	6.07757
No. 40	0.425	222.20	395.2	103.5	20.754	44.556	1.25	9.98268	55.5021
No. 60	0.250	80.70	475.9	22.8	4.572	16.182	1.25	18.4072	68.5358
No. 100	0.150	14.60	490.5	8.2	1.644	2.928	1.25	30.9839	35.1313
No. 140	0.106	2.10	492.6	6.1	1.223	0.421	1.1	47.5831	10.4876
No. 200	0.075	1.50	494.1	4.6	0.922	0.301	1.1	67.2927	14.9824
Pan	0.000	4.60	498.7	0	0.000				
	Total	498.7				Total mm^2			191.215

Table E.25: Particle size analysis and specific surface area for KRS

Kentucky River Sand						Specific Surface Area			
Sieve Number	Opening (mm)	Weight Retained Each Sieve (g)	Weight of Soil Retained (g)	Weight of Soil Passed (g)	Percent Finer	Proportion of total by mass P %	Angularity factor f	Specific Surface mm^{-1}	(P/100)* (S^2)*f
3/8"	9.500	0.00	0	1175.6	100.000				
No. 4	4.750	0.00	0	1175.6	100.000	0.000	1.25	0.89319	0
No. 10	2.000	0.00	0	1175.6	100.000	0.000	1.25	1.94666	0
No. 20	0.850	9.30	9.3	1166.3	99.209	0.791	1.25	4.60179	0.2094
No. 40	0.425	13.10	22.4	1153.2	98.095	1.114	1.25	9.98268	1.38809
No. 60	0.250	144.50	166.9	1008.7	85.803	12.292	1.25	18.4072	52.0585
No. 100	0.150	797.00	963.9	211.7	18.008	67.795	1.25	30.9839	813.542
No. 140	0.106	102.00	1065.9	109.7	9.331	8.676	1.1	47.5831	216.092
No. 200	0.075	53.00	1118.9	56.7	4.823	4.508	1.1	67.2927	224.566
Pan	0.000	56.70	1175.6	0	0.000	Total mm^2			1307.86
	Total	1175.6							

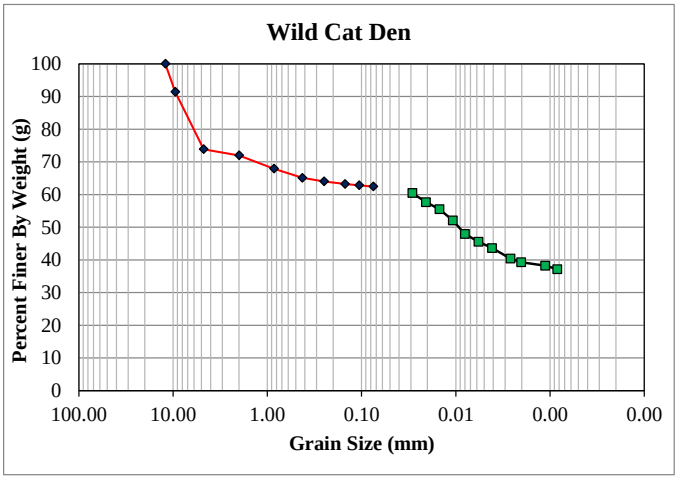

Figure E.9: Grain size distribution curve for Wild Cat Den

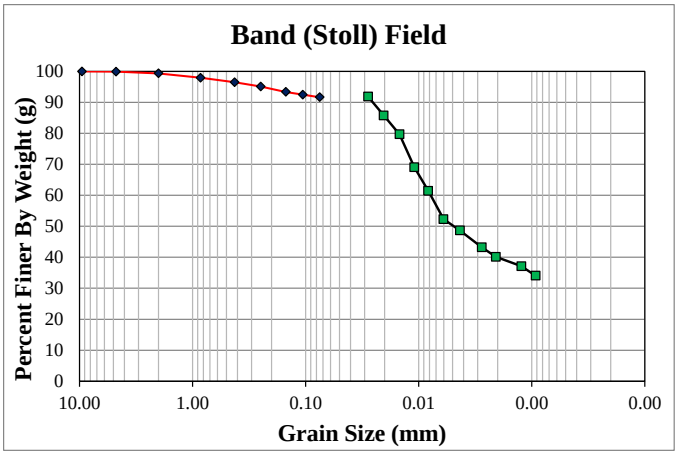

Figure E.10: Grain size distribution curve for Band Stoll Field

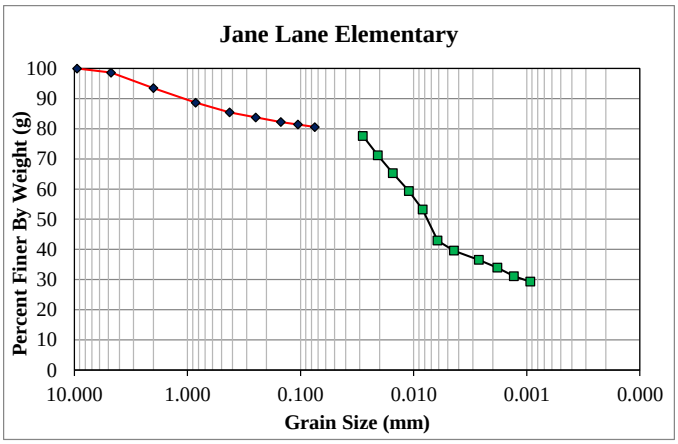

Figure E.11: Grain size distribution curve for Jane Lane

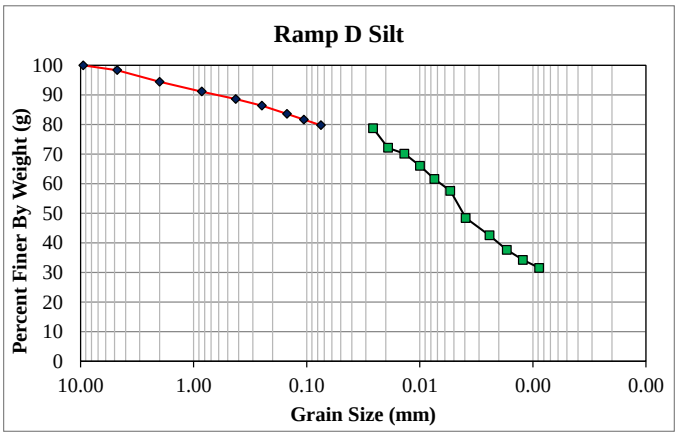

Figure E.12: Grain size distribution curve for Ramp D Silt

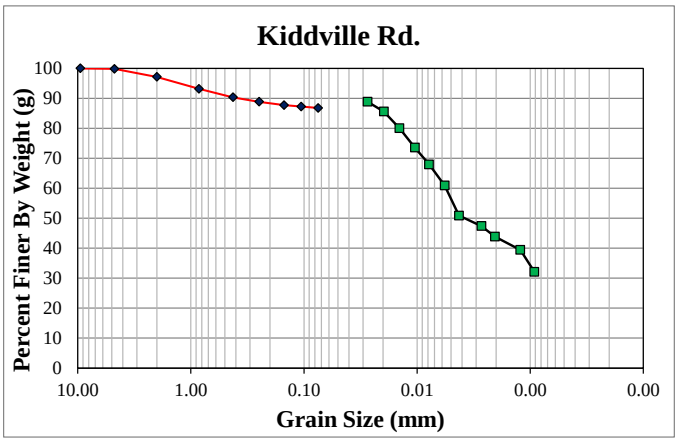

Figure E.13: Grain size distribution curve for Kiddville Road

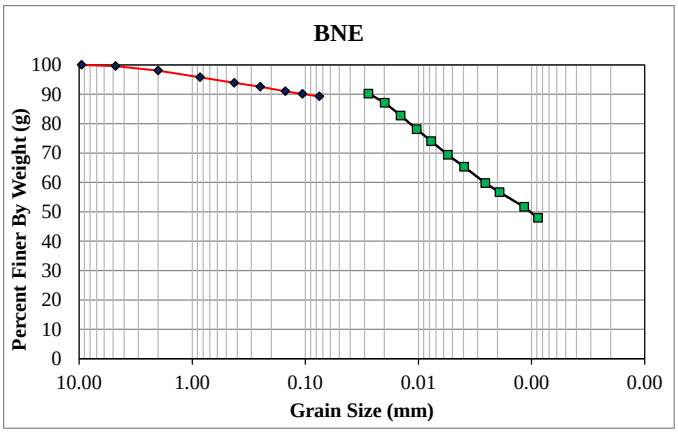

Figure E.14: Grain size distribution curve for BNE

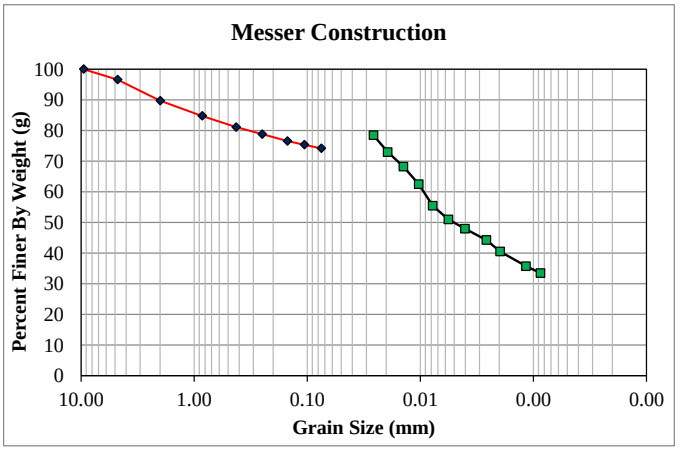

Figure E.15: Grain size distribution curve for Messer

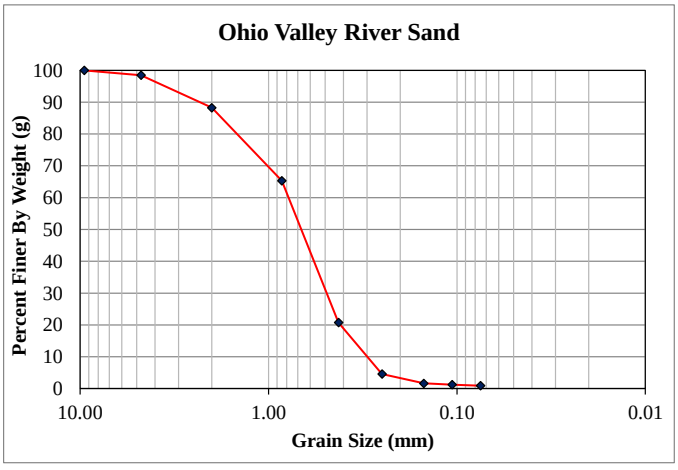

Figure E.16: Grain size distribution curve for OVRS

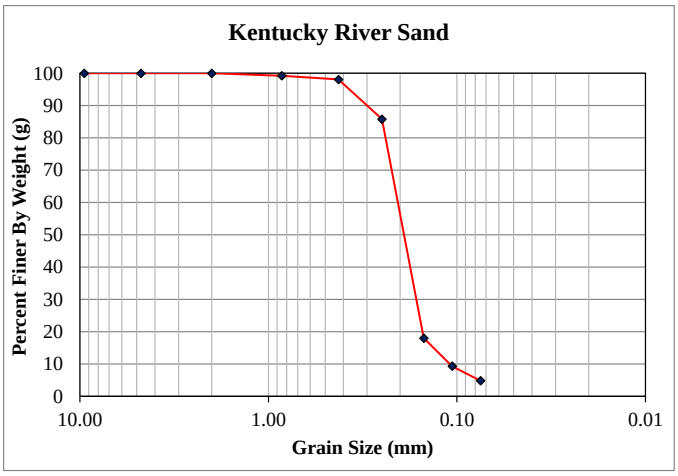

Figure E.17: Grain size distribution curve for KRS

References

Agilent Technologies. (2006). “Agilent Basics of Measuring the Dielectric Properties of Materials.” *Report 5989-2589EN*. June, 2006.

ASTM International. (2012). D698-12: “Standard Test for Laboratory Compaction Characteristics of Soil Using Standard Effort (600 kN-m^3)”. West Conshohocken, PA: ASTM International.

ASTM International. (2011). D1556-11: “Standard Test Method for Density and Unit Weight of Soil in Place by the Sand-Cone Method”. West Conshohocken, PA: ASTM International.

ASTM International. (2011). D2487-11: “Standard Practice for Classification of Soils for Engineering Purposes (Unified Soil Classification System)”. West Conshohocken, PA: ASTM International.

Altun, S., Goktepe, A.B., Sezer, A. (2008). “Investigation of Parameters of Compaction Testing.” *Turkish J. Eng. Env. Sci*. 32, 201-209

Ayers, P.D., and Bowen, H.D. (2008). "Laboratory Investigation of Nuclear Density Gauge Operation." *TRANSACTIONS of the ASAE*, ASAE, 31(3), 658-661.

Bellingham, K. (2007). “The Stevens Hydra Probe Inorganic Soil Calibrations.” Stevens Water Monitoring Systems Inc., Portland, Oregon.

Berney IV, E.S., Kyzar, J., and Oyelam L. (2011). “Device Comparison for Determining Field Soil Moisture Content.” Report No. ERDC/GSL TR-11-42. US Army Corps of Engineers Geotechnical and Structures Laboratory, Vicksburg, MS

Brown, J. (2007). “Non-Nuclear Compaction Gauge Comparison Study Final Report.” *Report 2007 – 19*. State of Vermont Agency of Transportation Materials and Research Section. December, 2007.

Campbell, J. E. (1990). “Dielectric Properties and Influence of Conductivity in Soils at One to Fifty Megahertz” *Soil Sci. Soc. Am. J.* (54) 332-341.

Carteret, R., Buzzi, O., and Fityus, S. (2013). “Installation, Calibration, and Application of Dielectric Sensors in Laboratory Studies of Compacted Unsaturated Granular Materials.” *Geotechnical Testing Journal,* 36(5),1-12

Delta-T Devices Ltd. (1999). *Theta Probe Soil Moisture Sensor User Manual: Type ML2x*. Cambridge, CB5 0EJ, England.

Drnevich, V. P., Lin, C.-P., Yi, Q., and Lovell, J. (2001). "Real-Time Determination of Soil Type, Water Content, and Density using Electromagnetics." *Report FHWA/IN/JTRP-2000/20,* Joint Transportation Research Program, West Lafayette, IN.

Evett, S. R. (2000). "Nuclear Gauge Design, Theory and Operation." *Nuclear Gauge Train-the-Trainer Course*, USDA-Radiation Safety Staff, Beltsville, MA.

Hu, Y., Vu, H., and Hubble, D. (2010). "Evaluation of Dielectric-Based Probes for Expansive Soils: Application to Regina Clay." *Canadian Geotechnical Journal.* 47 (3) 346-358

Kaleita, A., Heitman, J., and Logsdon, S. (2005) "Field Calibration of the Theta Probe for Des Moines Lobe Soils." *American Society of Agricultural Engineers*. 21(5): 865-870

Kelleners, T., Ayars, J., Robinson, D., Shouse, P., and Skaggs, T. (2005). "Frequency Dependence of the Complex Permittivity and Its Impact on Dielectric Sensor Calibration in Soils." *J. Soil Sci. Soc. Am. J.* 69 (1) 67-76.

Lee, K. (2005). "A Dielectric Permittivity Sensor for Simultaneous Measurement of Multiple Soil Properties." *PhD Dissertation*, Kansas State University, Manhattan, Kansas.

Mejias-Santiago, M., E.S. Berney IV, and C.T. Bradley. (2013). *Evaluation of A Non-Nuclear Soil Density Gauge on Fine-Grained Soils.*Vicksburg, MS: Report No. ERDC/GSL TR-13-20. U.S. Army Engineer Research and Development Center.

Miller, J.D., Gaskin, G.J. (1999) "Theta Probe ML2x. Principles of operation and applications. MLURI Technical Note (2^{nd} edn)

Mitchell, J., and Soga, K. (2005). *Fundamentals of Soil Behavior.* John Wiley and Sons, Inc. Hoboken, NJ.

Parilkova, J., Veselý, J., Pavlík, J., and Stoklásek, R. (2009). "Monitoring Of The Soil Status Using Electrical Impedance Spectrometry Method Developed In Project

E!3838 Of The Europe International Program Eureka." *XIX IMEKO World Congress*, Lisbon, Portugal, 2234-2237.

Pluta, S. E., and Hewitt, J. W. (2009). "Non-Destructive Impedance Spectroscopy Measurement for Soil Characteristics." *Characterization, Modeling, and Performance of Geomaterials: Selected Papers From the 2009 GeoHunan International Conference (GSP 189)*, 144-149.

Rathje, E. M., Wright, S. G., Stokoe, K. H. II, Adams, A., Tobin, R., and Salem, M. (2006). "Evaluation of Non-Nuclear Methods for Compaction Control." *Report FHWA/TX-06/0-4835-1,* Texas Department of Transportation, Austin, TX.

Rose, M. (2013). "Evaluation of Non-Nuclear Density Gauges for Determining In-Place Density of Unbound Materials" *Master's Thesis*, Washington State University of Civil and Environmental Engineering, Pullman, Washington.

Saito, T., Fujimaki, H., Yasuda, H., Inosako, K., and Inoue, M. (2013). "Calibration of Temperature Effect on Dielectric Probes Using Time Series Field Data." *Vadose Zone Journal* vol. 12. doi: 10.2136/vzj2012.0184

Schmutz, P., and Namikas, S. (2011) "Utility of the Delta-T Theta Probe for Obtaining Surface Moisture Measurements from Beaches." *Journal of Coastal Research.* 27 (3) 478-484

Sebesta, S., Oh, J., Lee, S., Sanchez, M., and Taylor, R. (2013). "Initial Review of Rapid Moisture Measurement for Roadway Base and Subgrade" *Report FHWA/TX-13/0-6676-1,* Joint Transportation Research Program, College Station, Texas

Seyfried, M., Grant, L., Du, E., Humes, K. (2005). "Dielectric Loss and Calibration of the Hydra Probe Soil Water Sensor." *Vadose Zone Journal*. 4:1070-1079

Seyfried, M. and Murdock, M. (2004). "Measurement of Soil Water Content with a 50-MHz Soil Dielectric Sensor" *Soil Sci. Soc. Am. J.* 68:394-403.

Sotelo, M., Mazari, M., and Nazarian, S. (2014). "Evaluation of Non-Nuclear Devices in Measuring Moisture Content and Density of Soils" Transportation Research Record, Journal of the Transportation Research Board, No. 14-4381.

Stevens Water Monitoring Systems, Inc. (2008). *Comprehensive Stevens Hydra Probe Users Manual*. User Manual, Portland: Stevens Water, Inc.

Topp, G., Davis, J., and Annan, A. (1980). "Electromagnetic Determination of Soil Water Content: Measurements in Coaxial Transmission Lines." *Water Resources Research*. 16 (3) 574- 582.

TransTech Systems, Inc. (2013). *Soil Density Gauge 200 Operator's Handbook.* User Manual, Schenectady: TransTech Systems, Inc.

Vaz, C., Jones, S., Meding, M., and Tuller, M. (2013). "Evaluation of Standard Calibration Functions of Eight Electromagnetic Soil Moisture Sensors." *Vadose Zone Journal* vol. 12. doi:10.2136/vzj2012.0160

Vita

Joshua Eli Robert Wells was born in Charleston, South Carolina and raised in Middletown, Ohio. He graduated top twenty in his class from Madison Jr./Sr. High School in 2007. Josh attended Western Kentucky University and graduated with a Bachelor's in Science in Civil Engineering in 2012. He obtained his Engineering in Training (EIT) Certificate in April of 2012 in the State of Kentucky. As an undergraduate at WKU, Joshua was active with Sigma Alpha Epsilon Fraternity, and the American Society of Civil Engineers (served as the WKU Chapter President and concrete canoe captain). He also received the Kentucky Section ASCE annual scholarship in 2011. After graduation from the University of Kentucky, Joshua will reside in Charlotte, North Carolina to stay close to his family. Joshua is the first author on one publication:

Wells, J.E.R., Bryson, L.S., Wilder, Z. (2014). "Performance of Non-Nuclear Devices for Insitu Moisture and Density Determination". *Geo-Congress Technical Papers*: 2450-2459